# *RETENTION FOR 3D PRINTED HOLLOW IMMEDIATE SURGICAL OBTURATORS FOR MAXILLECTOMY PATIENTS*

## T.L. COENRAAD

# Retention for 3D-printed hollow Immediate Surgical Obturators for Maxillectomy Patients

Master of Science in Technical Medicine
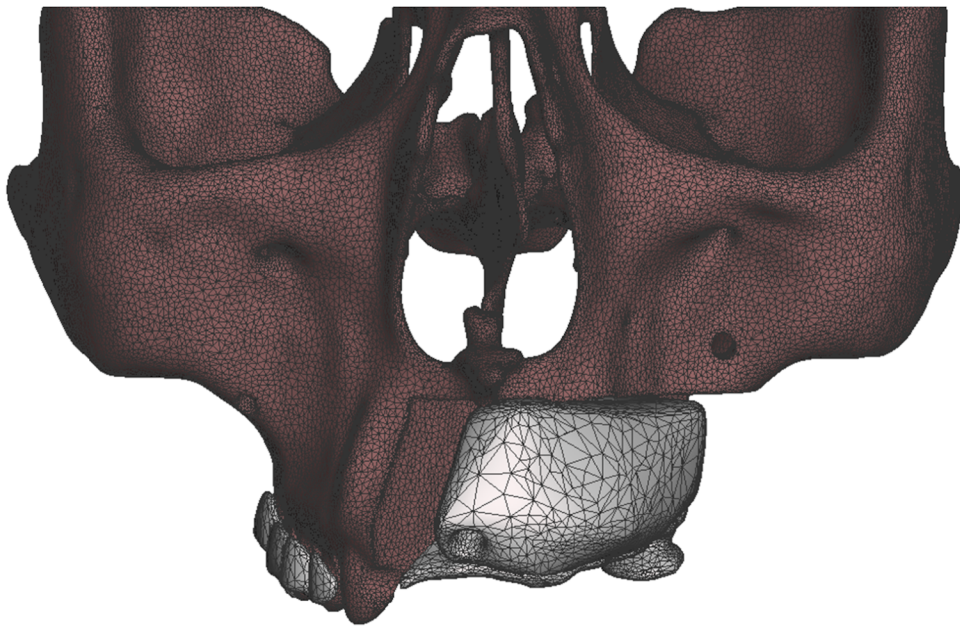


The work in this thesis was made in the:

Verwelius 3D Lab
Department of Head and Neck Oncology and Surgery
The Netherlands Cancer Institute

Technical Medicine
Medical Imaging and Interventions
Faculty of Science and Technology
University of Twente

# THESIS COMMITTEE

**Chairman**

Prof. Dr. I.A.M.J. Broeders

Surgeon
Centre for Artificial Intelligence
Meander Medisch Centrum
Amersfoort, the Netherlands
Professor
Robotics and Mechatronics group
University of Twente
Enschede, The Netherlands

**Medical supervisors**

Dr. M. B. Karakullukçu

Head and Neck Surgeon
Department of Head and Neck Surgery & Oncology
Verwelius 3D Lab
Netherlands Cancer Institute
Amsterdam, The Netherlands

Drs. M. Krap

Maxillofacial prosthodontist
Department of Head and Neck Surgery & Oncology Netherlands Cancer Institute
Amsterdam, The Netherlands

**Technical supervisor**

Dr. F.J. Siepel

Associate Professor - Technical Physician
Robotics and Mechatronics group
Faculty of EEMCS
University of Twente
Enschede, The Netherlands

**Technical Medicine supervisor**

Dr. M.J.A. van Alphen

Technical Physician and Postdoctoral researcher
Department of Head and Neck Surgery & Oncology
Verwelius 3D lab
Netherlands Cancer Institute Amsterdam, The Netherlands

**Process supervisor**

MSc. B.J.C.C. Sweep

Social psychologist - Lecturer Professional behaviour
Faculty Science and Technology
University of Twente
Enschede, The Netherlands

**External committee member**

Dr. A.T.M. Bellos-Grob

Assistant Professor - Technical Physician
Faculty Science and Technology
University of Twente
Enschede, The Netherlands

# ACKNOWLEDGEMENTS

I want to say thank you to everyone who made my research year at Antoni van Leeuwenhoek Hospital a memorable and enriching experience.

Menno, your expertise in dentistry and maxillofacial prosthetics has been invaluable. Your guidance and insights have taught me many things that cannot be read in books. Maarten and Robert, our regular biweekly conversations were a source of support and a space where I could freely discuss many things. Your willingness to listen and engage in discussions meant a lot. Baris, your openness created a positive atmosphere where I could learn. Your guidance and the clinical opportunities you offered me have taught me very much this past year. Wilfred, your assistance with 3D printing and our discussions about my future direction were incredibly valuable. Your support during the technical aspects of my work is deeply appreciated.

Francoise, your enthusiasm and meticulous approach were truly commendable. Your support, along with Vincent, at the RAM lab, significantly contributed to the line of research I performed the past year. Bregje, your creation of the intervision space provided a safe environment for reflection and growth, for which I am very grateful.

To the 3D-lab students, your collaboration and shared experience have made our work environment very pleasant. And with the daily snacks, coming into the hospital was no punishment!

I extend my deepest appreciation to my friends and family for their unwavering support throughout this journey. And to Rick, thank you for being a constant source of encouragement and understanding.

Thank you all for being an important part of my thesis year and contributing to its success.

Sincerely,
Tessa Coenraad

Amsterdam, November 2023

# ABSTRACT

Introduction - Retention of heavy obturators for maxillectomy patients can be challenging. Weight reduction can be achieved by hollow bulbs. A CAD/CAM workflow for a 3D-printed hollow Immediate Surgical Obturator (hISO) is developed in our centre. This workflow currently consists of data acquisition and the design of the baseplate and bulb. To implement the hISO in the clinic, retention is necessary. This study aims to provide the current 3D-printed hISO with retention.

Method - The proposed workflow for 3D-printable retention clasps includes design criteria, such as a safe and solid design, sufficient retention, free gingival sulcus and cementoenamel junction, and compatibility with oral structures and the hISO. These clasps are tested in a phantom study, simulating the outward force of exudate and contracting tissue and the force on the obturator during deglutition. A study is performed to determine the tongue-palate pressure (TPP) in three locations for young, healthy females during deglutition. A classification system is proposed that guides digital bulb-shape design, with corresponding 3D-printed clasps tested for each class to determine their retention. These clasps are compared against conventional circumferential wires around teeth combined with zygomatic wire and boulder, along with assessing additional retention when used in combination with a palatal screw. The retention is measured in terms of displacement, measured with an EM navigation system.

Results - The proposed NKI classification system consists of four alveolar classes and three zygomatic classes. Although the final design of the 3D-printed retention clasps met all design criteria, determining undercuts and insertion paths remained challenging, initiating exploration into a digital surveyor. TPP averages 17 kPa across anterior, medial, and posterior locations in the three subjects. According to the phantom study, the 3D-printed clasps outperform the circumferential wires around the teeth for all alveolar classes when combined with a zygomatic wire. For the zygomatic classes, retention was insufficient, which is in line with the literature. The 3D-printed clasps did not add retention in combination with a palatal screw.

Conclusion - This study provides a workflow for 3D-printed retention clasps, enhancing the hISO clinical viability. The 3D-printed clasps provide sufficient retention when combined with a zygomatic wire for the alveolar classes of the NKI classification. Future research should explore alternative retention methods, such as zygomatic implants, for retention of the zygomatic classes.

# LIST OF ABBREVIATIONS

| | |
|---|---|
| 3D | Three dimensional |
| C | Canine |
| CAD | Computer-Aided Design |
| CAM | Computer-Aided Manufacturing |
| CEJ | Cementoenamel junction |
| CN | Cranial nerve |
| CSM | Closed Surface Model |
| CT | Computed Tomography |
| DI | Dental Implants |
| DOF | Degrees of freedom |
| DSC | Dice Score Coefficient |
| EAT-10 | Eating Assessment Tool |
| EBV | Epstein-Barr virus |
| EM | Electromagnetic |
| FG | Field Generator |
| FRE | Fiducial Registration Error |
| HD | Hausdorff Distance |
| hISO | hollow Immediate Surgical Obturator |
| HNC | Head-and-Neck Cancer |
| HPV | Human Papilloma virus |
| HU | Hounsfield Unit |
| I | Incisor |
| IOPI | Iowa Oral Performance Instrument |
| IOS | Intraoral Scan |
| ISO | Immediate Surgical Obturator |
| M | Molar |
| MRI | Magnetic Resonance Imaging |
| NKI-AvL | Netherlands Cancer Institute – Antoni van Leeuwenhoek |
| OR | Operation Room |
| PM | Premolar |
| Q | Quadrant |
| RMS | Root Mean Square |
| RPD | Removable Partial Denture |
| SCC | Squamous Cell Carcinoma |
| SLA | Stereolithography (type of printing) |
| STL | Stereolithography (type of model) |
| TPP | Tongue-Palate Pressure |
| UV | Ultra Violet |
| ZI | Zygoma Implants |

# CONTENTS

# CONTENTS

# CHAPTER 1. GENERAL INTRODUCTION

# Chapter 1.
# Background information

*Anatomy*

## Maxilla

The maxillae are a pair of symmetrical bones connected at the intermaxillary suture, forming the upper jaw. The maxillae contribute to the formation of the nasal cavity, oral cavity, orbital cavity, while also supporting the upper teeth. Each maxilla is composed of a body, which forms a major part of the bone, and four processes: the *zygomatic process*, articulating with the zygomatic bone to form the cheekbone; the *alveolar process*, supporting the upper teeth; the *palatine process*, forming the anterior part of the hard palate; and the *frontal process*, forming the lateral boundary of the nose. The maxilla and its processes are shown in Figure **1.1**. [1–4]
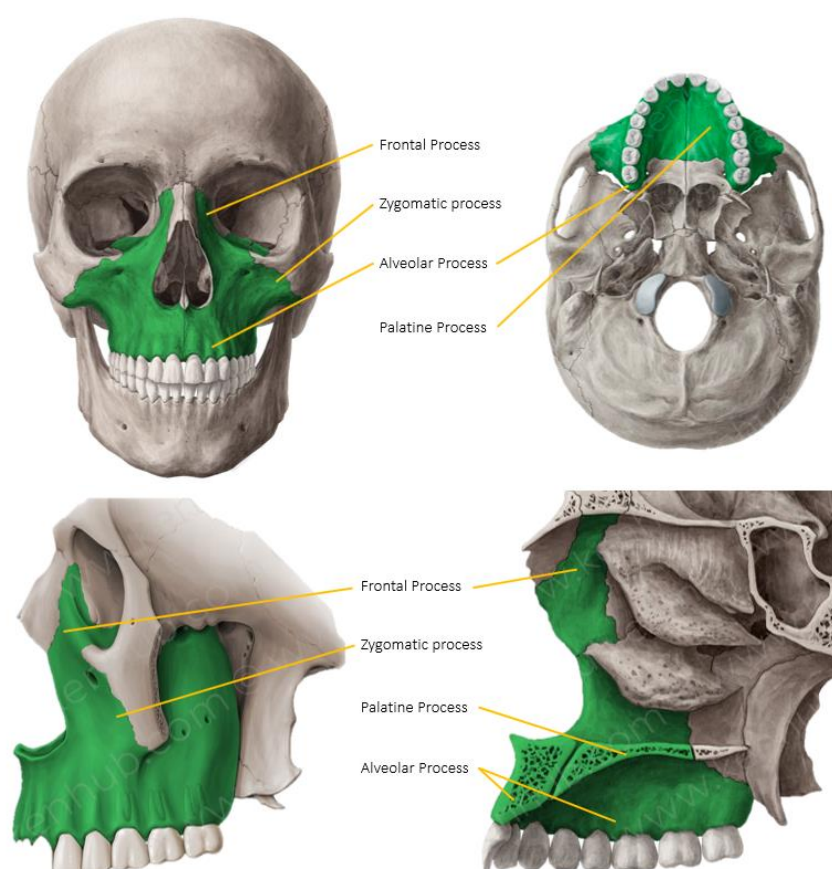


*Figure **1.1**. Maxilla bone from different angles. Four processes of the maxilla are shown: the frontal process forming the lateral boundary of the nose, the zygomatic process forming the cheekbone with the zygomatic bone, the alveolar process holding the upper teeth, and the palatine process forming the anterior part of the hard palate.[5]*

The paired, pyramid-shaped maxillary sinus is within the maxillae, as shown in Figure **1.2**. The orbital floor forms its roof, the maxilla's alveolar process forms the floor, and the lateral border of the nose is the medial border. The apex extends towards the zygomatic process.[6] The maxillary sinus is the largest of the four paranasal sinuses, serving several functions, including skull weight reduction, air humidification, and assistance in voice resonance.[7] The maxillary sinus is lined with mucus cells, providing mucus to the nose.[8]

*Figure **1.2**. Maxillary sinuses are highlighted in purple in the cross-sectional CT scan (A), and they are depicted together with the other paranasal sinuses (B).* [7,8]

## Palate

The palate serves as the roof of the oral cavity and consists of two parts: the hard palate (*palatum durum*) and the soft palate (*palatum molle*). The hard palate is formed by the *palatine process* of the maxillae and the horizontal plates of the *palatine bone*, with the *interpalatine suture* (existing of the *in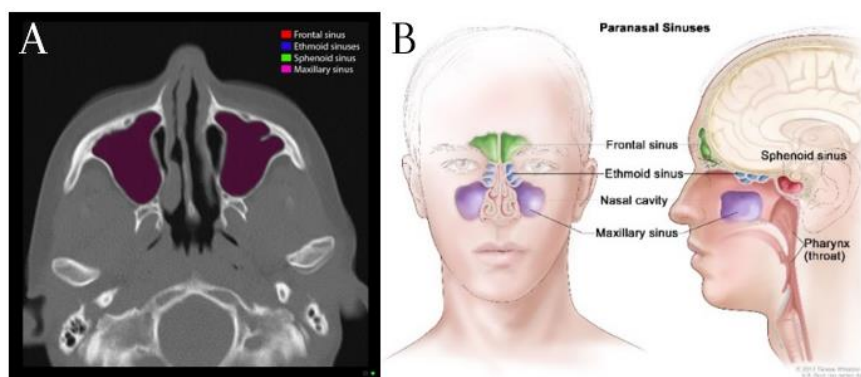termaxillary suture* and *the median palatine* suture) combining both sides (fig **3.1**). The *incisive foramen*, situated directly posterior to the incisors on the midline, transmits nerves and arteries such as the *sphenopalatine artery* supplying the mucous membrane of the hard palate, and the *nasopalatine nerves* innervating the hard palate.[1,2]

The *greater and lesser palatine foramina* are both bilaterally located and medial from the third molar. The lesser palatine foramen posterior to the greater palatine foramen. They respectively transmit the *greater and lesser palatine vessels and nerves.*[1,2,9]
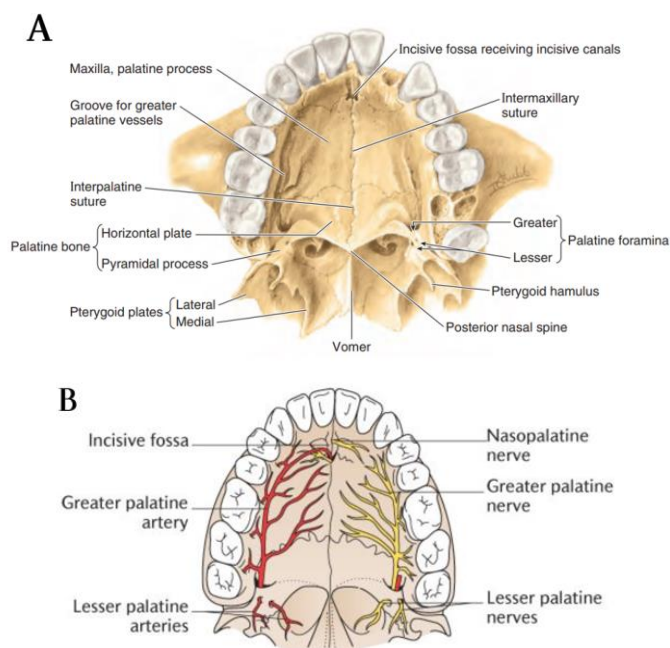


*Figure **1.3**. A) The bony anatomy of the hard palate. B) The nerves and arteries emerging from the incisive foramen, and the greater and lesser palatine foramina.*[2,10]

## Maxillary dentition

Teeth are essential for cutting, reducing and mixing food with saliva during mastication. They also play a role in the articulation of some sounds.[2] To enable clear communication about dentition, the mouth is divided into four quadrants: the right maxillary quadrant (Q1), the left maxillary quadrant(Q2), the left mandibular quadrant (Q3) and the right mandibular quadrant (Q4). The teeth are numbered from the midline in the distal direction (fig **1.4.A**).

There are four different types of teeth present in the maxilla: incisors (I2 and I2), canine (C), premolars (PM1 and PM2) and molars (M1, M2, and M3), see Figure **1.4**. The surfaces of those teeth are described as follows (see Figure **1.5**):

1.        The **lingual** surface is directed inward, towards the tongue *(lingua)*, also called the **palatal** surface for the maxillary teeth;
2.        The **buccal** surface is directed to the cheek;
3.        The **labial** surface is directed to the lip;
4.        The **mesial** surface is the one closest to the midline, present between 11-21 and 41-31;
5.        The **distal** surface is the one the furthest away from the midline;
6.        The **occlusal** surface is the masticatory surface.
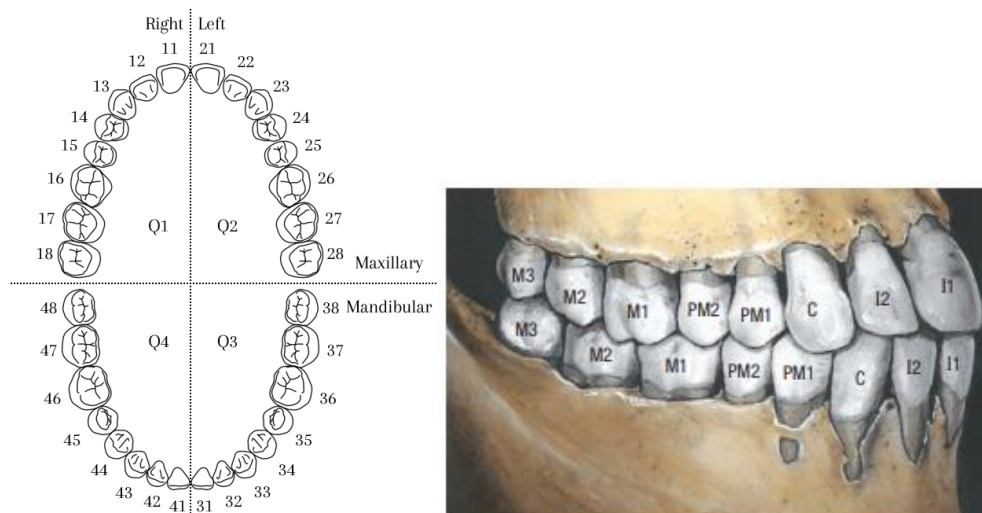
*Figure **1.4**. A) Dental quadrants; Q1) right maxillary, Q2) left maxillary, Q3) left mandibular, and Q4) right mandibular. The teeth are numbered from 1-8 from the medial line in the distal direction. B) Different types of dentition from anterolateral view. I1 and I2 are incisors, C are canine, PM1 and PM2 are the premolars and M1-M3 are the molars.* [1]
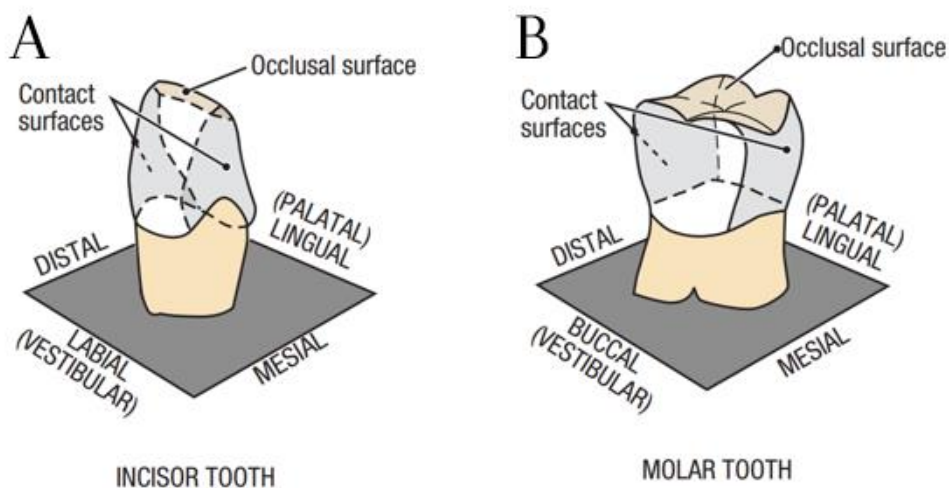
*Figure **1.5**. Incisor (A) and molar (B) are shown with their surfaces.* [1]

Teeth are composed of a crown and root, connected by the neck. Focusing on maxillary dentition, the root(s) (one or multiple) are fixated into the tooth socket in the alveolar process of the maxilla. The crown of the teeth is covered with enamel, whereas the root and neck are covered with dental cement. Where the two meet is called the cemento-enamel junction (CEJ). Figure **1.6** shows the anatomy of the tooth.

The alveolar process and the necks of the teeth are covered with mucosal tissue called gingiva. The marginal gingiva surrounds the necks of the dentition. The gingival sulcus is located between the teeth and the marginal gingiva (see Figure **1.6**).

Maxillary teeth are innervated by the superior alveolar nerves, stemming from the maxillary root of the facial nerve (see Figure **1.7**)
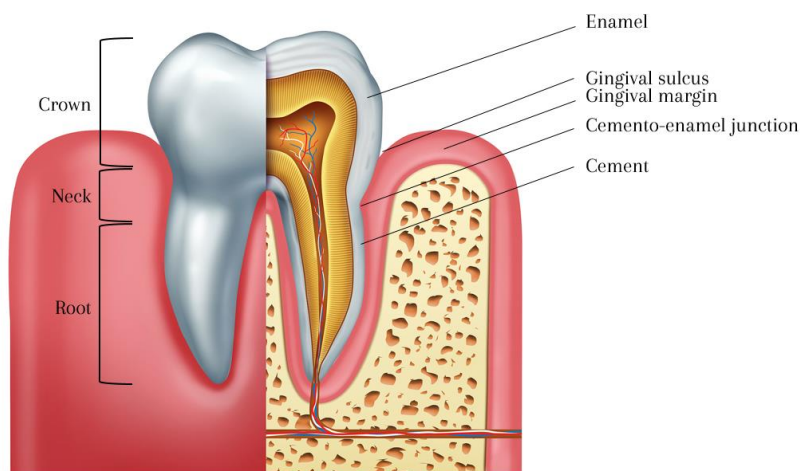


*Figure **1.6**. Anatomy of a tooth in its alveolar socket. The tooth is divided into the crown, neck and root. The location where the enamel meets the cement is called the cemento-enamel junction. Where the gingival margin and the neck of the tooth meet, the gingival sulcus occurs.* [11]
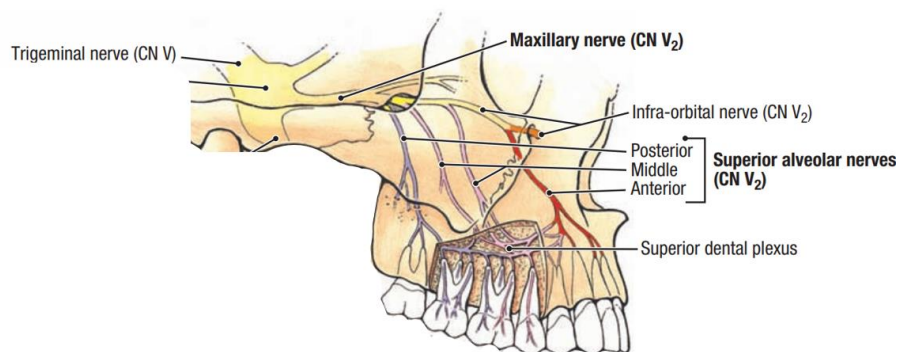


*Figure **1.7**. The maxillary root of the facial nerve is shown with its branches innervating the maxillary teeth.*[1]

## Maxillary cancer

### Epidemiology

Over the last decade, head-and-neck cancer (HNC) has been the ninth most frequently diagnosed cancer in the Netherlands. HNC predominantly affects men over 50 years old. [12–15] Oral cavity cancer constitutes the majority of HNC cases, with oral and nasal cavity cancer combined having an incidence of 6.8 per 100,000 capita in 2022. Oral cancer can occur in various intraoral sites, including the tongue, lips, floor of the mouth, buccal and palatal mucosa, gingiva and alveolar process of the mandible or maxilla. [16] Tumours affecting the maxilla can be involved with different structures, such as the maxillary sinuses, palate, alveolar bone/mucosa or the nasal cavity. [17–19] Cancer involving the hard palate was diagnosed 43 times in the Netherlands in 2022. [14]

Smoking and alcohol consumption are the main risk factors for oral and nasal cavity cancer. Exposure to carcinogenic substances like nickel and asbestos, as well as the HPV16 and EBV virus, is also proven to increase the risk of HNC. [15,17,20] Ninety per cent of oral cavity tumours are squamous cell carcinoma (SCC). [21]

### Maxillectomy

The indication for a maxillectomy is the surgical excision of tumours involving the maxilla. Maxillectomy is a commonly used treatment for maxillary tumours, possibly with adjuvant radiotherapy or chemotherapy. [22–24] Patients should be evaluated through a CT scan, MRI scan, or possibly both. While a CT scan assesses the bony anatomy of the patient, an MRI scan is superior in distinguishing the tumour from soft tissue. [25] Understanding the tumour's extent is crucial to decide on a partial or total maxillectomy, and to determine which adjacent tissue should be included in the resection. A maxillectomy involves three stages; soft tissue dissection and bone exposure; bony resection; closure and reconstruction. [26]

To achieve adequate soft tissue dissection and bone exposure, three traditional approaches can be performed based on the tumour's size and location: midfacial degloving, lateral rhinotomy, and Weber-Ferguson approach. The choice of approach depends on adequate exposure, function, and cosmesis. [26–29]

The next step is the bony resection, classified according to Brown's classification, illustrated in Figure **1.8** and described in Table **1.1**. [30] The classification offers a framework for the identification of different challenges and complexities of each defect, the planning of the maxillectomy as well as an indication for reconstructive options. It is important to perform the cuts through the tooth sockets when necessary, to prevent devitalization and destabilization of the adjacent tooth. [31]

Following the bony resection, wound closure and reconstruction are achieved. Various reconstruction options are available after a maxillectomy, including local/regional flaps, free flaps or prosthetic obturation. Reconstruction aims to achieve oronasal separation for restored eating and speaking ability, preserve facial contours and symmetry, minimize eye dislocation, maintain the nasal airway, and restore dentition. [26,32–34]
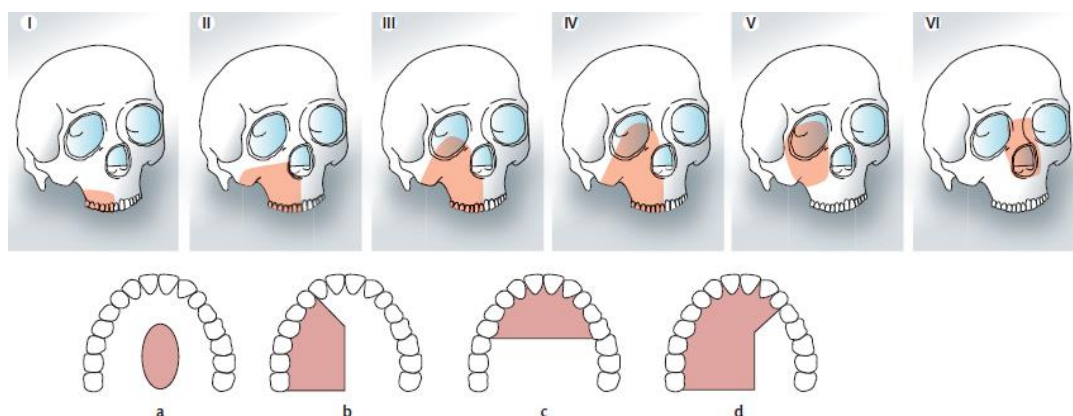


*Figure **1.8**. Browns classification.* [30]

Table **1.1** Browns classification system. [30]

| | |
|---|---|
| ***Vertical*** | |
| I | Maxillectomy without oronasal fistula |
| II | Maxillectomy not involving the orbit |
| III | Maxillectomy involving the peri-orbital area or with orbital floor |
| IV | Maxillectomy with orbital enucleation or exenteration |
| V | Orbitomaxillary defect |
| VI | Nasomaxillary defect |
| ***Horizontal*** | |
| a | Palatal defect without alveolus |
| b | Defect is ≤1/2 unilateral |
| c | Defect is ≤1/2 bilateral or transverse anterior |
| d | Defect is >1/2 maxillectomy |

## Obturator

The focus of this research is on maxillectomy reconstruction using a prosthetic obturator. Prosthesis obturation offers advantages such as reduced hospital time and cost, the immediate restoration of facial and dental morphology and oral function, and the early inspection of the surgical site for possible malignancy recurrence.[33,35-38] Prosthetic obturation can be divided into three phases, each with distinct objectives.[33,34]

### Immediate surgical obturator

During the maxillectomy, an immediate surgical obturator (ISO) is placed to ensure oronasal separation, allowing the patient to speak and eat after the surgery. It also provides a matrix for the placement of a skin graft for the wound, reduces oral contamination, and applies pressure on the soft tissue surrounding the defect. The ISO is not removed for the initial phase of wound healing. [34,39,40]

Comprising two parts, the ISO includes the palatal plate, also known as the baseplate, and the bulb. Before surgery, the baseplate is prepared using a working cast of the patient's teeth and palate. The planned resection is marked on the cast, and within that area, the teeth are removed, and the alveolar process is smoothed. The baseplate is created by pressing clear acrylic resin over the processed cast.[33,34,41]

The bulb is made from mouldable thermoplastic silicone putty and is hand-moulded by the prosthodontist during surgery. The putty is pressed into the defect. The prosthodontist can extend the bulb when necessary, to ensure pressure on the soft tissue to counteract the contraction of scar tissue developed by wound healing. The baseplate is adhered to the putty bulb. Figure **1.9** shows an example of an ISO before the surgery, comprising the baseplate, retention methods like (Adams) clasps, and a part where the bulb is built on. The bulb serves as a carrier for the skin graft covering the defect, often creating a ridge between the mucosa-skin graft junction. This ridge can aid in the retention of the ISO. Retention is frequently achieved by a wire bent around the zygomatic process of the temporal bone and wired around a bolder created on the prosthesis. Another widely used retention method involves wires around the patient's teeth.[33,34,41,42]
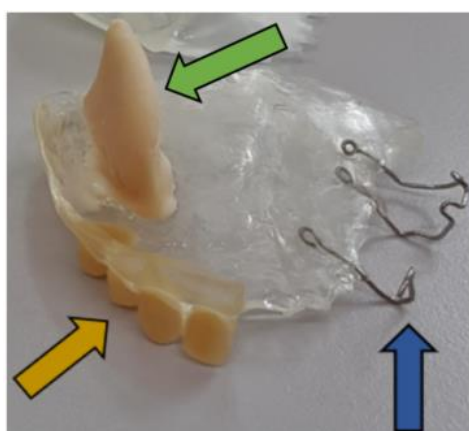


*Figure **1.9**. An example of an Immediate Surgical Obturator, with dentition (yellow), retention wires (blue), and an attachment for the bulb (green).*

## Interim obturator

Because of rapid soft tissue changes in the defect, the fit of the ISO is assessed 2-4 weeks after surgery. An interim obturator is developed, by modifying and relining the ISO or creating a new bulb. Changing the lining material of the bulb is essential due to its porosity, which may lead to bacterial contamination, unpleasant odours, and irritation of the mucous membranes. This obturator is used until the surgical site is completely healed and the defect is dimensionally stable. The interim obturator often includes dentition for cosmetic purposes and psychological benefits. A well-created interim obturator can serve as a backup obturator when the definitive obturator is in use. [31,33,34,39]

## Definitive obturator

A definitive obturator is created after the defect is completely stable and healed, mostly after 3-6 months. The definitive obturator is a newly crafted prosthesis designed to best fit the defect, ensuring comfort and preventing any potential leakage. For (partially) dentate patients, the retention of the definitive obturator is obtained from the potential skin-mucosal ridge, clasps around remaining teeth and/or implants. For edentulous patients, this skin-mucosal ridge is important, along with the presence of implants. [31,33,39]

## Problem statement

Despite conventional obturators being a good reconstructive option after maxillectomy, some drawbacks occur. The primary challenge lies in the obturator's weight. This is particularly challenging for larger defects requiring a large bulb, that can weigh up to 70-80 grams.[43] Achieving sufficient retention is a challenge for heavily weighted obturators, causing patient discomfort.[44] Moreover, the bulb's porous material facilitates bacterial and nasal mucus infiltration, leading to unpleasant odours and irritation of mucous membranes. [34,45] Furthermore, the intraoperative fabrication of the bulb increases the operating room (OR) time.

To achieve weight reduction of the ISO, a hollow bulb can be used. A hollow bulb can reduce the weight of the ISO by 7-47%. The literature describes different techniques for the development of hollow obturators, including an open or closed approach [44,46–48]. An open obturator can allow fluid accumulation, causing foul odour and taste.[37] Therefore, it is desired to develop closed hollow obturators, offering the advantage of eliminating fluid accumulation and providing superior extension into the defect.[49]

Literature suggests using CAD/CAM and 3D printing as a way to design and develop hollow closed obturators, which would overcome the limitations associated with the conventional ISO.[50–52] Opting for thermoplastic material, instead of porous material, prevents bacterial and mucus infiltration. Moreover, this approach can decrease OR time, as ISO development can be completed before surgery.

At the NKI-AvL, there is ongoing research that examines a CAD/CAM workflow for designing and fabricating hollow ISOs.

### CAD/CAM workflow

Steenhuis[53] and Ooms[43] established a CAD/CAM workflow for a patient-specific 3D-printed hollow ISO. Using an intraoral scan (IOS), the baseplate of the ISO is designed in Meshmixer. By using the preoperative CT scan and planned resection, a 2 mm thick hollow closed surface bulb is designed in 3D slicer. The IOS is registered to the CT-scan coordinate system using fiducial registration, which relies on handpicked fiducials to ensure the correct location of the bulb on the baseplate. Figure **1.10** shows the state-of-the-art workflow, while Figure **1.11** shows the ISO resulting from this workflow.
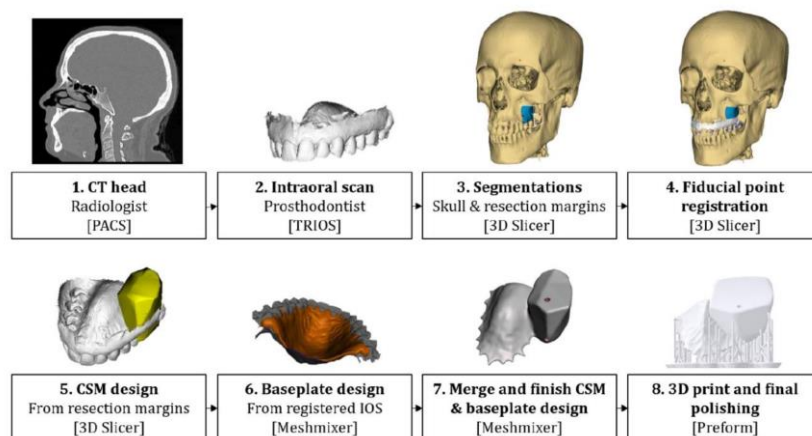


*Figure **1.10**. The CAD/CAM workflow for the development of a 3D hollow closed surface model immediate surgical obturator.*[43]
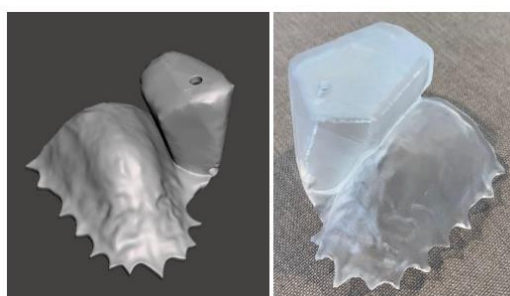


*Figure **1.11**. The left image shows a hollow closed surface immediate surgical obturator as a 3D model. The right image is the resulting obturator after 3D printing and post-processing.*

## Thesis objective and outline

As described in the previous section, Steenhuis and Ooms have already taken several steps towards creating a user-friendly workflow for a patient-specific hollow ISO (hISO) for (partially) dentate patients. However, the obturator resulting from this workflow cannot be clinically implemented due to its lack of retention. During this research, a focus will be on this crucial step required for the implementation of the hISO.

The main objective of this research is:

*To provide the current 3D-printed hollow immediate surgical obturator with retention.*

The research is divided into four parts, each offering distinct insights leading up to the phantom study in **Chapter 6**, where various retention methods are assessed for different defects.

**Chapter 2** provides technical background information to understand the techniques that are used throughout this year of research.

Despite the medical and technical jargon, clear communication about the shape of an obturator can be challenging. Especially with digital workflows for the design of prostheses on the rise, a clear guideline is missing. Previous research investigated bulb shapes from digital designs for different maxillectomy defects, and **Chapter 3** proposes a classification system with design principles based on those tests. This classification system functions as a framework for the phantom study.

Adams clamps are widely used for conventional obturators, but they cannot be incorporated into the CAD/CAM hISO workflow. Therefore, **Chapter 4** proposes and evaluates a CAD/CAM workflow for 3D printed retention clasps. This retention method will be tested in the phantom study.

In **Chapter 5**, the tongue-palate pressure during deglutition for young, healthy female subjects is tested. These outcomes are the basis for the simulation of deglutition in the phantom study.

In addition to the tongue palate pressure determined in Chapter 4, obturators are also subjected to an outward force of shrinking scar tissue and wound exudate after a maxillectomy. These two forces are simulated in the phantom study of **Chapter 6**, where three retention methods, including the clasps from Chapter 5, are tested amongst each other for each class from the classification system stated in Chapter 3.

In **Chapter 7**, the overall project will be discussed and future perspectives will be stated.

**Remark**: All following chapters of this thesis are written so that they can be read separately. Therefore, some

chapters contain overlapping information.

REFERENCES

1.      Agur AMR, Dalley AF. *Grant's Atlas of Anatomy*. 14th ed. Wolters Kluwer/Lippincott Williams & Wilkins,; 2017.

2.      Moore KL, Dalley AF, Agur AMR. *Clinically Oriented Anatomy*. 7th ed. Wolters Kluwer/Lippincott Williams & Wilkins; 2014. doi:10.1002/ca.22316

3.      Radlanski RJ, Wesker KH. *Het Gezicht: Atlas van de Klinische Anatomie*. 2nd ed. (Koolstra JH, Langenbach GEJ, eds.). Prelum uitgevers; 2013.

4.      Hacking C, Glick Y. Maxilla. *Radiopaedia.org*. Published online April 20, 2017. doi:10.53347/RID-52768

5.      Maxilla: Anatomy, function and clinical notes | Kenhub. Accessed February 7, 2023. https://www.kenhub.com/en/library/anatomy/the-maxilla

6.      Jones J, St-Amant M. Maxillary sinus. *Radiopaedia.org*. Published online October 22, 2013. doi:10.53347/RID-25379

7.      Hapugoda S, St-Amant M. Paranasal sinuses. *Radiopaedia.org*. Published online October 22, 2013. doi:10.53347/RID-25381

8.      Definition of maxillary sinus - NCI Dictionary of Cancer Terms - NCI. Accessed January 4, 2023. https://www.cancer.gov/publications/dictionaries/cancer-terms/def/maxillary-sinus

9.      Iwanaga J, Tubbs RS. *Atlas of Oral and Maxillofacial Anatomy*. Springer International Publishing; 2021. doi:10.1007/978-3-030-78327-3

10.     25 The oral cavity and related structures | Pocket Dentistry. Accessed October 4, 2023. https://pocketdentistry.com/25-the-oral-cavity-and-related-structures/

11.     The Anatomy and Structure of a Tooth - Tuxedo Dental Group. Accessed October 4, 2023. https://www.tuxedodental.ca/dental_library/the-anatomy-and-structure-of-a-tooth/

12.     Oral Cavity & Oropharyngeal Cancer Key Statistics 2021. Accessed January 5, 2023. https://www.cancer.org/cancer/oral-cavity-and-oropharyngeal-cancer/about/key-statistics.html

13.     Dubal PM, Bhojwani A, Patel TD, et al. Squamous cell carcinoma of the maxillary sinus: A population-based analysis. *Laryngoscope*. 2016;126(2):399-404. doi:10.1002/LARY.25601

14.     NKR Cijfers. Accessed October 6, 2023. https://iknl.nl/nkr-cijfers

15.     Dhull AK, Atri R, Dhankhar R, Chauhan AK, Kaushal V. Major Risk Factors in Head and Neck Cancer: A Retrospective Analysis of 12-Year Experiences. *World J Oncol*. 2018;9(3):80-84. doi:10.14740/wjon1104w

16.     Mehanna P, Smith G. Maxillary carcinoma: A wolf in sheep's clothing. *Canadian Family Physician*. 2009;55(3):262-264.

17.     Chi AC, Day TA, Neville BW. Oral cavity and oropharyngeal squamous cell carcinoma-an update. *CA Cancer J Clin*. 2015;65(5):401-421. doi:10.3322/CAAC.21293

18.     Paranasal sinus cancer - UpToDate. Accessed January 6, 2023. https://www.uptodate.com/contents/paranasal-sinus-cancer

19.     Incidentie hoofd-halskanker. Accessed October 4, 2023. https://iknl.nl/kankersoorten/hoofd-halskanker/registratie/incidentie

20.     Lacko M. Hoofd-hals kanker epidemiologie, etiologie, symptomatologie en diagnostiek. Published online 2015. https://oncologie.mumc.nl/sites/oncologie/files/2.epidemiologie.pdf

21.     Al-Jamaei AAH, van Dijk BAC, Helder MN, Forouzanfar T, Leemans CR, de Visscher JGAM. A population-based study of the epidemiology of oral squamous cell carcinoma in the Netherlands 1989–2018, with emphasis on young adults. *Int J Oral Maxillofac Surg*. 2022;51(1):18-26. doi:10.1016/J.IJOM.2021.03.006

22.     Startpagina - Hoofd-halstumoren - Richtlijn - Richtlijnendatabase. Accessed January 6, 2023. https://richtlijnendatabase.nl/richtlijn/hoofd-halstumoren/hoofd-halstumoren_-_korte_beschrijving.html

23.     Byrd JK, Clair JMS, El-Sayed I. AHNS Series: Do you know your guidelines? Principles for treatment of cancer of the paranasal sinuses: A review of the National Comprehensive Cancer Network guidelines. *Head Neck*. 2018;40(9):1889-1896. doi:10.1002/hed.25143

24.     Charles Catton. Princess Margaret Cancer Centre Clinical Practice Guidelines. *Princess Margaret Cancer Centre*.                         Published                         online                         2012:1-10. http://www.uhn.ca/PrincessMargaret/Health_Professionals/Programs_Departments/Gastrointestinal_GI/D ocuments/CPG_GI_PancreaticCancer.pdf

25.     Pittman AL, Zender CA. Total maxillectomy. *Oper Tech Otolayngol Head Neck Surg*. 2010;21(3):166-170. doi:10.1016/j.otot.2010.07.005

26.     Fagan J. Open Access Atlas of Otolaryngology , Head & Neck Operative Surgery. *Atlas of Otolaryngology , Head & Neck Operative Surgery*. 2008;(Figure 1):1-12. www.entdev.uct.ac.za

27.     Partial and Total Maxillectomy | Ento Key. Accessed January 10, 2023. https://entokey.com/partial-and-total-maxillectomy/

28.     Maxillectomy  |  Iowa  Head  and  Neck  Protocols.  Accessed  January  10,  2023. https://medicine.uiowa.edu/iowaprotocols/maxillectomy

29.     Helman JI. Maxillectomy. *Atlas of the Oral and Maxillofacial Surgery Clinics*. 1997;5(2):75-90. doi:10.1016/S1061-3315(18)30084-2

30.     Brown JS, Shaw RJ. Reconstruction of the maxilla and midface: Introducing a new classification. *Lancet Oncol*. 2010;11(10):1001-1008. doi:10.1016/S1470-2045(10)70113-3

31.     Pool C, Shokri T, Vincent A, Wang W, Kadakia S, Ducic Y. Special Topics in Palatal and Maxillary Reconstruction: Prosthetic Reconstruction of the Maxilla and Palate. *Semin Plast Surg*. 2020;34(2):114. doi:10.1055/S-0040-1709143

32.     Andrades P, Militsakh O, Hanasono MM, Rieger J, Rosenthal EL. Current Strategies in Reconstruction of Maxillectomy Defects. *Arch Otolaryngol Head Neck Surg*. 2011;137(8):806. doi:10.1001/ARCHOTO.2011.132

33.     Haribhakti V V. *Restoration, Reconstruction and Rehabilitation in Head and Neck Cancer*. Springer Singapore; 2019. doi:10.1007/978-981-13-2736-0

34.     Beumer III J, Marunick MT, Esposito SJ. *Maxillofacial Rehabilitation: Prosthodontic and Surgical Management of Cancer-Related, Acquired, and Congenital Defects of the Head and Neck*. Third Edit. Quintessence Publishing Co, Inc; 2011.

35.     Hanawa S, Kitaoka A, Koyama S, Sasaki K. Influence of maxillary obturator prostheses on facial morphology in   patients   with   unilateral   maxillary   defects.   *J   Prosthet   Dent*.   2015;113(1):62-70. doi:10.1016/J.PROSDENT.2014.06.016

36.     dos Santos DM, de Caxias FP, Bitencourt SB, Turcio KH, Pesqueira AA, Goiato MC. Oral rehabilitation of patients after maxillectomy. A systematic review. *British Journal of Oral and Maxillofacial Surgery*. 2018;56(4):256-266. doi:10.1016/j.bjoms.2018.03.001

37.     Corsalini M, Barile G, Catapano S, et al. Obturator prosthesis rehabilitation after maxillectomy: Functional and   aesthetical   analysis   in   25   patients.   *Int   J   Environ   Res   Public   Health*.   2021;18(23). doi:10.3390/ijerph182312524

38.     Miloro M, Ghali GE, Larsen PE, Waite P, eds. *Peterson's Principles of Oral and Maxillofacial Surgery*. Fourth Edition. Springer International Publishing; 2022. doi:10.1007/978-3-030-91920-7

39.     Keyf F. Review Obturator prostheses for hemimaxillectomy patients. doi:10.1111/j.1365-2842.2001.00754.x

40.     Rathee M, Bhoria M, Malik P. Prosthodontic Rehabilitatative Therapy through Surgical Obturator for Maxillectomy    Patients:    A    Review.    *Cancers    Review*.    2014;1(2):52-58. doi:10.18488/journal.95/2014.1.2/95.2.52.58

41.     Maxillary Prostheses | Iowa Head and Neck Protocols. Accessed January 11, 2023. https://medicine.uiowa.edu/iowaprotocols/maxillary-prostheses

42.     Carrau RL, Prosser JD, Solares AA, Panizza BJ. Maxillectomy. Published September 24, 2019. https://emedicine.medscape.com/article/1890955-overview?form=fpf

43.     Ooms A. Optimized and user-friendly workflow for the fabrication of 3D printed maxillary hollow closed surface model obturator using CT, intraoral scanning technology, and computer aided/manufacturing | Master Thesis. 2022;(October).

44.     Wu Y low, Schaaf NG. Comparison of weight reduction in different designs of solid and hollow obturator prostheses. *J Prosthet Dent*. 1989;62(2):214-217. doi:10.1016/0022-3913(89)90317-X

45.     Ikusika OF, Dosumu OO, Ajayi DM, Ogunrinde TJ. Effect of resilient lining of obturator bulbs on patients with maxillectomies.     *Journal       of       Prosthetic       Dentistry.*       2016;116(6):932-936.e1. doi:10.1016/j.prosdent.2016.04.011

46.     Tanaka Y, Gold H 0, Pruzansky S. *A Simplified Technique for Fabricating a Lightweight Obturator.*

47.     Parathasarathy N, Anusha K, Madhan Kumar S, Shanmuganathan N. Maxillary Defect Rehabilitation Using a Hollow Bulb Obturator. *Cureus*. Published online November 10, 2022. doi:10.7759/cureus.31326

48.     Patil PG, Patil SP. A hollow definitive obturator fabrication technique for management of partial maxillectomy. *J Adv Prosthodont*. 2012;4(4):248. doi:10.4047/JAP.2012.4.4.248

49.     Padmanabhan T V., Kumar VA, Mohamed KK, Unnikrishnan N. Prosthetic Rehabilitation of a Maxillectomy with a Two-Piece Hollow Bulb Obturator. A Clinical Report. *Journal of Prosthodontics*. 2011;20(5):397-401. doi:10.1111/j.1532-849X.2011.00712.x

50.     Arun Kumar VR, Jagdish SK, Prabhu K, Ramesh AS, Venkatesan N. Rehabilitation of maxillary defect by three different types of obturators – A case series. *Journal of Pierre Fauchard Academy (India Section)*. 2016;30(1):1-5. doi:10.1016/j.jpfa.2016.10.004

51.     Mazzola F, Smithers F, Cheng K, et al. Time and cost-analysis of virtual surgical planning for head and neck reconstruction: A matched pair analysis. *Oral Oncol*. 2020;100. doi:10.1016/j.oraloncology.2019.104491

52.     Callahan N, Moles SL, Markiewicz MR. The Use of a CAD/CAM Surgical Obturator Without Impressions to Restore    a    Maxillectomy    Defect.    *Craniomaxillofacial    Trauma    &    Reconstruction    Open*. 2021;6:247275122199297. doi:10.1177/2472751221992972

53.     Steenhuis A. *Fabrication Process of Maxillary Hollow Bulb Immediate Surgical Oburator Using Intraoral Scanning Technology and Computer Aided Design/Manufacturing*.; 2021.

# CHAPTER 2. TECHNICAL BACKGROUND

# Chapter 2.
# Technical background

This chapter provides technical background on techniques used during this year of research. The information will include principles of operation and specifics of equipment used in the NCI-AvL.

## Imaging techniques

Medical imaging is an indispensable tool for the diagnosis and treatment of various diseases. Among the commonly used imaging techniques are X-ray scans, Computed Tomography (CT) scans, Magnetic Resonance Imaging (MRI) scans, Ultrasound (US) and Positron Emission Tomography (PET). Each technique is based on different principles, resulting in different information provided by the scans. US is a non-invasive imaging technique that utilizes the impedance of tissue and reflection of sound waves to produce a real-time image of tissue. However, it cannot penetrate through bone or air, US has limited penetration depth, and the quality of images varies considerably based on the operator's skill. X-ray scans are a quick imaging method that utilizes radiation absorption in tissue to depict a 2D image. It is widely used to detect fractures, visualize dentition, or for inspection of the lungs and heart. However, X-ray is less effective in imaging soft tissues, and only shows a 2D projection image. MRI scans on the other provide a cross-sectional image with superior soft tissue detail, by using the spins of hydrogen nuclei and a magnetic field.

A CT scan can be considered a 3D version of an X-ray image, which combines X-ray images from different angles to create a cross-sectional image of bones and soft tissue. These greyscale images are based on the Hounsfield Units (HU) of the depicted tissue, which are directly related to the physical density of the tissue and the x-ray beam attenuation. Water has an HU value of 0, whereas air has an HU of -1000. Bone has a HU of approximately 1000-2000 based on its density. The zygomatic bone is very dense (approx. 2000 HU and much cortical bone), whereas the alveolar bone is less dense (approx. 1000 HU for the cortical bone).[1,2]

Because the bony anatomy is very important for a suspected maxillary tumour, patients who have a suspicion of cancer in the maxillary region get a CT scan in our centre. This CT scan is performed from the cranial roof to the lowest point of the mandible, with the following settings: Gantry angle 0°, FOV 220-250 (including tip of nose, auricles, and mastoid), slice thickness 1 mm, 135 kV, 400 mAs.

Moreover, CT scans offer an advantage over MRI scans for possible maxillectomy patients as the HU's of CT scans can be used for image segmentation. When the treatment plan involves a maxillectomy, a skull segmentation is made using thresholding from 200-250 HU and up, to include the cortical and trabecular bone and the possible dental fillings. Together with the surgeon, the planning for the resection is determined and separated from the original segmentation of the skull. Figure **2.1** shows a skull segmentation and the preoperative planned excision in red.
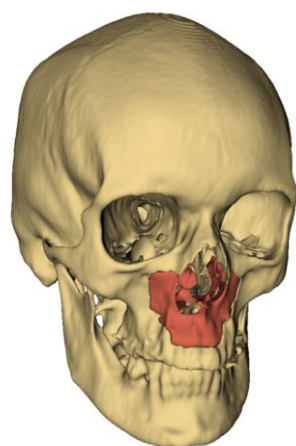


*Figure **2.1**. Image of a bone segmentation of a skull, based on HU thresholding of a head-and-neck CT scan. Red shows the preoperative planned excision.*

# Navigation

Surgical navigation plays a crucial role in maxillofacial surgery, serving as a valuable tool for surgeons.[3,4] The preoperative planning segmentation serves as a guide during maxillectomies, with the preoperative CT scan used to determine the intraoperative planning. To use this planning during surgery, the CT scan is modified by altering the voxels within the planned excision to -1000, causing them to appear black in the modified scan (see Figure **2.2**). This is referred to as the planning CT.



*Figure **2.2**. Axial slice of the navigation CT scan for intraoperative navigation. The voxels of the original CT scan of the patient within the preoperative maxillectomy planning are altered to -1000, showing black on the image. This is called the planning CT.*

During the surgery, a Medtronic stealthstation ENT Navigation system (Medtronic, ENT, Minneapolis, Minnesota, U.S. [5]) is used for intraoperative navigation. The planning CT is loaded into the system, and the position of the patient is matched to the CT scan using image-to-patient registration. The stealthstation navigation system operates on electromagnetic (EM) tracking, wherein the position of sensors is measured through an inhomogeneous magnetic field. This magnetic field is generated by a field generator (FG), which is placed near the surgery site. For maxillectomies, the Medtronic tabletop FG is placed under the patient's head.

Within this inhomogeneous field, magnetic sensors can determine their position and orientation. These sensors feature three orthogonally aligned coils, where the magnetic field induces a voltage. The system control unit then measures and amplifies these electric signals, determining the position and orientation of the sensors. [6–8]

Sensors can be defined based on their degrees of freedom (DOF), which describe the number of axes along which changes in the sensor's position can be detected. For instance, a 6DOF sensor detects translation in the x-, y-, and z-axis, as well as orientation in yaw, pitch and roll (see Figure **2.3**).
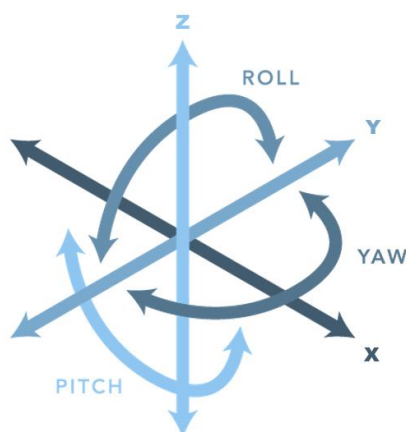


*Figure **2.3**. The six degrees of movement. The x-, y-, and x-axis define the translation of an object, whereas the yaw, pitch and roll define the orientation.*

## 3D-scanning

To obtain patient-specific dental and palatal anatomy, three-dimensional (3D) scanning can be used. At our centre, these 3D scans are made with a 3Shape (Copenhagen, Denmark) Trios 3 Intraoral scanner (see Figure **2.4**). This scanner created a 3D model using confocal microscopy. By focusing a light source and detection optics on the same spot, using a dichromatic mirror, thousands of images are captured and combined to produce an accurate 3D surface model.[9–13] This 3D scan will be called the intraoral scan (IOS) in this thesis. The Trios scanner has software to visualise the IOS and export it as an STL file for further processing.



*Figure **2.4**. The 3Shape (Copenhagen, Denmark) Trios 3 intraoral scanner.* [14]

## Registration

To ensure proper alignment of the bulb to the baseplate, the IOS must be registered to the skull segmentation from the CT scan. There are various registration methods, each utilizing different principles to transform datasets into the same coordinate system. One of these datasets is transformed towards the other set, by using a transformation model. For this study, fiducial registration is used, which creates a linear rigid transformation based on manually selected points that are identical in both scans, called fiducials. A linear rigid transformation applies only translation and rotation to create the transformation model, so the transformation is performed with 6DOF. No scaling or warping is performed with a linear rigid transformation. [15–17]

The registration error can be measured by the fiducial registration error (FRE), which calculates the root-mean-square (RMS) of the differences between matching fiducial pairs after registration.[18,19] An example of the FRE is shown in Figure **2.5**.
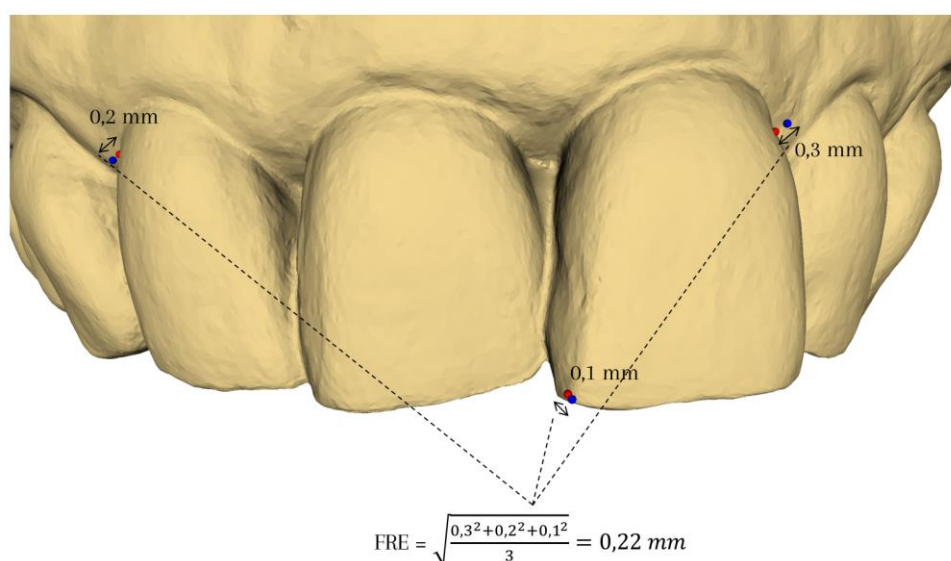


$$FRE = \sqrt{\frac{0,3^2 + 0,2^2 + 0,1^2}{3}} = 0,22 \ mm$$

*Figure **2.5**. An example of a fiducial registration error calculation, which is the root-mean-square of the distance of the paired fiducials.*

## CAD/CAM

Computer Aided Design (CAD) and Computer Aided Manufacturing (CAM) are two important technologies that involve the use of computers in designing and manufacturing. CAD software, such as AutoCAD and Solidworks, is used to create 2D and 3D models. Mesh-based models can also be digitally designed using software like 3Matic and Meshmixer, which construct the designs via a triangular polygon mesh consisting of many small triangles that form a 3D model. The Meshmixer object is represented as a face-vertex mesh, with a certain connectivity of the vertices. Figure **2.6** shows an example of a face-vertex mesh. These designs are then exported to a Stereolithography (STL) file, which is opened with CAM software to translate the 3D model into a job for the manufacturing machine.
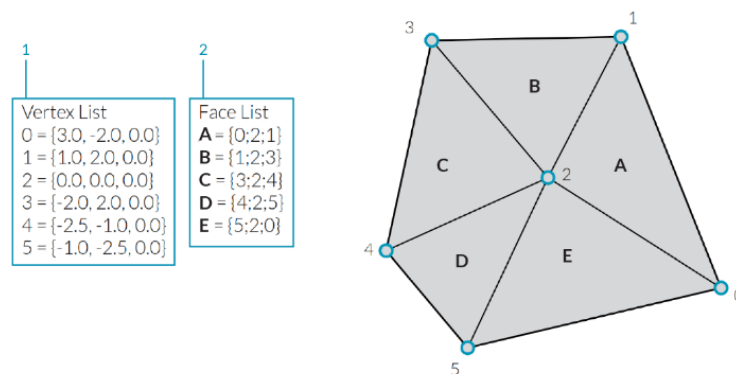


*Figure **2.6**. An example of a triangular polygon mesh, existing of faces (the grey surface indicated with a letter) and vertices (the blue dots, having an x- y- and z-axis location).*[20]

The use of CAD/CAM technology has seen a rise in head and neck oncologic surgery, particularly in virtual surgery planning and the development of patient-specific implants and prostheses.[21] In the maxillofacial prosthodontic field, 3D scanning and planning are commonly used.[22] During this research, the software Meshmixer (RRID:SCR_015736, ©2020 Autodesk, Inc.) is used for the design of the obturators and phantoms. These designs are then exported to Preform (Formlabs, Somerville, Massachusetts, U.S.), a CAM software that prepares the parts for 3D printing.

## 3D-printing

3D printing is a manufacturing method involving CAD/CAM software. There are various types of 3D-printing, such as selective laser sintering, fused deposit modelling and stereolithography (SLA). A Formlabs SLA 3D printer (Form 3B) is used for prototypes at the NKI-AvL. SLA printing is commonly known as resin 3D printing, and it involves using a laser or projector to cure the liquid thermoset resin into hardened plastic onto a platform, creating a 3D printed object (see Figure **2.7**). Supports are printed to secure the stability of the printed object, enabling complex shapes to be printed.
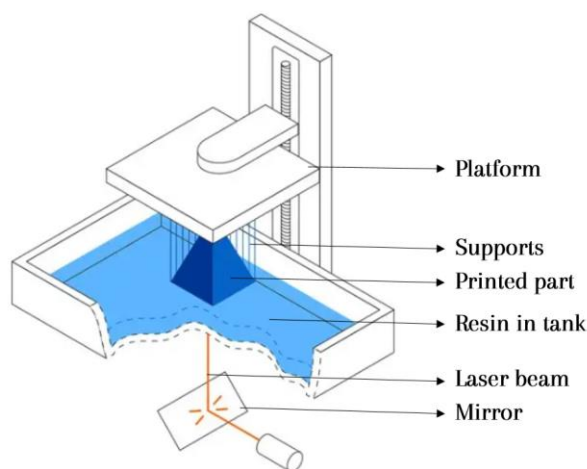


*Figure **2.7**. Schematic image of a Stereolithographic (SLA) 3D printer. A laser cures the thermoset resin into hard plastic on a platform to create the part.*[23]

Post-processing is a crucial step after 3D-printing. The object is washed in isopropyl alcohol to remove the liquid resin sticking to it. When the object is dry, it is post-cured in a chamber providing heat and UV radiation. This process finalizes the cross-linking of the polymer network, thereby improving the material properties of the polymer. The temperature and duration of the post-curing are specific to each type of resin.

During this research, Formlabs Clear Resin (V4) is used for the ISO, enabling vision on the surgery site when fitting the ISO. Clear resin is washed for 10 minutes, and post-processed for 15 minutes at a temperature of 60 degrees Celsius.[24] However, it is important to note that this resin is not biocompatible, and thus cannot be used when the 3D-printed ISO is clinically implemented. Due to the cost and availability of the biocompatible clear resin, non-biocompatible clear resin is used during this research.

# REFERENCES

1.  DenOtter TD, Schubert J. Hounsfield Unit. *Radiopaedia.org*. Published online March 6, 2023. doi:10.53347/rid-38181

2.  Computed Tomography (CT). Accessed October 5, 2023. https://www.nibib.nih.gov/science-education/science-topics/computed-tomography-ct

3.  Azarmehr I, Stokbro K, Bell RB, Thygesen T. Surgical Navigation: A Systematic Review of Indications, Treatments, and Outcomes in Oral and Maxillofacial Surgery. *Journal of Oral and Maxillofacial Surgery*. 2017;75(9):1987-2005. doi:10.1016/J.JOMS.2017.01.004

4.  Nijmeh AD, Goodger NM, Hawkes D, Edwards PJ, McGurk M. Image-guided navigation in oral and maxillofacial surgery. *Br J Oral Maxillofac Surg*. 2005;43(4):294-302. doi:10.1016/J.BJOMS.2004.11.018

5.  ENT Navigation System | Medtronic. Accessed October 5, 2023. https://www.medtronic.com/ca-en/healthcare-professionals/products/neurological/surgical-navigation-systems/stealthstation/ent-navigation.html

6.  Franz AM, Haidegger T, Birkfellner W, Cleary K, Peters TM, Maier-Hein L. Electromagnetic tracking in medicine -A review of technology, validation, and applications. *IEEE Trans Med Imaging*. 2014;33(8):1702-1725. doi:10.1109/TMI.2014.2321777

7.  van der Heijden F. Sensor systems for tracking - Surgical Navigation Technologies . *Lecture notes Surgical Navigation Technologies, Technical Medicine - Medical Imaging and Interventions*. Published online 2020.

8.  Electromagnetic Tracking Systems - NDI. Accessed October 6, 2023. https://www.ndigital.com/electromagnetic-tracking-technology/

9.  Mangano F, Gandolfi A, Luongo G, Logozzo S. Intraoral scanners in dentistry: a review of the current literature. *BMC Oral Health*. 2017;17(1):149. doi:10.1186/s12903-017-0442-x

10. Dental 3D Scanners & Software for CAD/CAM Dentistry | 3shape. Accessed October 6, 2023. https://www.3shape.com/en

11. Ting-shu S, Jian S. Intraoral Digital Impression Technique: A Review. *Journal of Prosthodontics*. 2015;24(4):313-321. doi:10.1111/jopr.12218

12. 3Shape. European Patent Specification EP 2822444B1. *2013*.

13. Elliott AD. Confocal Microscopy: Principles and Modern Practices. *Curr Protoc Cytom*. 2020;92(1):e68. doi:10.1002/CPCY.68

14. The 3Shape TRIOS® Intraoral Scanner. Accessed October 6, 2023. https://alphaplusdentalcenter.com/the-3shape-trios-intraoral-scanner/

15. Registration — 3D Slicer documentation. Accessed October 6, 2023. https://slicer.readthedocs.io/en/latest/user_guide/registration.html

16. Saiti E, Theoharis T. An application independent review of multimodal 3D registration methods. *Computers and Graphics (Pergamon)*. 2020;91:153-178. doi:10.1016/j.cag.2020.07.012

17. Fiducial Registration — 3D Slicer documentation. Accessed October 8, 2023. https://slicer.readthedocs.io/en/latest/user_guide/modules/fiducialregistration.html#panels-and-their-use

18. Seginer A. Rigid-body point-based registration: The distribution of the target registration error when the fiducial registration errors are given. *Med Image Anal*. 2011;15(4):397-413. doi:10.1016/J.MEDIA.2011.01.001

19. Chen ECS, Lasso A, Fichtinger G. External tracking devices and tracked tool calibration. In: *Handbook of Medical Image Computing and Computer Assisted Intervention*. Elsevier; 2019:777-794. doi:10.1016/B978-0-12-816176-0.00036-3

20. What is a Mesh? | The Grasshopper Primer (EN). Accessed October 30, 2023. http://grasshopperprimer.com/en/1-foundations/1-6/1_What%20is%20a%20Mesh.html

21.    Nyirjesy SC, Heller M, von Windheim N, et al. The role of computer aided design/computer assisted manufacturing (CAD/CAM) and 3- dimensional printing in head and neck oncologic surgery: A review and future directions. *Oral Oncol.* 2022;132. doi:10.1016/j.oraloncology.2022.105976

22.    Cristache CM, Tudor I, Moraru L, Cristache G, Lanza A, Burlibasa M. Digital workflow in maxillofacial prosthodontics—an update on defect data acquisition, editing and design using open-source and commercial available software. *Applied Sciences (Switzerland)*. 2021;11(3):1-19. doi:10.3390/app11030973

23.    Guide to Stereolithography (SLA) 3D Printing | Formlabs. Accessed October 27, 2023. https://formlabs.com/eu/blog/ultimate-guide-to-stereolithography-sla-3d-printing/

24.    Form Cure time and temperature settings. Accessed October 17, 2023. https://support.formlabs.com/s/article/Form-Cure-Time-and-Temperature-Settings?language=en_US

# CHAPTER 3. THE NKI CLASSIFICATION: A NOVEL CLASSIFICATION SYSTEM FOR THE PREOPERATIVE PLANNING AND DESIGN OF IMMEDIATE SURGICAL OBTURATORS IN PATIENTS UNDERGOING MAXILLECTOMY.

# Chapter 3.

# The NKI Classification: A novel classification system for the preoperative planning and design of Immediate Surgical Obturators in patients undergoing maxillectomy

## ABSTRACT

Maxillectomy, a surgical procedure involving the marginal or segmental removal of the maxilla, presents complex challenges in functional and aesthetic rehabilitation. Obturators, designed to close oronasal communication and restore speech, swallowing, and facial aesthetics during the first healing phase, offer an effective solution for patients. While various classification systems exist for maxillectomy resections, there is no classification system enabling communication and guidelines for the design of the obturator. This article introduces a novel classification system for preoperative obturator planning and design in maxillectomy patients. Six different obturator designs were tested intraoperatively to establish design principles for each class. The resulting classification system consists of seven classes, each with its specific design principles. A validation dataset of 17 patients confirmed the classification system's usefulness in obtaining accurate and customized obturator designs. The system's implementation allows for streamlined fabrication processes, improved obturator design accuracy, and enhanced patient outcomes.

## Introduction

Maxillectomy, a surgical procedure involving the removal of (part of the) the maxilla, presents complex challenges for functional and aesthetic rehabilitation in patients[1,2]. Various classification systems have been developed to categorize maxillectomy resections, providing some guidance for surgical planning and reconstruction options.[1,3–6] These existing classification systems primarily focus on the extent and location of the maxillary resection, providing a framework for decision-making regarding reconstructive techniques.

During maxillectomy procedures, surgeons have two primary options for restoration: reconstruction or the use of an obturator [1,7,8]. While reconstructive techniques are the best option for some patients, surgical obturators have emerged as an effective solution for functional and aesthetic rehabilitation for many patients. Immediate surgical obturators are designed to close the oronasal communication and restore speech, swallowing, and facial aesthetics during the first healing phase.[2,9,10] However, the specific design and classification of obturators have received relatively less attention compared to the extensive classifications available for reconstructive options.

With the advancement of preoperative planning and design techniques, particularly the integration of Computer-Aided Design and Computer-Aided Manufacturing (CAD/CAM) technology, there is a growing need for a comprehensive classification system specifically addressing the preoperative design of obturators. The design of the obturator bulb i.e. that fills the defect, which determines its size, shape, and contour, plays a crucial role in achieving optimal results[10]. A classification system focusing on the obturator design can provide a standardized framework for communication and anticipation of obturator requirements preoperatively.

This article aims to introduce a novel classification system for the preoperative planning and design of obturators in patients undergoing maxillectomy. The integration of this novel classification system into the preoperative planning process can enable clinicians, prosthodontists, and surgeons to anticipate and communicate the specific design requirements of obturators. This can streamline the fabrication process, improve the accuracy of obturator design, enable communication between professionals about the obturator and ultimately enhance patient outcomes.

## Materials and methods

<u>Study Design</u>

The obturator design consists of two parts: the baseplate and the bulb, which obturates the defect. This study aimed to develop and validate a classification system for the design of standardised CAD/CAM bulb shapes. Six different strategies for the design of the bulb are intraoperatively tested to establish principles of obturator design. The classification system is validated on a retrospective dataset.

<u>Designing, printing and fitting Process</u>

All designed bulb shapes are based on the resection that is planned prior to the OR on a segmentation of the CT scan and the intraoral scan (IOS). The IOS is made with 3Shape Trios (Copenhagen, Denmark), and loaded into Meshmixer (Autodesk, San Francisco, California, U.S.). The patient CT scan is loaded into 3D Slicer (Slicer 5.2.1 software, Surgical Planning Lab, Harvard Medical School, Harvard University, Boston, USA) to create a segmentation and plan the resection. To ensure the planned resection complies with the actual per-operative resection, a Medtronic StealthStation (Minneapolis, Minnesota, US) Surgical Navigation Tower is used.

For each patient, the resection is planned and six different bulb shapes are preoperatively designed: The first shape is a hollow dome design, existing of a sphere that is manually shaped around the segmented bone resection. The second bulb shape is based on a 3D optical scan of the obturator of a patient who had a resection in the same region, scaled to the defect. The third bulb shape is based on two different segmentations: the bone resection and the soft tissue resection. A surface model is automatically created around the outer surface points of the segmentations, also called a closed surface model (CSM). Figure **3.1** shows the design step for creating the CSM, and shows different segmentations. For the third bulb shape, a CSM around the bone resection and a CSM around the soft tissue resection will be created separately and combined, and then scaled to 0.8 for a layer of tissue conditioner around the bulb. The fourth bulb shape is based on the CSM merely around the segmentation of the bone resection, which is also scaled to 0.8. The fifth bulb shape was created by shaping the CSM around manually selected points around the buccal fat pad, taking into account not blocking the lower jaw from closing. The sixth and last bulb shape is based on the segmentation of the bone resection and soft tissue resection combined. A CSM is created around the combined segmentation, and scaled to 0.8. The different order of steps between this bulb and the third bulb shape results in a different shape. Figure **3.2** shows the six bulb shapes craniocaudally.
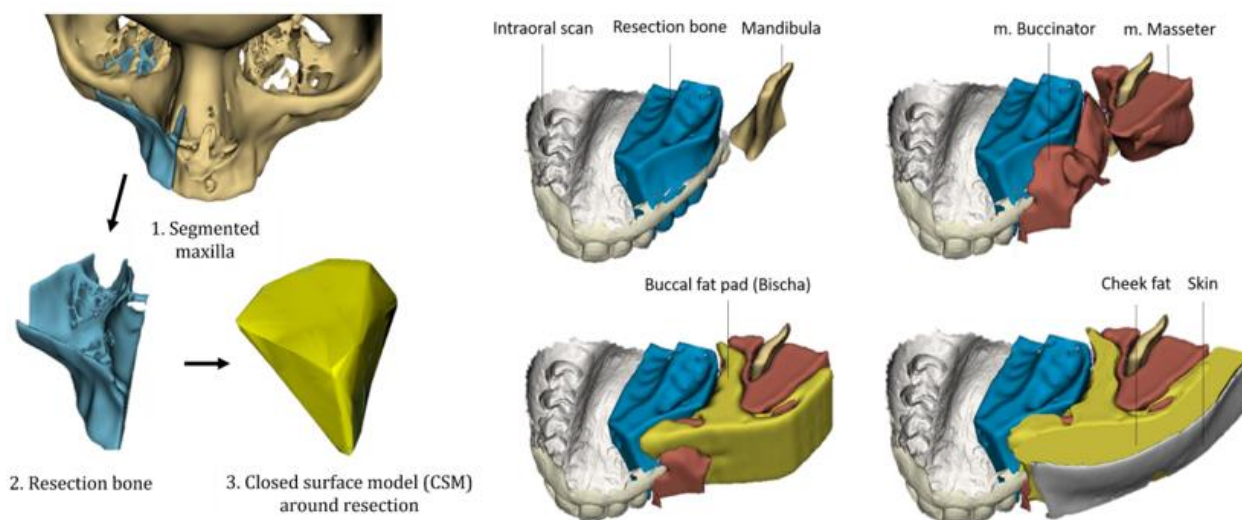


*Figure **3.1**. shows the bone segmentation and its closed surface model (CSM) on the left. On the right, different segmentations are shown, such as the bone resection, m. buccinator and m. masseter resection, the bischa resection and the cheek fat. A CSM can be designed around all different resections, combined or apart and later combined.*
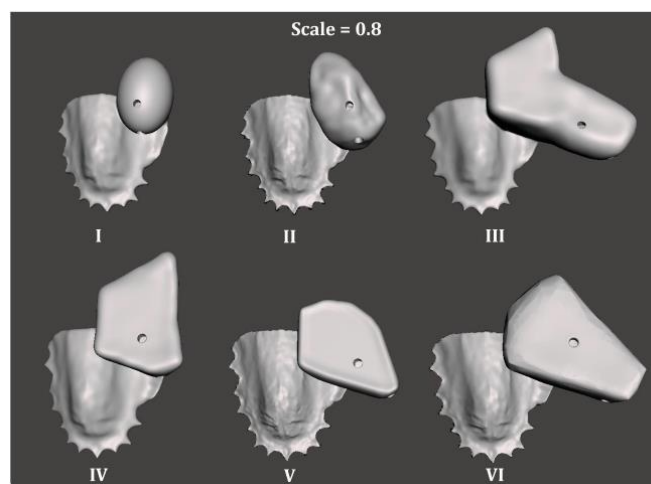
*Figure **3.2**. Six different patient-specific obturator designs that are intraoperatively fitted.*

The designed obturators are printed with Clear V4 in a Formlabs SLA printer (Form 3B, Somerville, Massachusetts, U.S.) and post-processed as intended. During the OR, the maxillectomy is performed according to the 3D pre-operative planning and confirmed by EM navigation intra-operatively and the 3D printed obturators are individually fitted into the resection. However, it is crucial to emphasize that these obturators were not used for treatment; they were solely utilized to derive the design principles for each class of the classification system.

Evaluation of Bulb Shapes and Classification System Creation

During the intraoperative placement, the clinical fit is examined. The following parameters were important to describe the clinical fit of the obturator: 1) the bulb has to fit in the defect; 2) the bulb does not block occlusion; 3) the defect gives enough counter pressure to the surrounding wound tissue; 4) the cheek or lip shape is aesthetically acceptable; 5) the obturator can be inserted and removed with the (sometimes limited) mouth opening of the patient; and 6) general expert opinion of the maxillofacial prosthodontist.

Based on the results of the fitting process, a classification system for obturator design was empirically created. The different defects encountered during oral surgeries were categorized into distinct classes within the classification system, based on differences of optimal bulb shape per defect. For each class, specific design principles were identified, documented, and associated with the corresponding defect. These design principles formed the basis for creating obturators that effectively addressed each class of defects.

Classification System Validation Dataset

To evaluate the performance of the classification system, a dataset was compiled including patients who underwent a maxillectomy between 2009 – and 2020 in the NKI-AvL hospital. The inclusion criteria included that both a pre- and postoperative CT scan were available for each patient. In addition, the conventional bulb could be distinguished in grayscale and therefore segmented from the postoperative CT scan. This inclusion left 17 patients who were enrolled in the dataset. This dataset is used for the validation, the data is not used to develop the classification system.

Data Collection and Analysis

For each patient in the validation dataset, their resection was assigned to the corresponding class of the classification system. Their conventional bulb was segmented and a new bulb was designed according to the described process and scaled, both with the use of 3D Slicer. It is important to mention that the design of the new bulb was done in a blinded fashion, without knowledge of the conventional bulb shape. The shape comparison between the conventional obturator and the new design according to the classification system was also assessed in 3D Slicer by one of the most used overlap-based segmentation metrics: the Hausdorff Distance (HD). The HD calculates the largest distance (d) between point set X (newly designed obturator) to Y (conventional obturator) as schematically visualized in Figure **3.3**. Furthermore, the maximum HD without outliers is calculated, called the 95th percentile (95%) HD. In addition, the average HD was calculated, including outliers. To validate the classification system, the newly designed obturator must have a small HD with the conventional obturator.

The CAD/CAM-designed bulb must fit into the conventional bulb, to ensure that it can fit into the resection. Therefore, the Dice Similarity Coefficient (DSC) is evaluated. The DSC measures the similarity between two sets of binary data, with values between 0 and 1, where 0 indicates no overlap, and 1 represents a perfect overlap. The first binary set is the CSM, and the second is the Boolean Intersection of the CSM and the Conventional bulb, resulting in a segmentation of the CSM, which is inside the conventional bulb. This is schematically shown in Figure **3.3**. The DSC of those two binary sets gives the percentage of the CSM that fits into the conventional bulb. The DSC is determined in 3D Slicer.
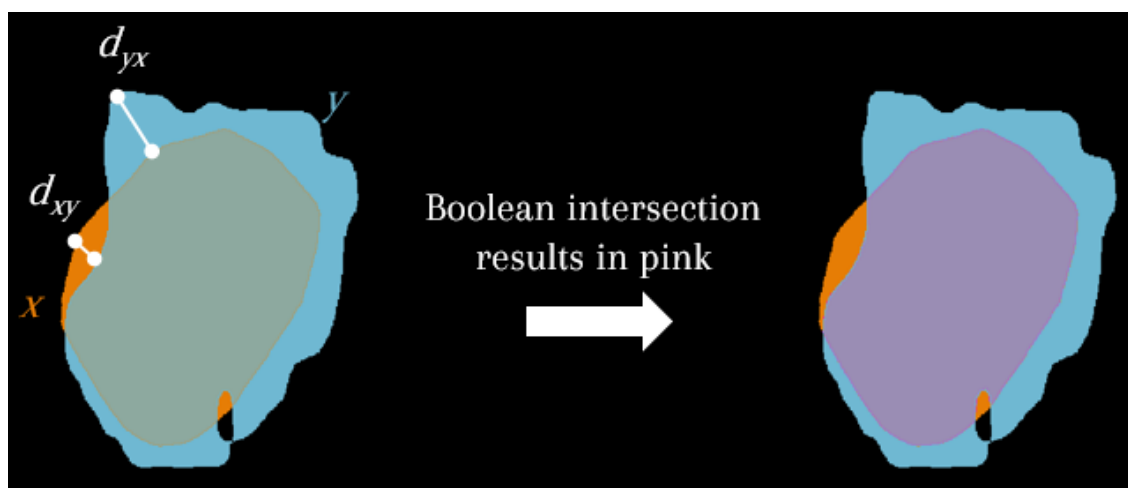


*Figure **3.3**. On the left, a schematic overview of distances between two obturator bulbs is shown. Blue represents the conventional bulb, and orange represents the CAD/CAM bulb. $D_{xy}$ and $d_{yx}$ represent distances between the two bulbs, the Hausdorff distance is the biggest distance. On the right image, the pink represents the result of the Boolean intersection. When the Dice Score Coefficient is determined between the pink and the orange bulb, the result tells which percentage of the CAD/CAM bulb fits inside the conventional bulb.*

## Results

<u>Classification System</u>

The case studies resulted in the identification of two important factors affecting the bulb shape: the involvement of the canine tooth, the height of the resection, and the involvement of the anterior nasal spina. When the resection includes the canine, the lip needs to be supported; therefore, the m. buccinator segmentation should be taken into account for the CSM design. The zygomatic arch and process are the support of the cheek and are important for the facial structure. When the resection involves the zygomatic process of the maxilla, the obturator should extend to cover this defect and provide support. Therefore, the CSM must extend from the alveolar process to the zygomatic process in a direct plane, or with a slight curve outward. When the resection involves the anterior nasal spina, the support of the nose is removed. The bulb design should replace the support of the spina to prevent the nose from sagging. It is also important to provide pressure from within the lip, to prevent the scar tissue from contracting and change the shape of the lip in a later stage.

The outcomes described above result in the following classification system, which consists of seven distinct classes, each with its own set of design principles. Figure **3.5** illustrates the classification system. The classification system takes into consideration the height of the defect, ranging from the alveolar bone to the orbital floor.
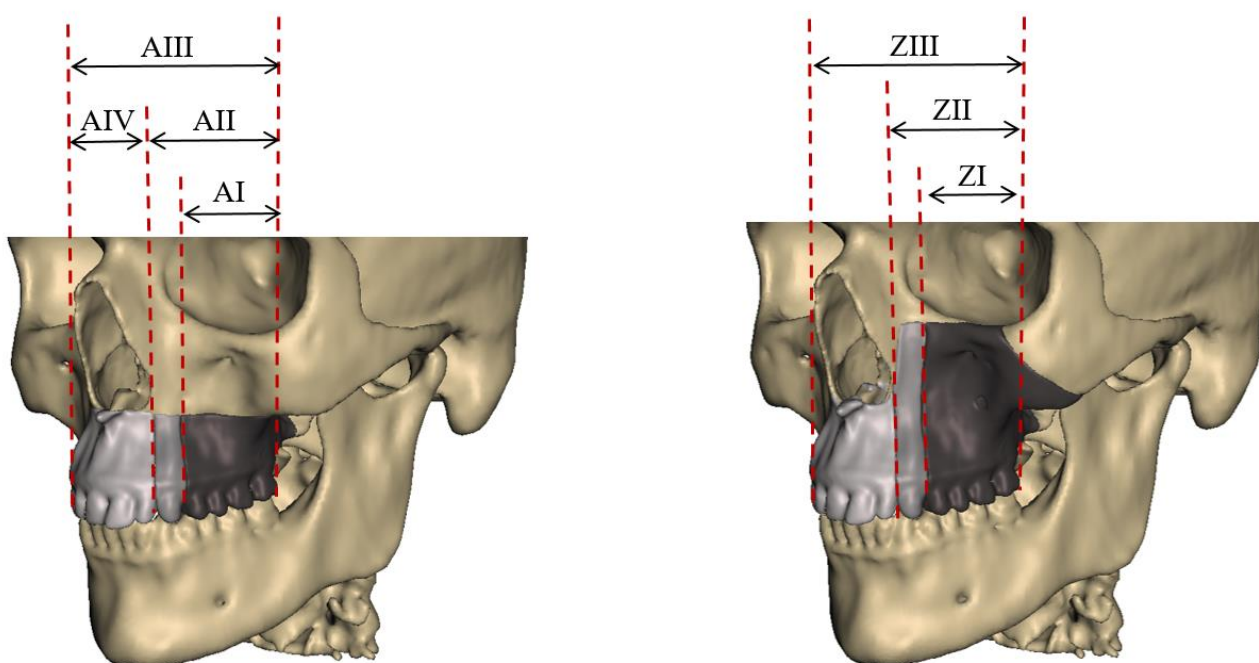


*Figure **3.5**. Classification system for the design principles immediate surgical obturators based post-operative resections after maxillectomy. The left image shows maxillectomy resection not extending the alveolar maxilla (A). The right image shows maxillectomy resections to the height of the zygomatic process (Z). I represents a resection including (pre)molars, II represents a resection including (pre)molars and the canine, III represents a resection including (pre)molars, the canine and the incisors, and IV represents a resection of the incisors.*

<u>Design Principles</u>

Each class within the classification system is associated with specific design principles that guide the fabrication of the obturator bulb. The design principles address the unique requirements of the bulb design for each class, ensuring optimal fit, functional restoration and optimal aesthetics. Table **3.1** summarizes the design principles for each class, highlighting the key considerations and recommendations for obturator design. The design principles associated with the classification system provide guidance for fabricating obturators tailored to specific defect characteristics.

Table **3.1** Design principles for the NKI – obturator classification system

| Alveolar class | |
|---|---|
| Class A1 | Maxilla resection involves the (pre)molars and is limited to the alveolar bone. The ISO remains narrow, slightly exceeding the bony resection margins. Therefore, only the resection bone is considered in the ISO design. The height of the ISO is limited to the vertical resection margin. |
| Class A2 | Maxilla resection involves (pre)molars and the canine. The height is limited to the alveolar bone. Because the canine is involved, the bulb should provide pressure to the surrounding soft tissue of the cheek and lip. This results in a wide-shaped ISO exceeding the lateral bony resection margins. Therefore, both the resected bone as the m. buccinator are considered in the ISO design. The height of the ISO is limited to the vertical resection margin. |
| Class A3 | Maxilla resection involves the anterior and lateral alveolar bone, including all teeth from the molars to the incisors. This ISO design is a combination of A2 and A4, taking the m. buccinator and nasal spina into account. |
| Class A4 | Maxilla resection involves the incisors and the canine. It is limited to the anterior alveolar bone. The ISO should support the nose due to the removal of the anterior nasal spina. The bony resection is taken into account for the CSM, which should extend to the spina for support. The maximal height is limited to the upper bound of the nasal spina. |
| Zygomatic class | |
| Class Z1 | Maxilla resection involves both the alveolar bone and zygomatic process and (pre)molars. The ISO is narrow and tall, slightly exceeding the contours of the bony resection. Therefore, only the resection bone including the zygomatic process is considered in the ISO design. The bulb extends from the alveolar process to the zygomatic process in a direct plane. The height is limited to the vertical resection with its maximum reach until the orbital floor. |
| Class Z2 | Maxilla resection involves the alveolar bone and zygomatic process, (pre)molars, and canine. The involvement of the canine and the zygomatic process results in a tall and wide ISO, extensively supporting the cheeks. Therefore, the bulb extends from the alveolar process to the zygomatic process in a direct plane. The height is limited to the vertical resection with its maximum reach until the orbital floor. |
| Class Z3 | Maxilla resection involves the anterior- and lateral alveolar bone, the zygomatic process, and all teeth from the molars to the incisors. This ISO design is a combination of A4 and Z2. |

Validation of the Classification System

To validate the effectiveness and reliability of the classification system and design principles, a validation dataset as described in the method section was utilized. This dataset consisted of 17 patients with diverse defects. The validation dataset was independent of the data used to develop the classification system.

For each obturator case in the validation dataset, the classification system assigned a specific class based on the corresponding defect characteristics. The assigned class indicated the appropriate design principles for the given defect. This design is compared to the shape of the conventional obturator, the HD and DSC are calculated as the outcome and shown in Table **3.2**.

Table **3.2**: Hausdorff distances (HD), presenting minimum, maximum, mean (μ) values and standard deviation (σ), and Dice Score Coefficient (DSC) of the conventional bulb versus the Boolean intersection of the conventional bulb and the CAD/CAM bulb.

| Patient No. | NKI – class | Tumor site | Bulb shape | HD max (mm) | HD average (mm) | HD 95th percentile (mm) | DSC |
|---|---|---|---|---|---|---|---|
| 1 | Z1 | Left | IV | 3.15 | 0.07 | 0.68 | 0.991 |
| 2 | Z3 | Left | VI | 15.9 | 1.59 | 9.92 | 0.886 |
| 3 | A1 | Left | IV | 6.20 | 0.43 | 3.00 | 0.954 |
| 4 | Z2 | Right | VI | 20.84 | 6.57 | 13.18 | 0.819 |
| 5 | Z3 | Left | IV | 8.01 | 0.71 | 3.62 | 0.899 |
| 6 | Z3 | Left | IV | 14.79 | 1.77 | 8.26 | 0.857 |
| 7 | A1 | Right | IV | 4.88 | 0.41 | 2.79 | 0.956 |
| 8 | Z2 | Right | IV | 10.37 | 0.34 | 2.88 | 0.981 |
| 9 | Z2 | Left | IV | 5.42 | 0.25 | 1.86 | 0.974 |
| 10 | Z3 | Left | IV | 6.07 | 0.47 | 3.65 | 0.950 |
| 11 | A3 | Right | IV | 10.77 | 0.23 | 1.77 | 0.972 |
| 12 | Z3 | Right | VI | 16.15 | 1.89 | 9.83 | 0.801 |
| 13 | Z3 | Right | VI | 12.00 | 0.88 | 5.12 | 0.939 |
| 14 | Z3 | Left | IV | 9.25 | 1.09 | 5.61 | 0.910 |
| 15 | A3 | Right | VI | 16.59 | 5.08 | 10.72 | 0.959 |
| 16 | Z3 | Left | IV | 10.35 | 0.64 | 5.05 | 0.934 |
| Minimum | - | - | - | 3.15 | 0.07 | 0.68 | 0.819 |
| Maximum | - | - | - | 20.84 | 1.8 | 8.7 | 0.991 |
| μ±σ | - | - | - | 9.99 ± 4.26 | 1.06 ± 1.21 | 4.89 ± 3.13 | 0.924 ± 0.056 |

## Discussion

The present study aimed to investigate the fitting of bulb shapes for different classes of patients based on bone and soft-tissue segmentation. Prior to the tests, for classes A2, A3, Z2, and Z3, the bone-and-soft-tissue CSM (III or VI) was expected to fit best. The results revealed that bulb shape IV, based only on bony resection, provided the best overall fit for all classes. In addition, bulb shape VI was a good fit for classes A3, Z2, and Z3, which is consistent with the design principles of these classes. Furthermore, it was observed that manual adaptation of the bulbs according to the design principles is crucial, and can be done digitally. However, if shape IV is chosen, the bulb can be intraoperatively extended with tissue conditioner.

The study also revealed significant differences between the maximum HD and the 95% HD, which may be due to the resolution of the segmentations. Although there is no cut-off value for the HD, a lower HD average signifies greater similarity in shape. The DSC was used to evaluate the similarity in shape. The average DSC for all patients was found to be 0.924 with a low standard deviation, which is considered reasonable. However, values below 90% were observed for half of the Z2 and Z3 class bulbs, mainly for bulb VI. Therefore, it can be concluded that the complete soft-tissue-and-bone CSM overestimates the shape, while the use of only bone segmentation tends to underestimate it.

Future research should focus on developing an optimal segmentation method to create the CSM according to the design principles. In the meantime, bone segmentation can be used for all classes, with manual adjustments based on the design principles.

To our best knowledge, there is no classification system providing a framework for (digital) bulb design. Hazra et al.[11] also mentioned this gap and proposed a prosthetically driven classification system from the prosthodontist's standpoint. This classification system focuses on retention options and implant placement, rather than the bulb shape.

The development and validation of the classification system for obturator design represent an advancement in the field of obturators for maxillectomy defects. This classification system provides a framework for effectively addressing various maxillectomy defects, allowing guidelines for customized obturator designs that enhance patient comfort and oral function. However, it is important to acknowledge certain limitations and considerations that should be taken into account when interpreting the validity of this system.

The validation dataset consisted of 17 patients, which did not cover all classes equally. Especially class A1, A2 and Z3 are underrepresented in the dataset and should be further validated. Future studies should aim to expand the dataset to include a larger and more diverse patient population to further validate and refine the design principles per class.

Furthermore, it is essential to highlight that the classification system has undergone validation using a retrospective approach with a validation dataset. While the validation process provides valuable insights into the system's performance and reliability, it falls short of prospective implementation in real-time clinical settings. Prospective studies involving a larger sample size and longer-term follow-up are necessary to evaluate the system's performance and validate its efficacy.

On the other hand, it is worth mentioning that within our centre, the classification system has been tested in practice on 4 occasions, yielding promising results. These initial experiences demonstrate the potential benefits and feasibility of implementing the system in clinical settings. The system has provided valuable guidance for CAD/CAM of immediate surgical obturators in our centre. However, it is important to acknowledge that these limited experiences within a single centre cannot substitute for comprehensive validation through larger-scale prospective studies involving multiple centres and diverse patient populations.

## Conclusions

In conclusion, the classification system can enable experts to communicate about maxillectomy defects and the design of the corresponding obturator. Surgeons and maxillofacial prosthodontists can more easily align their expectations pre- and peroperatively. With CAD/CAM, also for obturators, it is important to gain communicative frameworks to consult about the optimal patient-specific obturator, within but also between institutions. The design of obturators is still one like craftsmanship, but with a tool for communication, knowledge sharing between institutions can be enhanced. This way, the fabrication process can be streamlined, the accuracy of obturator design can be improved and ultimately patient outcomes can be enhanced.

## REFERENCES

1.    dos Santos DM, de Caxias FP, Bitencourt SB, Turcio KH, Pesqueira AA, Goiato MC. Oral rehabilitation of patients after maxillectomy. A systematic review. *British Journal of Oral and Maxillofacial Surgery*. 2018;56(4):256-266. doi:10.1016/j.bjoms.2018.03.001

2.    Beumer III J, Marunick MT, Esposito SJ. *Maxillofacial Rehabilitation: Prosthodontic and Surgical Management of Cancer-Related, Acquired, and Congenital Defects of the Head and Neck*. Third Edit. Quintessence Publishing Co, Inc; 2011.

3.    Brown JS, Shaw RJ. Reconstruction of the maxilla and midface: Introducing a new classification. *Lancet Oncol*. 2010;11(10):1001-1008. doi:10.1016/S1470-2045(10)70113-3

4.    Okay DJ, Genden E, Buchbinder D, Urken M. Prosthodontic guidelines for surgical reconstruction of the maxilla: A classification system of defects. *J Prosthet Dent*. 2001;86(4):352-363.

5.    Boucher LJ, Aramany MA. MAXILLOFACIAL PROSTHETICS Basic principles of obturator design for partially edentulous patients. Part I: Classification.

6.    Cordeiro PG, Santamaria EN, York NY. *A Classification System and Algorithm for Reconstruction of Maxillectomy and Midfacial Defects*.

7.    Breeze J, Rennie A, Morrison A, et al. Health-related quality of life after maxillectomy: obturator rehabilitation compared with flap reconstruction. *British Journal of Oral and Maxillofacial Surgery*. 2016;54:857-862. doi:10.1016/j.bjoms.2016.05.024

8.    Andrades P, Militsakh O, Hanasono MM, Rieger J, Rosenthal EL. Current Strategies in Reconstruction of Maxillectomy Defects. *Arch Otolaryngol Head Neck Surg*. 2011;137(8):806. doi:10.1001/ARCHOTO.2011.132

9.    Keyf F. Review Obturator prostheses for hemimaxillectomy patients. doi:10.1111/j.1365-2842.2001.00754.x

10.    Haribhakti V V. *Restoration, Reconstruction and Rehabilitation in Head and Neck Cancer*. Springer Singapore; 2019. doi:10.1007/978-981-13-2736-0

11.    Hazra R, Srivastava A, Kumar D. Obturators: A proposed classification and its associated techniques. *J Indian Prosthodont Soc*. 2023;23(2):192-197. doi:10.4103/jips.jips_313_22

# CHAPTER 4. WORKFLOW FOR THE DESIGN OF CLASP RETENTION FOR CAD/CAM IMMEDIATE SURGICAL OBTURATORS.

# Chapter 4.
# Workflow for the design of clasp retention for CAD/CAM immediate surgical obturators

## *Introduction*

An obturator is a commonly used reconstruction option for patients who have undergone maxillectomy. The primary challenge with the obturator is inadequate retention of the prosthesis.[1–3] To enhance retention, a more lightweight prosthesis can be designed.[2,4,5] A way to achieve this is by designing a hollow bulb, which can reduce the obturator's weight by 7-47%.[6–8] Various methods can be used to create a hollow bulb obturator, including the use of a CAD/CAM workflow for the hollow Immediate Surgical Obturator (hISO), which is currently being explored at our centre.[8,9] In this workflow, the bulb of the hISO is designed based on preoperative planning using the CT scan of the patient. The bulb is created around the planned resection, scaled to 0.8 to enable space for tissue conditioner, and made hollow. The baseplate is designed using a 3D-Intra Oral Scan (IOS) of the patient. The bulb and baseplate are connected using handpicked fiducial registration to create the hISO, which is then 3D-printed before the maxillectomy. However, this workflow is not yet suitable for clinical application due to the lack of retention on the 3D-printed obturator.

For conventional obturators, Adams clasps are widely used to provide retention, together with a boulder and zygomatic wire combination or a palatal screw. These Adams clasps are metal wires that are bent to create two arrowheads, fitting around the mesiobuccal and distobuccal undercuts of the teeth.[10] Retention is provided by engaging with these undercuts. The undercut is defined as "the portion of the surface of an object that is below the height of contour in relationship to the path of placement".[11] A surveyor (see Figure **4.1**) is used on a plaster cast of the patient's teeth and hard palate to determine where the undercut is located. First, the height of contour is determined on the cast, delineating the biggest circumference for a certain alignment of the cast, shown as the orange line in Figure **4.2**. The area under this line is the undercut of the tooth (see Figure **4.2**). When the clasps are located in the non-undercut area, they provide no retention.
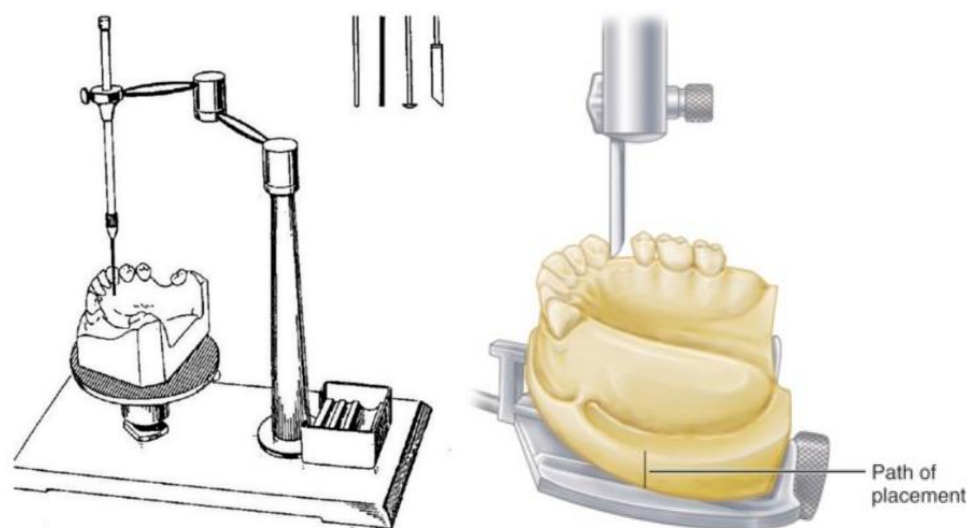


*Figure **4.1**. Examples of dental surveyors. A dental cast is put in a surveyor, to observe the optimal path of placement and determine the undercuts of the teeth.[12,13]*

*Figure **4.2**. A survey line is shown in orange, delineating the biggest circumference of the tooth from one path. Beneath this line, the undercut of the tooth is located, where retentive arms should be located to provide retention.* [14]

The metal wires are positioned on the plaster cast made from the teeth and hard palate, located around the remaining or available teeth needed for retention. Guidelines on the placement of the clasps are described by Aramany et al.[15] The wires are bent over the occlusal embrasure and are called the minor connectors (see Figure **4.3**), leaving the ends of the metal wire on the palate, creating retentive tags (see Figure **4.3**). These retentive tags are encapsulated in the acrylic baseplate that is pressed over this cast to fixate the Adams clasp into the baseplate.

For a 3D-printed hISO, it is not possible to encapsulate these retentive tags after or during 3D-printing, because the hISO goes from a liquid resin to a solid object. Therefore, another method must be developed to create retention options for the 3D-printed hISO. This study aims to develop a workflow for the design of 3D-printed retention clasps, which can be added to the CAD/CAM workflow for hISOs.



*Figure **4.3**. On the left, the location of the occlusal embrasure is shown with the yellow v, being the opening between the two curved proximal surfaces of adjacent posterior teeth.* [16] *The right image shows a completed Adams clasp on a plaster cast. The retentive tags are encapsulated in the acrylic baseplate that is pressed over the cast, to fixate the Adams clasp into the baseplate. The minor connectors are also shown in the image, going from the buccal undercut over the occlusal embrasure.* [10]

## Method

To create 3D-printed retention clasps, design criteria are set up with the expertise and proficiency of a maxillofacial prosthodontist from our centre and a dental technician specialized in the design of (Adams) clasps and other retention methods for dental prostheses. With their knowledge, a starting prototype for the retention clasps is designed using the design criteria as a guideline for the workflow (see Figure **4.4**). The workflow and the design are iteratively tested on 3D-printed dental models and on patients during surgery. During this process, the workflow is altered and design criteria are added to the list. In this section, the design criteria are stated and the workflow is described. To test the workflow, the clasps resulting from the final workflow are tested on a dental cast. When the design criteria are met with this test, the workflow for the clasp retention can be added to the CAD/CAM workflow for ISOs.

*Figure **4.4**. In beige, a 3D-printed model of a 3D-intraoral scan of the upper jaw. On the premolars and molars, an initial design for 3D-printable retention clasps is placed.*

### Design criteria

*Provide retention* - The clasps must provide retention to the ISO by covering the buccal undercut. The design of these clasps must be tested for their retention by the maxillofacial prosthodontist during fitting. Ultimately, these 3D-printed retention clasps must provide comparable to superior retention when compared to retention methods of the conventional ISO. This will be tested on a phantom in Chapter 6.

*Dental bulge* – For the clasps to provide retention with the use of the undercut, they need to first pass the bulge of the teeth (see Figure **4.5**). The design must be compatible with this bulge, and thus fit over the bulge of the teeth.

*Free gingival sulcus* –The ISO is secured for the initial recovery period after the maxillectomy. It is important to maintain oral hygiene by cleaning the gingival sulcus (see Figure **4.5**). Poor gingival sulcus hygiene can lead to gingivitis and periodontitis, which can lead to instability of the remaining teeth due to alveolar bone loss. Preservation of the remaining teeth is crucial for retention.[17] Therefore, the retention clasps must keep clear from the gingival sulcus.[10]

*Dental enamel* – Gingival recession can be present in some patients. This means that the gingival margin and possibly the free gingiva are withdrawn back. In this case, the cemento-enamel junction (CEJ) is emerged. To prevent the patient from experiencing dentin hypersensitivity, it is important to stay on dental enamel and not cross the CEJ.[18] The CEJ is visible on the teeth of the patient, as well as on the IOS as can be seen in Figure **4.6**.



*Figure **4.5**. Schematic overview of a molar with its gingival sulcus, the height of contour that is drawn with a surveyor and the delineation of the bulge of the molar, and the undercut under the bulge.*
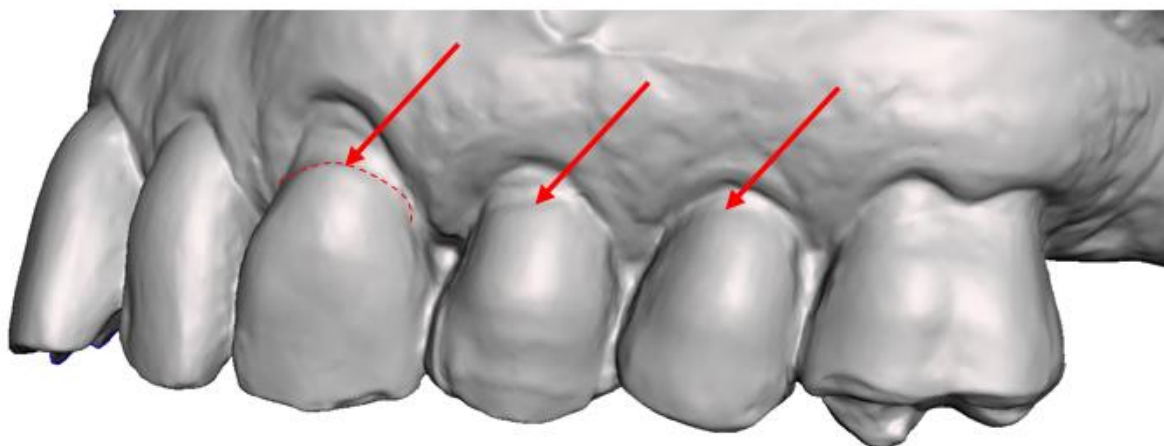
*Figure **4.6**. The buccal part of some teeth of an STL of an intraoral scan of a patient is shown. The red arrows point at the visible cemento-enamel junction.*

*Material* – The retention clasps are added to the existing CAD/CAM workflow for the fabrication of the hISO, creating a one-piece 3D-printed hISO with clasps. Thus, the material for the clasps must be the same as the resin used for the hISO. The material should ultimately be biocompatible. Because the hISO is not yet clinically used during this study, it is sufficient to use a non-biocompatible material with properties alike the final material. The resin used during this study is Clear Resin (Clear Resin V4, Formlabs, Somerville Mas., U.S. [19]).

*Solidity* – The clasps should be solid and not break off during use. The material properties of 3D-printing resins are different from the stainless steel that is used for the Adams clasps. Especially the difference in Ultimate Tensile Strength (65 MPa for Formlabs Clear V4 resin [19], and 320-795 MPa for SS 316 [20]) show that the resin will break more easily when there are forces applied. The design should be tested for solidity during intended use.

*Obturator fit* – The obturator must fit as intended. The retention clasps should not alter the position of the obturator.

*Safe design* – The design must be safe, with no small parts that can break off easily or sharp edges that can harm patients or staff. The design must not consist of unnecessary crevices to maintain hygiene.

*3D-printing properties* – The minimal wall thickness and layer thickness should be considered specifically for the chosen material and 3D-printer. The design must be 3D-printed as intended.

Table **4.1** shows the design criteria and the evaluation method.

Table **4.1**. Design criteria for 3D-printable retention clasps for a 3D-printed hollow obturator with their evaluation method.

| CRITERIA | EVALUATION |
|---|---|
| Provide retention | Tested by maxillofacial prosthodontist. |
| Dental bulge | The clasps get over the bulge of the teeth, and "click" in their intended place. |
| Gingival sulcus | Gingival sulcus must be free. |
| Dental enamel | The clasps must not cross CEJ. |
| Material | Same material as hISO. |
| Solidity | No breach after 10 times of placement and removal. |
| Obturator fit | hISO fits as intended. |
| Safe design | No parts break off during the fitting process. No sharp edges, no unnecessary crevices. |
| 3D-printable | The clasps are 3D-printed as intended. |

### Iterative testing and evaluation

The retention clasps are iteratively tested on three patients. For each patient, a dental cast was 3D-printed from the IOS, on which the retention clasp designs were tested. For two patients, the hISO and clasp design is also tested intraoperatively during their maxillectomy surgery. The 3D-printed dental cast of patient 3 is used for the final evaluation of the workflow and clasp design. Table **4.2** provides an overview of the tests performed per patient.

Table **4.2**. Testing method per patient for the workflow of 3D-printed retention clasps.

| PATIENT | DENTAL CAST TEST | INTRAOPERATIVE TEST |
|---|---|---|
| 1 | ✓ | |
| 2 | ✓ | ✓ |
| 3 | **Evaluation** | ✓ |

## Results

The result of this study is the evaluated workflow for 3D-printed retention clasps for obturators with its corresponding design principles that follow from the design criteria.

### Design principles

Throughout the iterative tests, a set of design principles was established to meet the design criteria. In order to ensure solidity and cover the bulge, flexibility must be the primary focus. The minor connectors were observed to be susceptible to bending forces when the clasps pass the bulge, which led to frequent breakage during the iterative tests. Figure **4.7** demonstrates the designated terminology. The following design principles were established:

*Buccal undercut* – The clasps should only cover a portion of the buccal undercut in order to provide sufficient retention. The distal undercut must **not** be covered by the clasps.

*Interproximal space* – During the design process, protrusions that extend into the interproximal space are often observed. To reduce the bending forces exerted on the minor connectors, the protrusions should be trimmed as much as possible.

*Thin distal minor connector* – The minor connector should be kept thin to increase flexibility.

*Minor connectors* – To ensure enough strength, the minor connectors should have a thickness of 1mm.
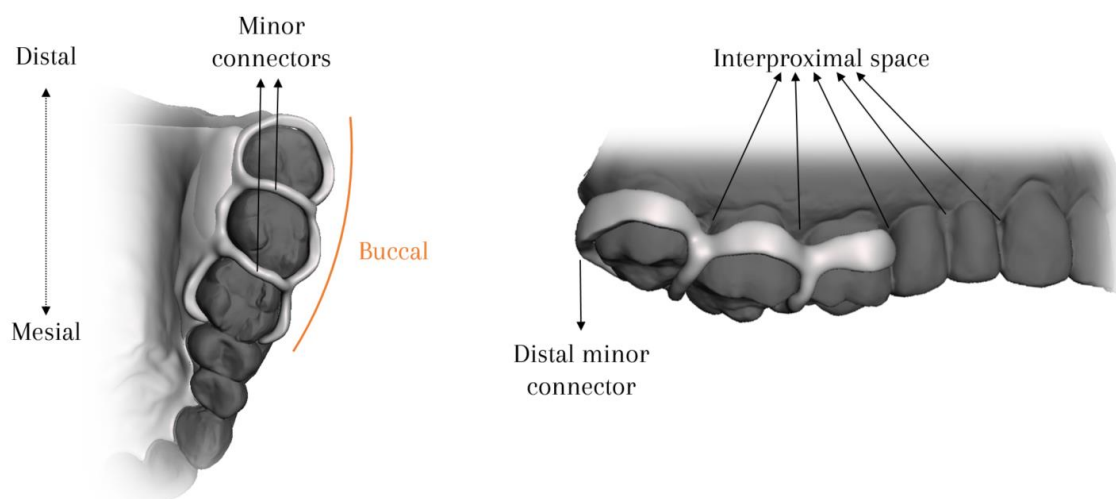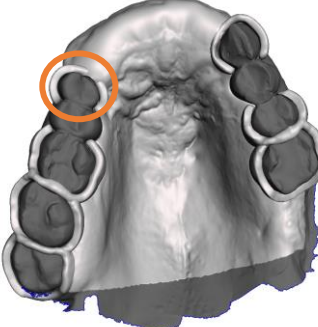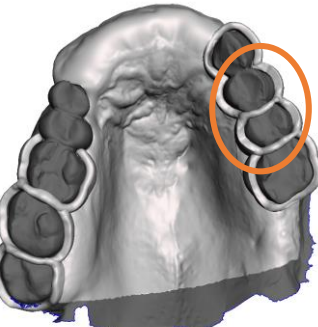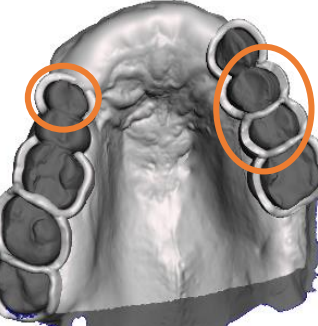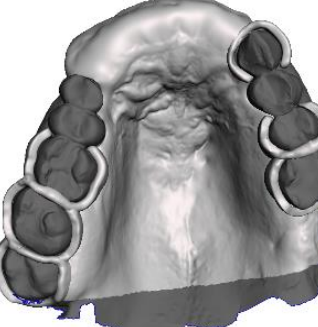


*Figure **4.7**. On the left is the inferior view of the palate, showing the left maxillary teeth (dark grey) and retention clasps (light grey). The buccal side of the teeth is annotated in orange. The bridges over the occlusion are called the minor connectors. On the right, the buccal side of the teeth is shown (dark grey) with the retention clasps in light grey. The distal minor connecter is shown, as are the interproximal spaces between the adjacent teeth.*

*Teeth selection* – During the iterative tests, various configurations of teeth were selected for the design of the retention clasps and tested. Table **4.3** shows the different configurations that were tested intraoperatively on patient 3. The principle resulting from these tests is to select <u>no more than three adjacent teeth</u>. The design of 3D-printed retention clasps on four adjacent teeth decreases flexibility and causes failure.

For a conventional ISO, the <u>canine</u> and the tooth adjacent to the defect are included in the retention.[15] During the iterative tests for the 3D-printed clasps, including those teeth did not provide additional retention. Especially for patient 3, the right PM1 did not have much undercut. Therefore, this tooth is not included in the final evaluation of the clasps on the dental cast.

Table **4.3**. Different configurations of retention clasps tested on a 3D-printed maxillary cast.

| SELECTED TEETH | IMAGE | RESULT OF THE FITTING |
|---|---|---|
| Left: C PM2 M1<br>Right: PM1 M1 M2 M3 |  | The right PM1 did not provide extra retention.<br>The left M1 buccal surface is troubling. |
| Left: C PM1 PM2 M1<br>Right: M1 M2 M3 |  | Left side failure. |
| Left: C PM1 PM2 M1<br>Right: PM1 M1 M2 M3 |  | Left side failure. |
| Left: C PM2 M1<br>Right: M1 M2 M3 |  | The right side fits well; the left M1 buccal surface is troubling. |

## Workflow

*Intraoral Scan* – First, an IOS is made with the Trios 3Shape (Copenhagen, Denmark) and loaded into Autodesk Meshmixer (RRID:SCR_015736, ©2020 Autodesk, Inc.). The ISO is designed and the STL file is altered according to the workflow designed by S. Steenhuis[9] and A. Ooms[8].

*Determine the included teeth for retention* – Include the most distal tooth on the opposite side of the defect, with one or two adjacent teeth when available, no more than three adjacent teeth, teeth adjacent to the defect, and the canine when available. An example of teeth included for retention is shown in Figure **4.8**.
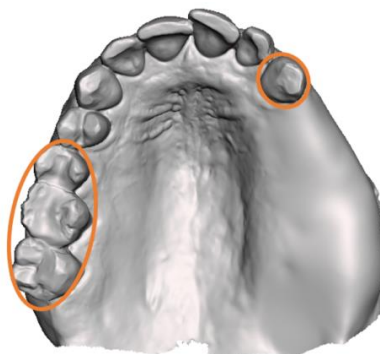


*Figure **4.8**. Example of the teeth included for the retention clasps.*

*Selection* – The area directly on the chosen teeth is then selected, keeping in mind the undercut of the teeth and the thin distal minor connector. The minor connectors over the occlusal embrasure are also selected with a size of about 25. Once the selection is made according to the criteria, the boundary is optimized and smoothed. Figure **4.9** shows the selected area with optimized and smoothed boundaries.
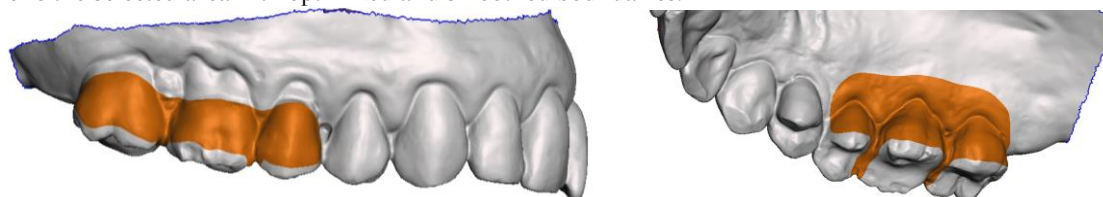


*Figure **4.9**. The selected area for retention clasp design is shown in orange, with optimized and smoothed boundaries.*

*Offset and separate* – An offset of 0.2 mm is applied to correct for 3D-scanning and printing errors. The outer selection is then separated into its own group. Work with this new group.

*Extrusion* – Perform an extrusion of 1.5 mm towards the normal of the triangles. The spikes that arise with this performance are smoothed out. Figure **4.10** shows the clasps after extrusion on the left and on the right the clasps after smoothing.
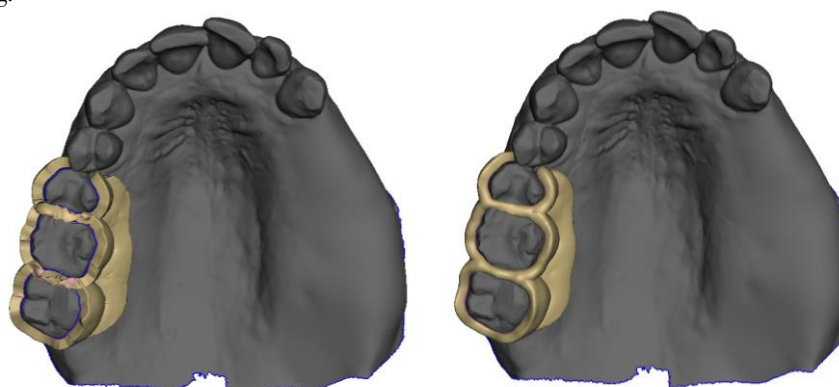


*Figure **4.10**. On the left retention clasps after extrusion. The right image shows the clasps after smoothing and sculpting.*

*Offset check* – The part is checked for the offset, as the sculpting may cause it to not fit over the teeth anymore. Corrections can be made from the inside of the IOS using the sculpt *ShrinkSmooth* brush or the *Move* brush. Figure **4.11** shows the clasp exceeding the IOS STL on the left, and the right image shows the result after this offset check.
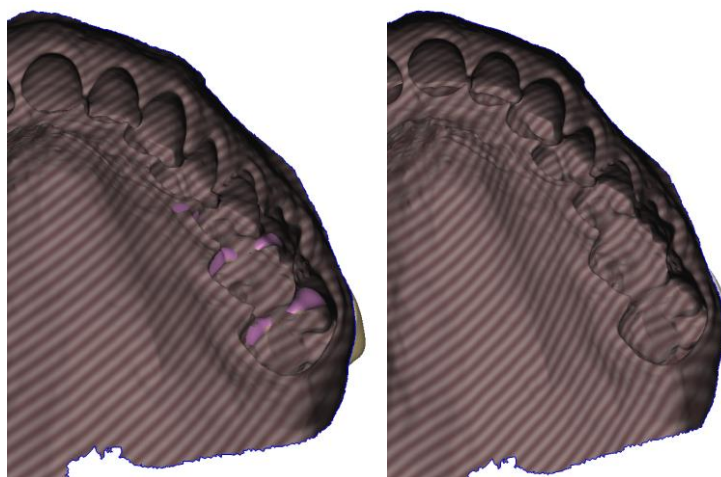
*Figure **4.11**. Sculpting of the retention clasps can result in the part exceeding the intraoral scan, which causes the clasps to not fit anymore, as shown in the left image. The right image shows the result after sculpting the part from the inside.*

*Smooth and sculpt* – Check the design for unnecessary crevices or spikes and remove or alter them when present. Always check the inside of the IOS to check the offset when the part is altered to check the offset. Decrease the protrusions at the interproximal space. Smooth the part. Figure **4.12** shows the retention clasps before (left) and after (right) smoothing and sculpting.
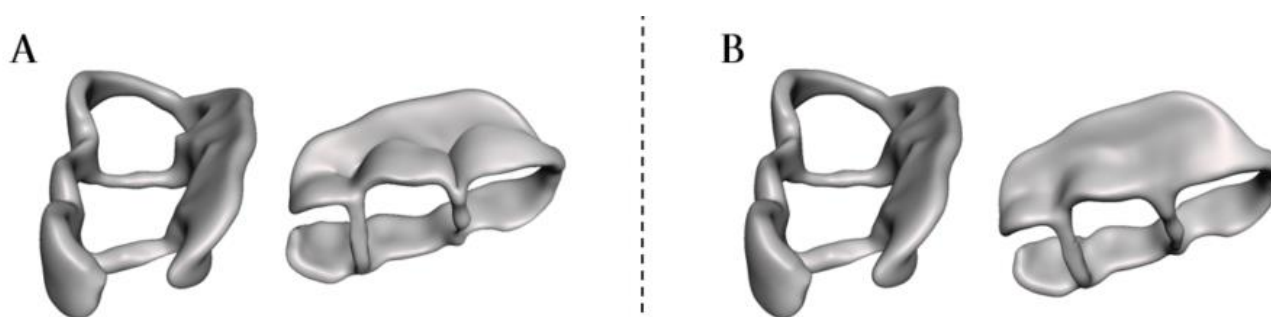


*Figure **4.12**. Retention clasps, before smoothing and sculpting (A), and after (B).*

*Merge* – Finally, the retention clasps are merged with the baseplate of the ISO to be 3D-printed as one part. Hard transitions should be smoothed.

Figure **4.13** shows the complete workflow.
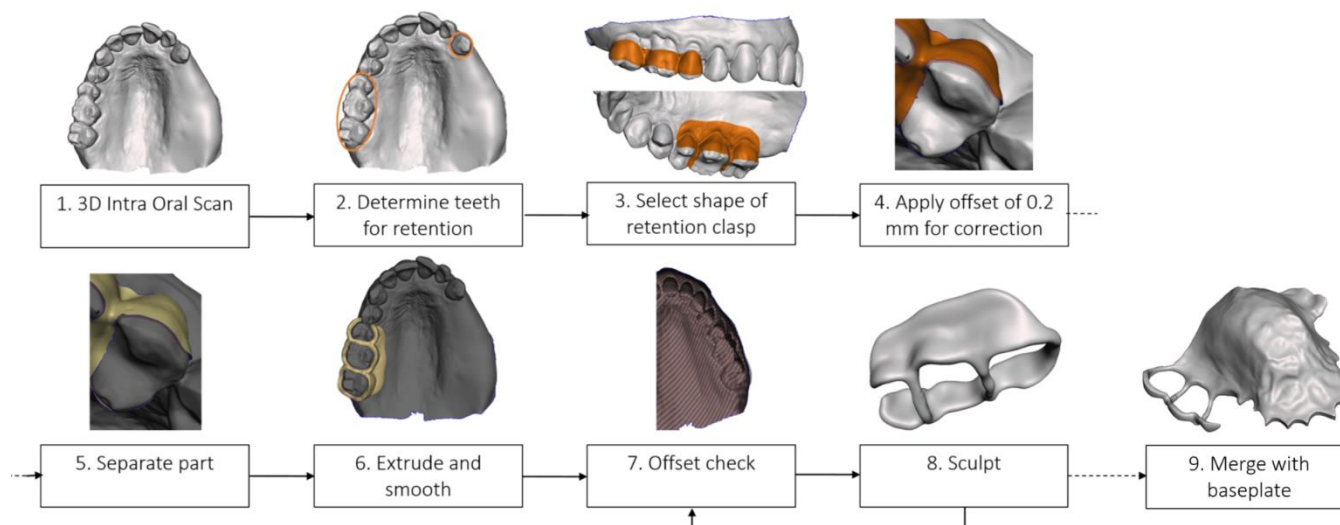


*Figure **4.13**. The CAD/CAM workflow for 3D-printable retention clasps. To be fabricated in one piece with a 3D-printed hollow obturator.*

## Evaluation

The 3D-printed dental cast of patient 3 is used for the final evaluation of the design. Figure **4.14** shows the fitting of the 3D-printed baseplate and retention clasps on the cast model. Table **4.4** shows the list of design criteria and the evaluation.



*Figure **4.14**. 3D-printed baseplate and retention clasps fitted on a 3D-printed dental cast. The clasps are evaluated according to the design criteria stated in Table **4.4**.*

Table **4.4**. Design criteria for 3D-printed retention clasps, evaluated on a dental cast.

| CRITERIA | EVALUATION |
| --- | --- |
| Provide retention | The clasps provide sufficient retention according to the maxillofacial prosthodontist. |
| Bulge | The clasps get over the bulge of the teeth. They "click" in place. |
| Gingival sulcus | Gingival sulcus is free. |
| Dental enamel | Clasps do not extend the CEJ. |
| Material | The material is the same as for the hISO (Clear V4). |
| Solidity | The clasps do not break when placed and removed 10+ times. |
| Obturator fit | hISO fits as intended. |
| Safe design | The design is smooth. No parts break off. No sharp edges. |
| 3D-printable | Successfully 3D-printed in one-piece with the baseplate. |

## Discussion

This study aimed to develop and evaluate a workflow for 3D-printed retention clasps for the hISO. The final workflow and clasp design met all design criteria. However, determining the undercuts was the most common limitation during the iterative process. Specifically, patients with significant bulges on the distal side of the last molar presented challenges, as the workflow focused on the buccal undercut and lacked flexibility in the distal direction. For patients with bilateral retention clasps, undefined undercuts caused problems with finding the path of insertion and fitting the clasps over bulges. All teeth have a certain mesial distal angulation, which is different for each patient.[21] This angulation causes the direction of insertion of the prosthesis to be important. The use of a digital surveyor could address these issues.

Digital surveying for removable partial dentures (RPD) is described in the literature, which has similar retention clasps as an obturator. Previous studies have used the 3Shape CAD software for electronic surveying.[22–25] Lee et al. [27] describe the use of the path of placement for the undercut areas, determined in 3-Matic (3-Matic; Materialise NV). Williams et al. [26] describe a method for electronic surveying using MATLAB software (MATLAB; The MathWorks, Inc., Natick, Mass) that marks downward-facing triangle surfaces from the registered and aligned STL, which enables automation of the surveying process.

Based on these literature findings, a first attempt at a digital surveyor is performed. A PLY file of the IOS is loaded into MATLAB. This file is a triangular polygon mesh, consisting of many faces and vertices, together creating the 3D-image of the intraoral scan. The normal of each vertex is determined as a vector. The faces with an upward normal in the z-axis (z>0) are depicted as red, and the rest of the faces are white (see Figure **4.14**). Appendix B elaborates on this method of digital surveying. This digital surveying shows promise, but validation is necessary before clinical use.
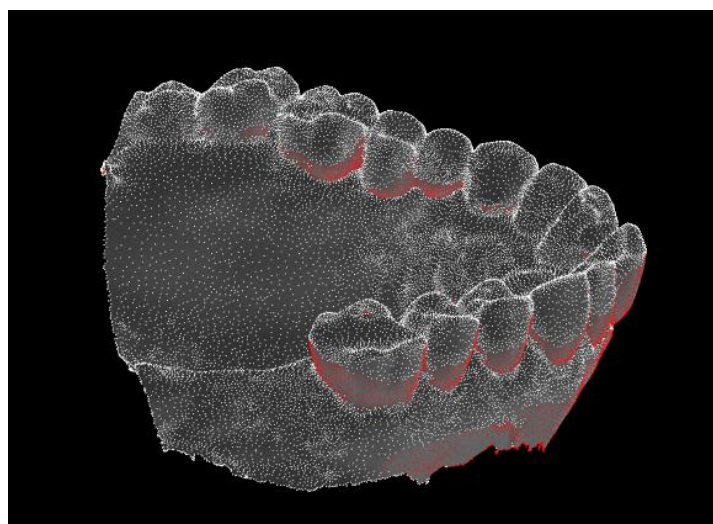


*Figure **4.14**. Example of a 3D-model of an intraoral scan after being digitally surveyed. Red shows the undercuts.*

The retention clasps are 3D-printed in Formlabs Clear Resin. However, for optimal results, it is recommended to print them in biocompatible resin, such as Formlabs Dental LT Clear Resin. The material properties of Dental LT Clear Resin are different from Clear Resin, with a lower ultimate tensile strength (52 MPa vs 65 MPa for clear resin), higher flexural modulus (2.3 GPa vs. 2.2 GPa for clear resin), and higher notched Izod test (449 J/m vs 25 J/m for clear resin). This indicates that Dental LT Clear Resin can bear more load before breaking. Other clear, biocompatible resins for Formlabs SLA printers include Formlabs BioMed Durable Resin and Formlabs BioMed Clear Resin. However, BioMed Durable Resin can only be used for short-term dentin contact (<24 h), which is not useful for the ISO that needs to stay in place for at least 2 weeks.

To evaluate the clinical implementation of this workflow, tests should be performed with Dental LT Clear Resin. Because most mechanical properties are in the same order of magnitude, it is expected that the workflow is also usable when biocompatible material is used for 3D-printing.

It is important to note that the retention of dental prostheses is highly patient-specific and dependent on various factors. Therefore, the results of this report only indicate the usability of these 3D-printable retention clasps. Clinical reports are needed to evaluate the 3D-printed retention clasps in a more complex clinical situation.

**Future perspectives**

In this study, evaluation of the retention relies on the expert's proficiency, as there is a lack of a measurable outcome for sufficient retention for obturator prostheses, other than patient satisfaction. The literature suggests that insufficient retention is a factor for prosthesis failure, based on clinical experience.[1–3] Because the 3D-printed retention clasps cannot be clinically tested yet, their performance should be evaluated in a comparison study with the conventional method. For clinical implementation, the new technique must meet or exceed the performance of the conventional retention clasps. Chapter 6 describes a phantom study that examines the performance of this new retention method technique.

Moreover, it is important to emphasise the importance of stability and support in maxillofacial prostheses. Stability is defined as the resistance to horizontal and rotational forces. Figure **4.15** shows a tooth with its survey line, where the upper part plays a role in the stability of the prosthesis. The design of the 3D-printed retention clasps includes this side of the survey line, and could thus provide some level of stability. Future research should evaluate if this level of stability is sufficient.
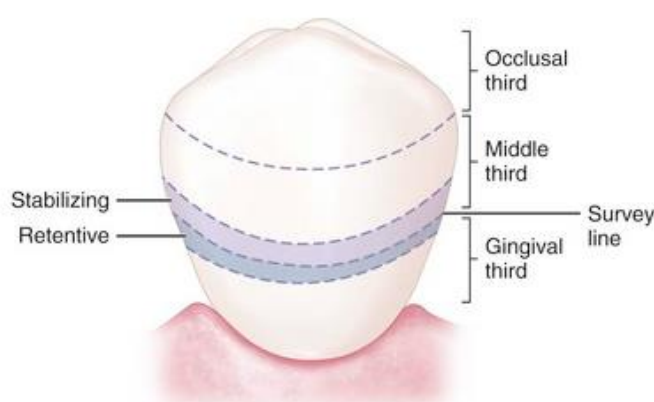


*Figure **4.15**. Tooth with survey line. In blue, part of the undercut is shown which provides retention when a clasp is placed in this area. In purple, the region providing stabilization is shown when a clasp is placed in this area.* [28]

Support is vital to resist cranial vertical forces, which is specifically important in obturators to prevent the bulb from pushing into the wound tissue, causing pain. It can be achieved by designing rests on the teeth or with maximum extension onto the residual palate and contact with residual bony structures.[29] The minor connectors of the design of the 3D-printed retention clasps could provide some level of support, which can be evaluated in future research.

As stated, further research should be done to develop and validate a digital surveyor. With a digital surveyor, the path of insertion and the undercuts can be visualized. Future research can also look into other options for digital surveying, such as the 3Shape digital surveyor or the 3Matic function.

## Conclusion

In summary, this research presents a practical CAD/CAM workflow that enables the addition of 3D-printed retention clasps to an existing CAD/CAM workflow for a 3D-printed hollow obturator. The retention clasps designed in this study satisfy all design criteria, thus proving the feasibility of this workflow. However, it is worth noting that the path of insertion for bilateral retention clasps is challenging to define, which can lead to misfit or breach. To overcome this issue, future research can focus on validating a proposed method for digital surveying using a digital surveyor on the digital cast model.

# REFERENCES

1.      Singh M, Kapoor S, Kumar L, Pal US, Singh A, Anwar Mohd. Prevalence of maxillectomy defects among patients visiting in an institutionalized hospital setting: A prospective, single-institute study. *Natl J Maxillofac Surg*. 2020;11(2):231. doi:10.4103/NJMS.NJMS_61_20

2.      Devlin H, Barker GR. *Prosthetic Rehabilitation of the Edentulous Patient Requiring a Partial Maxillectomy*.

3.      Murat S, Gurbuz A, Isayev A, Dokmez B, Cetin U. Enhanced retention of a maxillofacial prosthetic obturator using precision attachments: Two case reports. *Eur J Dent*. 2012;6(2):212-217. http://www.ncbi.nlm.nih.gov/pubmed/22509126

4.      Keyf F. Review Obturator prostheses for hemimaxillectomy patients. doi:10.1111/j.1365-2842.2001.00754.x

5.      Dalkiz M, Dalkiz AS. The Effect of Immediate Obturator Reconstruction after Radical Maxillary Resections on Speech and other Functions. *Dent J (Basel)*. 2018;6(3). doi:10.3390/DJ6030022

6.      Wu Y low, Schaaf NG. Comparison of weight reduction in different designs of solid and hollow obturator prostheses. *J Prosthet Dent*. 1989;62(2):214-217. doi:10.1016/0022-3913(89)90317-X

7.      Tanaka Y, Gold H 0, Pruzansky S. *A Simplified Technique for Fabricating a Lightweight Obturator*.

8.      Ooms A. Optimized and user-friendly workflow for the fabrication of 3D printed maxillary hollow closed surface model obturator using CT, intraoral scanning technology, and computer aided/manufacturing | Master Thesis. 2022;(October).

9.      Steenhuis A. *Fabrication Process of Maxillary Hollow Bulb Immediate Surgical Oburator Using Intraoral Scanning Technology and Computer Aided Design/Manufacturing*.; 2021.

10.     Green JIJ. Dental materials: The Adams family. *BDJ Team 2014 1:1*. 2014;1(1):14-17. doi:10.1038/bdjteam.2014.133

11.     The Glossary of Prosthodontic Terms: Ninth Edition. *J Prosthet Dent*. 2017;117(5):e1-e105. doi:10.1016/j.prosdent.2016.12.001

12.     Dental Surveyor & Surveying - Focus Dentistry. Accessed October 24, 2023. https://thefuturedentistry.com/dental-surveyor-surveying/

13.     11: Surveying | Pocket Dentistry. Accessed October 24, 2023. https://pocketdentistry.com/11-surveying/

14.     Removable Partial Denture – Dental Surveying – My Dental Technology Notes. Accessed October 24, 2023. https://mydentaltechnologynotes.wordpress.com/2018/07/15/removable-partial-denture-dental-surveying/

15.     Aramany MA. Basic principles of obturator design for partially edentulous patients. Part II: Design principles. *Journal of Prosthetic Dentistry*. 2001;86(6):562-568. doi:10.1067/mpr.2001.121619

16.     Ness Visual Dictionary. Accessed October 27, 2023. https://ptc-dental.com/dictionary/index.php

17.     Parr GR, Tharp GE, Rahn AO. *Prosthodontic Principles in the Framework Design of Maxillary Obturator Prostheses*. Vol 62.; 1989.

18.     Davari A, Araei E, Assarzadeh H. Dentin Hypersensitivity: Etiology, Diagnosis and Treatment; A Literature Review. *J Dent Shiraz Univ Med Sci, Sept*. 2013;14(3):136-145.

19.     Technical Datasheet - Formlabs. General Purpose Resins - Materials for High Resolution Models and Rapid Prototyping.

20.     316 Stainless Steel Mechanical Properties | E-Z LOK. Accessed September 27, 2023. https://www.ezlok.com/316-stainless-steel-properties

21.     Tong H, Kwon D, Shi J, Sakai N, Enciso R, Sameshima GT. Mesiodistal angulation and faciolingual inclination of each whole tooth in 3-dimensional space in patients with near-normal occlusion. *American Journal of Orthodontics and Dentofacial Orthopedics*. 2012;141(5):604-617. doi:10.1016/j.ajodo.2011.12.018

22.     Tamimi F, Almufleh B, Caron E, Alageel O. Digital removable partial dentures. *Clinical Dentistry Reviewed*. 2020;4(1). doi:10.1007/s41894-020-00074-y

23.     Bajunaid SO, Altwaim B, Alhassan M, Alammari R. The fit accuracy of removable partial denture metal frameworks using conventional and 3D printed techniques: An in vitro study. *Journal of Contemporary Dental Practice*. 2019;20(4):476-481. doi:10.5005/jp-journals-10024-2542

24.     Saad AS, Abbas FS, Elgharabawy SH. Clinical evaluation of removable partial denture constructed from 3d printed resin pattern designed using cad cam technology. *Alexandria Dental Journal*. 2019;44(2):15-21. doi:10.21608/ADJALEXU.2019.57357

25.     Al-Haj Husain N, Özcan M, Schimmel M, Abou-Ayash S. A digital cast-free clinical workflow for oral rehabilitation with removable partial dentures: A dental technique. *J Prosthet Dent*. 2020;123(5):680-685. doi:10.1016/j.prosdent.2019.05.008

26.     Williams RJ, Bibb R, Rafik T. *A Technique for Fabricating Patterns for Removable Partial Denture Frameworks Using Digitized Casts and Electronic Surveying*.

27.     Lee H, Kwon KR. *A CAD-CAM Device for Preparing Guide Planes for Removable Partial Dentures: A Dental Technique THE JOURNAL OF PROSTHETIC DENTISTRY*.

28.     7: Direct Retainers | Pocket Dentistry. Accessed October 27, 2023. https://pocketdentistry.com/7-direct-retainers/

29.     Raja HZ, Saleem MN. Gaining retention, support and stability of a maxillary obturator. *J Coll Physicians Surg Pak*. 2011;21(5):311-314. http://www.ncbi.nlm.nih.gov/pubmed/21575545

# CHAPTER 5. TONGUE PALATE PRESSURE FOR DEGLUTITION SIMULATION ON IMMEDIATE SURGICAL OBTURATORS

# Chapter 5.
# Tongue palate pressure for deglutition simulation on immediate surgical obturators

## Introduction

Immediate Surgical Obturators (ISO) are intraoperatively placed into the maxillectomy defect. The primary goal of the ISO is to restore oronasal separation, enabling the restoration of speech, swallowing, and facial aesthetics during the first healing phase. The ISO is secured in position using palate screws, zygomatic wires, retention wires and/or Adams clasps.[1–4]

During deglutition, speech, and mastication, the ISO undergoes various forces, including caudal pressure caused by tissue contraction and wound exudate. In the phantom study of Chapter 6, the aim is to simulate these forces to evaluate the 3D printed retention for all ISO classes. While studies have investigated the mastication function of patients with obturators[5–8], there is limited literature discussing the impact of other forces on the obturator.

As the current workflow for the 3D printed ISO does not incorporate dentition, mastication forces are excluded from this study. Yano et al.[9] assessed both swallowing and articulation pressure across five palatal locations. Their findings indicate that the tongue pressure during swallowing reached a 6.0-6.7 times higher maximal magnitude than during articulation. Therefore, the focus of this study is the tongue-palate pressure (TPP) during deglutition. This TPP is used in the phantom study to develop a tongue phantom.

During the oral stage of swallowing, the tongue executes a wave-like motion. The tip of the tongue exerts pressure on the alveolar ridge and front part of the hard palate while the back part of the tongue descends to allow the bolus to move towards the pharynx. Thereafter, the tongue gradually pushes against the palate from anterior to posterior to propel the bolus into the pharynx.[10] The final phantom study aims to mimic this tongue movement, to determine the maximum displacement of the obturator during deglutition. This displacement is responsible for prosthesis failure and lack of retention. Given the complexity of swallowing, the movement is simplified for the phantom study. The largest displacement of the obturator takes place when the anterior part of the obturator is pushed, directly followed by the posterior part. Therefore, our focus is on the TPP at these two locations. Additionally, a third location medially on the hard palate is examined, to replicate a wave-like motion. The measurements are taken at the midline of the hard palate since Miller et al.[11] found no difference in TPP between the mid-anterior tongue and the lateral sides.

## Method

TPP was measured using the Iowa Oral Performance Instrument (IOPI Medical LCC, Redmond, Washington). This instrument is a pneumatic device, measuring pressures in kPa. It consists of an air-filled balloon attached to a flexible plastic tube that is connected to the device. The balloon is approximately 3.5 cm in length, 1.5 cm in width and has an internal volume of 2.8 mL.

The TPP is measured at three locations along the tongue midline: anterior, posterior, and medial. To determine the location of the anterior TPP ($TPP_a$), the middle of the balloon is placed on the alveolar ridge, just posterior to the incisors. For the posterior TPP ($TPP_p$), the tip of the balloon is placed at the transition of hard to soft palate. The median TPP ($TPP_m$) is in the middle of the $TPP_a$ and $TPP_p$. An elastic band marks the location on the connecting tube for all three locations (see Figure **5.1**).
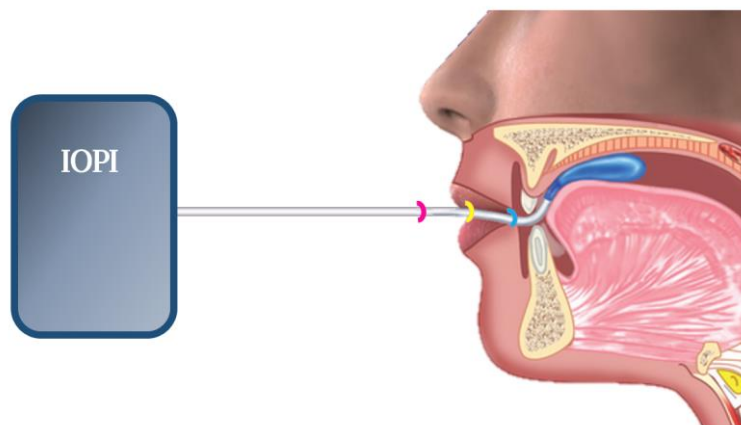
*Figure **5.1**. A schematic figure of the IOPI balloon placed on the medial part of the tongue. The blue, yellow and pink bands are elastic bands on the tube, marking the anterior, median and posterior location of the balloon on the hard palate, specific for each subject. This ensures that the placement of the balloon is identical for all three repetition measurements. The elastic band is placed just outside the lips.*[12]

The study enrolled three healthy, young (age 23-24) females, who were recruited from the NCI-AvL. To evaluate TPP during deglutition, the participants were asked to drink a small sip of water (10-20 mL [13]) through a straw. During one measurement repetition, each subject is seated in a chair facing forward and instructed to take three consecutive sips of water with the bulb in the anterior position, then three consecutive sips with the bulb in the middle position and finally three consecutive sips with the bulb in the posterior position. Each subject performs three of these measurement repetitions.

<u>Analysis</u>

The analysis is done in twofold. Firstly, the mean pressure is calculated for each location, averaging all 27 measurements taken at the location. Secondly, a Wilcoxon Signed Ranks Test is performed in SPSS software (IBM, New York, USA), to evaluate whether there are any differences between $TPP_a$, $TPP_m$ and $TPP_p$. This test compares population means to determine if there is a significant difference between related data sets.

In SPSS data contained three variables, $TPP_a$, $TPP_m$ and $TPP_p$, each with 27 measurements (3 subjects * 3 sips * 3 sets = 27 measurements). As the statistical analysis is used as substantiation for the hypotheses that $TPP_a$, $TPP_m$ and $TPP_p$ do not significantly differ ($H_0$: the groups differ), all measurements per location are aggregated. The confidence interval is set at 95%, with a significance level of 0.05. This means that a p-value of >0.05 suggests the similarity of the three locations, but does not provide conclusive evidence. For the 95% confidence interval, the Z-value cutoff is 1.96. A Z-value between -1.96 and 1.96 supports the hypothesis of the similarity of $TPP_a$, $TPP_m$ and $TPP_p$.

## *Results*

The raw data of the tongue pressure on the hard palate for $TPP_a$, $TPP_m$ and $TPP_p$ for three subjects that completed three measurement repetitions can be found in Appendix A.

The mean and standard deviation for all three locations (N=27) are shown in Table **5.1**.

Table **5.1**. mean and standard deviation of the tongue palate pressure on three locations measured on young healthy females.

|  | Average | Standard deviation |
| --- | --- | --- |
| **TPP$_A$** | 16.8 kPa | 5.5 |
| **TPP$_M$** | 17.6 kPa | 4.5 |
| **TPP$_P$** | 17.4 kPa | 3.2 |

*Retention for 3D-printed hollow immediate*
*surgical obturators for maxillectomy patients*
*TPP during swallowing*

Three Wilcoxon Signed Ranks Tests were performed to compare all three groups. The Z- and p-values of those three tests are shown in Table **5.2**.

Table **5.2**. Z- and p-value of three comparisons with the Wilcoxon Signed Ranks test.

|  | Z | P value |
|---|---|---|
| TPP$_A$ vs. TPP$_M$ | -.526 | .599 |
| TPP$_A$ vs. TPP$_P$ | -.789 | .430 |
| TPP$_M$ vs. TPP$_P$ | -.013 | .989 |

## Discussion

This study aims to investigate the TPP on three palate locations during deglutition of a sip of water. The results indicate a TPP of 17-18 kPa for all three locations. The Wilcoxon Signed Ranks test did not indicate a significant difference between all groups, thus the null hypothesis (H$_0$) is not rejected. This implies that the TPP is uniform across all three locations.

However, these results do not match with some literature. Yano et al.[9] measured the tongue pressure for articulation (monosyllable, Japanese) and deglutition (dry, saliva) with a sensor sheet attached to the hard palate. They found a dissimilarity between the anterior, medial and posterior measurement points on the palatal midline. Miller et al.[11] supported this finding, by concluding that the anterior-medial and posterior-lateral parts of the palate have a high maximal magnitude of tongue pressure for the bolus to propagate. One explanation for our results is the size of the balloon of the IOPI, which can lead to some overlay at the three locations.

The outcomes of this study will serve as the basis for designing a tongue phantom that can mimic a simplified swallowing motion. The tongue phantom will be configured with the IOPI to attain a pressure of 17 kPa, which will be measured at all three locations.

There are some limitations to this study. Firstly, the bolus size was not standardized. During the measurements, the subjects took a sip of water through a straw. Both the bolus size and viscosity affect the TPP.[11,14,15] Thus, we were unable to measure the maximum pressure the obturator will endure during swallowing, as the pressure can increase with a larger volume or when swallowing a thicker substance.

Another limitation is that these results are measured for healthy young female subjects. Age can influence tongue pressure.[14] The tongue function may also differ in maxillectomy patients. Ogino et al.[16] conducted a retrospective analysis of tongue function and swallowing in maxillectomy patients and found impaired EAT-10 scores. They also highlighted the importance of obturator retention, as poor retention can even lead to impaired tongue functions that can cause dysphagia. Therefore, the TPP may differ for maxillectomy patients compared to healthy young subjects. Literature is inconclusive about the effect of gender on tongue strength. Vanderwegen et al.[17] found that men, in general, showed higher tongue pressures, though Stierwalt et al.[18] found no significant difference.

## Conclusion

Within the limitations of this study, we can conclude that the TPP for young healthy female subjects is 17 kPa in three locations measured with the IOPI. The TPP is uniform across the three locations on the midline of the palate. These findings can be used in the deglutition test of the phantom study in Chapter 6.

# REFERENCES

1. Beumer III J, Marunick MT, Esposito SJ. *Maxillofacial Rehabilitation: Prosthodontic and Surgical Management of Cancer-Related, Acquired, and Congenital Defects of the Head and Neck.* Third Edit. Quintessence Publishing Co, Inc; 2011.

2. Keyf F. Review Obturator prostheses for hemimaxillectomy patients. doi:10.1111/j.1365-2842.2001.00754.x

3. Haribhakti V V. *Restoration, Reconstruction and Rehabilitation in Head and Neck Cancer.* Springer Singapore; 2019. doi:10.1007/978-981-13-2736-0

4. Iqbal Z, Murtaza S, Kazmi R, Yazdanie N, Mehmood Z, Ali S. Maxillary Obturator Prosthesis: Support and Retention Case Series.

5. Kreeft AM, Krap M, Wismeijer D, et al. Oral function after maxillectomy and reconstruction with an obturator. *Int J Oral Maxillofac Surg.* 2012;41(11):1387-1392. doi:10.1016/J.IJOM.2012.07.014

6. Vero N, Mishra N, Singh BP, Singh K, Jurel SK, Kumar V. Assessment of swallowing and masticatory performance in obturator wearers: A clinical study. *Journal of Advanced Prosthodontics.* 2015;7(1):8-14. doi:10.4047/jap.2015.7.1.8

7. de Groot RJ, Rieger JM, Rosenberg AJWP, Merkx MAW, Speksnijder CM. A pilot study of masticatory function after maxillectomy comparing rehabilitation with an obturator prosthesis and reconstruction with a digitally planned, prefabricated, free, vascularized fibula flap. *J Prosthet Dent.* 2020;124(5):616-622. doi:10.1016/J.PROSDENT.2019.06.005

8. Matsuyama M, Tsukiyama Y, Tomioka M, Koyano K. Clinical assessment of chewing function of obturator prosthesis wearers by objective measurement of masticatory performance and maximum occlusal force. *Int J Prosthodont.* 2006;19(3):253-257. http://www.ncbi.nlm.nih.gov/pubmed/16752621

9. Yano J, Kumakura I, Hori K, Tamine KI, Ono T. Differences in biomechanical features of tongue pressure production between articulation and swallow. *J Oral Rehabil.* 2012;39(2):118-125. doi:10.1111/j.1365-2842.2011.02258.x

10. Matsuo K, Palmer JB. Anatomy and Physiology of Feeding and Swallowing – Normal and Abnormal. *Phys Med Rehabil Clin N Am.* 2008;19(4):691. doi:10.1016/J.PMR.2008.06.001

11. Miller JL, Watkin KL. *The Influence of Bolus Volume and Viscosity on Anterior Lingual Force During the Oral Stage of Swallowing.* Vol 11.; 1996.

12. Home - IOPI Medical. Accessed October 4, 2023. https://iopimedical.com/

13. Lawless HT, Bender S, Oman C, Pelletier C. Gender, Age, Vessel Size, Cup vs. Straw Sipping, and Sequence Effects on Sip Volume. doi:10.1007/s00455-002-0105-0

14. Shaker R, Dodds WI, Hogan WJ. *Pressure-Flow Dynamics of the Oral Phase of Swallowing.*

15. Sugita K, Inoue M, Taniguchi H, Ootaki S, Igarashi A, Yamada Y. Effects of Food Consistency on Tongue Pressure during Swallowing. *J Oral Biosci.* 2006;48(4):278-285. doi:10.1016/S1349-0079(06)80010-1

16. Ogino Y, Fujikawa N, Koga S, Moroi R, Koyano K. A retrospective cross-sectional analysis of swallowing and tongue functions in maxillectomy patients. doi:10.1007/s00520-021-06186-w/Published

17. Vanderwegen J, Guns C, Van Nuffelen G, Elen R, De Bodt M. The influence of age, sex, bulb position, visual feedback, and the order of testing on maximum anterior and posterior tongue strength and endurance in healthy Belgian adults. *Dysphagia.* 2013;28(2):159-166. doi:10.1007/s00455-012-9425-x

18. Stierwalt JAG, Youmans SR. Tongue Measures in Individuals With Normal and Impaired Swallowing. *Am J Speech Lang Pathol.* 2007;16(2):148-156. doi:10.1044/1058-0360(2007/019)

# CHAPTER 6. RETENTION METHODS FOR 3D-PRINTED IMMEDIATE SURGICAL OBTURATORS: A PHANTOM STUDY.

# Chapter 6.
# Retention Methods for 3D-printed Immediate Surgical Obturators: A Phantom Study

## Introduction

The success of an obturator is dependent on many factors. Adequate retention contributes to the prosthesis' success. Retention of a dental prosthesis is defined as "the quality inherent in the dental prosthesis acting to resist the forces of dislodgment along the path of placement".[1] For some patients, a conventional obturator prosthesis with various retention methods such as clasps, wires and screws is sufficient for the phase of the immediate surgical obturator (ISO). Unfortunately, there are also patients where these methods do not suffice in retention, stability and support, leading to prosthesis dissatisfaction.[2] Reducing the weight of the bulb could enhance the retention and stability of an obturator.[3–6]

Designing a hollow bulb can reduce the weight of an obturator by 7-47%.[7,8] Within the NKI-AvL, a CAD/CAM workflow for the fabrication of 3D-printed hollow ISO (hISO) is developed.[9,10] The current workflow (see Figure **6.1**) consists of the data acquisition and registration, and the design and fabrication of the baseplate and the bulb. Before the hISO can be clinically implemented, retention must be included in this workflow.



**1. CT head**
Radiologist
[PACS]

**2. Intraoral scan**
Prosthodontist
[TRIOS]

**3. Segmentations**
Skull & resection margins
[3D Slicer]

**4. Fiducial point registration**
[3D Slicer]

**5. CSM design**
From resection margins
[3D Slicer]

**6. Baseplate design**
From registered IOS
[Meshmixer]

**7. Merge and finish CSM & baseplate design**
[Meshmixer]

**8. 3D print and final polishing**
[Preform]
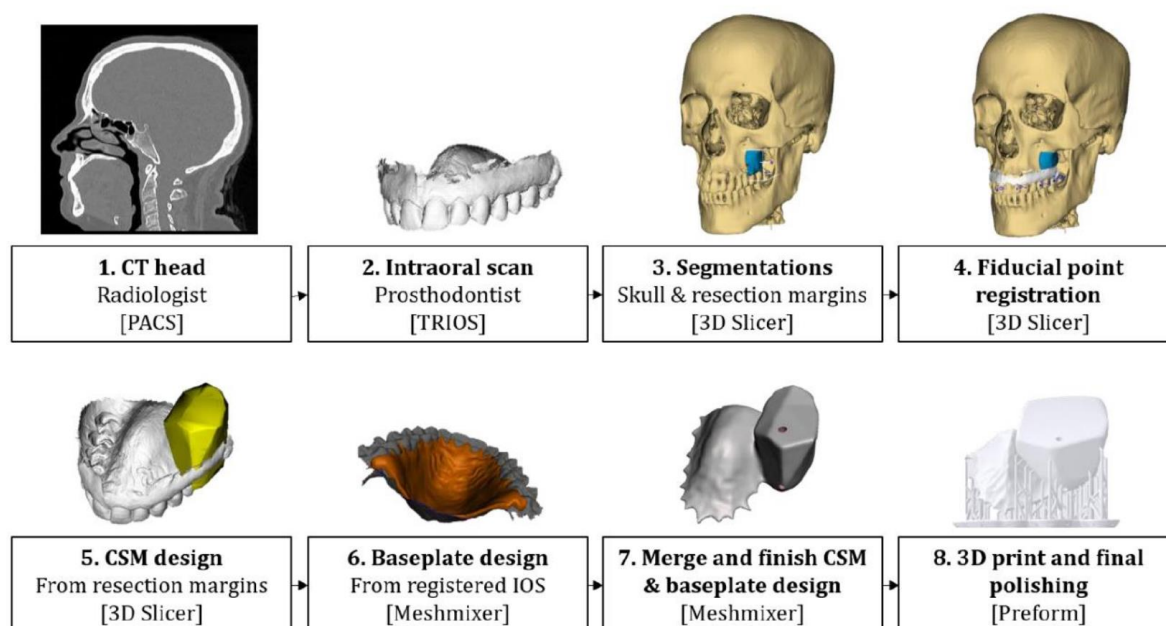
*Figure **6.1**. CAD/CAM workflow for the fabrication of a hollow bulb Immediate Surgical obturator. This workflow includes the data acquisition and registration, and the design and fabrication of the bulb and baseplate.*

Retention of an obturator is affected by many different aspects, such as the remaining teeth, the size of the defect, and the availability of tissue and muscles around the defect.[11] A conventional ISO is mainly secured with the following four different techniques, alone or combined[12]: Zygomatic wires and boulders, palatal screws, retentive clasps, and circumferential wires around teeth (see Figure **6.2**).

*Figure **6.2** Four different retention methods used for the fixation of a surgical obturator during maxillectomy. From left to right: Zygomatic wire and boulder; palatal screws; Adams clasp; and circumferential cerclage wires around the teeth, through holes in the baseplate.* [13–16]

Based on these retention methods for the conventional ISO, the retention methods for the 3-printed hISO are developed. A standardized boulder for the zygomatic wire is designed (see Figure **6.3**) that can be scaled and added to the digital design of the hISO. For the palatal screws and circumferential wires around the teeth, holes can be included in the design, or drilled in the desired locations after fabrication. In addition, Chapter 4 proposes a workflow for 3D-printable retention clasps. These clasps can be used on their own or in combination with other retention methods.
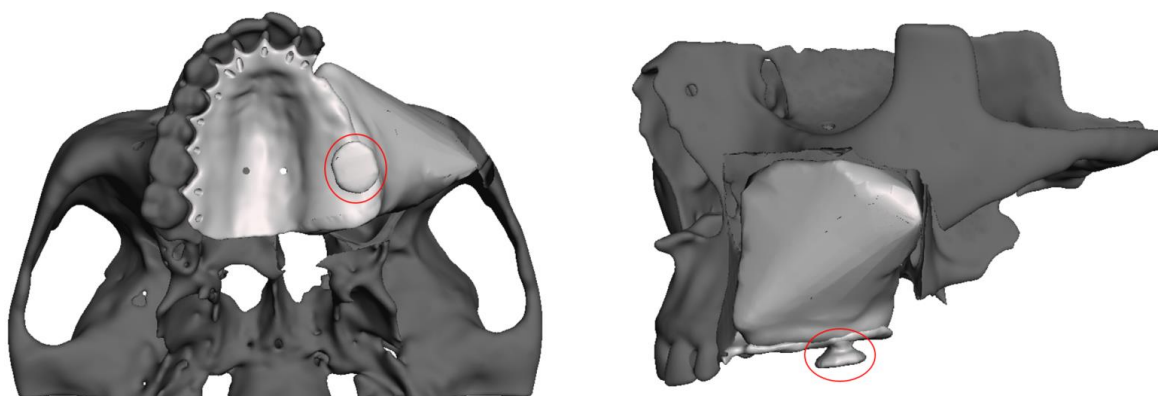


*Figure **6.3**. A digital design of an obturator, with the boulder delineated with red. A zygomatic wire can be placed around the boulder.*

This study aims to investigate the retentive value of these 3D-printed clasps in different combinations for different defects. This is done by performing a phantom study, which compares the retention clasps to the circumferential wires around the teeth in combination with the zygomatic wire and boulder. The retentive value of the clasps is also determined in combination with a palatal screw. These tests are performed for each NKI class, as stated in Chapter 3. The retentive value is measured as displacement under simulated forces of deglutition and wound tissue contraction and exudate, where less displacement means better retention.

## Methods

This phantom study includes skull phantoms in a steady mounting frame, obturators with different retention method combinations, a tongue phantom and a spring balance, which will be elaborated on in this method section.

The goal of the phantom study is to determine the displacement of the obturators relative to the skull phantom under two forces: deglutition and the outward force of tissue contraction and exudate. To determine this displacement, electromagnetic (EM) tracking is used. Two EM sensors are placed: one on the skull ($S_S$) and one on the obturator ($S_O$). This section elaborates on the measurements and set-up.

**Skull phantom and mounting frame design and fabrication**

Chapter 3 proposes a new classification system for the design of hISOs. This study aims to determine the implications of the use of 3D-printed clasps for each of these classes.

A skull phantom is designed for each class to mimic the corresponding defect. A CT scan and intraoral scan of a subject are used to design the skull phantom. As in the CAD/CAM workflow for the hISO, a skull segmentation is derived from the CT scan. This segmentation is merged with the intraoral scan in Artec Studios (Artec, Senningerberg, Luxembourg) to include more dental detail into the skull phantom. Also, the bone segmentation of the CT scan only includes the palatal bone, so the merge with the IOS provides the mucosal anatomy of the upper jaw. To shorten fabrication time and decrease costs, only the region of interest is included in the final digital design, including the maxilla and the zygomatic arch. Holes are created between the teeth present on the phantom to mimic the interproximal space, which is important for the circumferential wires around the teeth. Figure **6.4** shows the final designs of all seven skull phantoms. Note the adapters, for fixation to the mounting frame, which will be elaborated on later on.

All skulls are 3D-printed using a Formlabs SLA printer (Formlabs, Somerville Mas., U.S.) in Formlabs Tough 1500 Resin. To mimic the mucosa on the hard palate, a thin layer of tissue conditioner (Coe-Soft, GC America Inc., Alsip, IL, U.S.A.) is put on the palate of all phantoms.
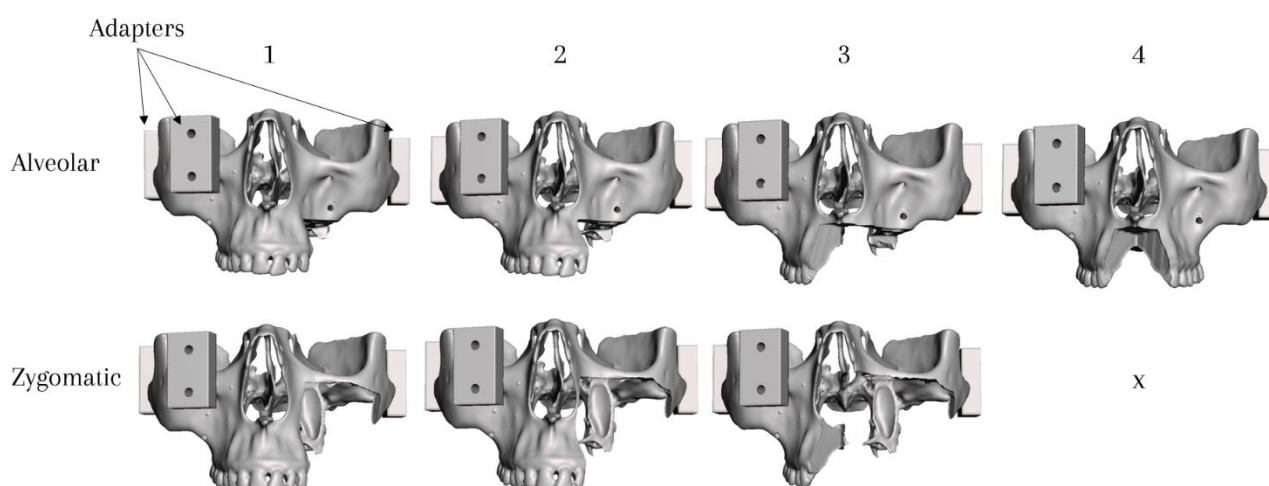


*Figure **6.4**. Seven digitally designed phantom skulls, each representing another NKI class defect. Note the adapters on the designs, for easy and repeatable montage on a mounting frame.*

The mounting frame (see Figure **6.5**) is made out of non-magnetic parts to minimize the disturbance on the EM field during measurements. This means plastic poles, plates, screws and nuts are used. The frame consists of three poles (20x20x200 mm) with vertical notches. As seen in Figure **6.4**, the skull phantoms have adapters, each corresponding to one pole. A screw and nut can be put through the adapter, and slide into the notch of the pole. This way, the skull phantoms can be easily swapped and tightly secured. Figure **6.6** also shows these adapters, to ensure the right location to the poles.

The base plate and tongue plate are made out of Perspex, which have been laser cut into the right shape. The tongue plate includes windows, so it can slide over the poles. Windows are cut into the tongue plate for it to slide over de poles, after which it is fixated on the right height with corner brackets. The poles are screwed onto the baseplate.
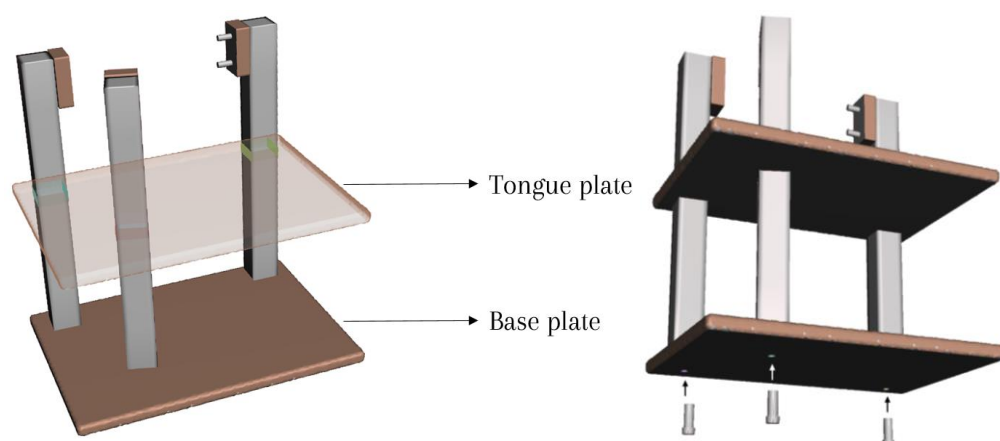
*Figure 6.5. Digital design of the mounting frame for the skull phantoms. The frame exists of a baseplate, tongue plate and three poles that are screwed into the baseplate. The tongue plate has windows to fit over the poles and is fixated on the right height with corner brackets in the eventual set-up. The image also shows the adapters on top of the poles, to determine their right location when added to the skull phantoms.*
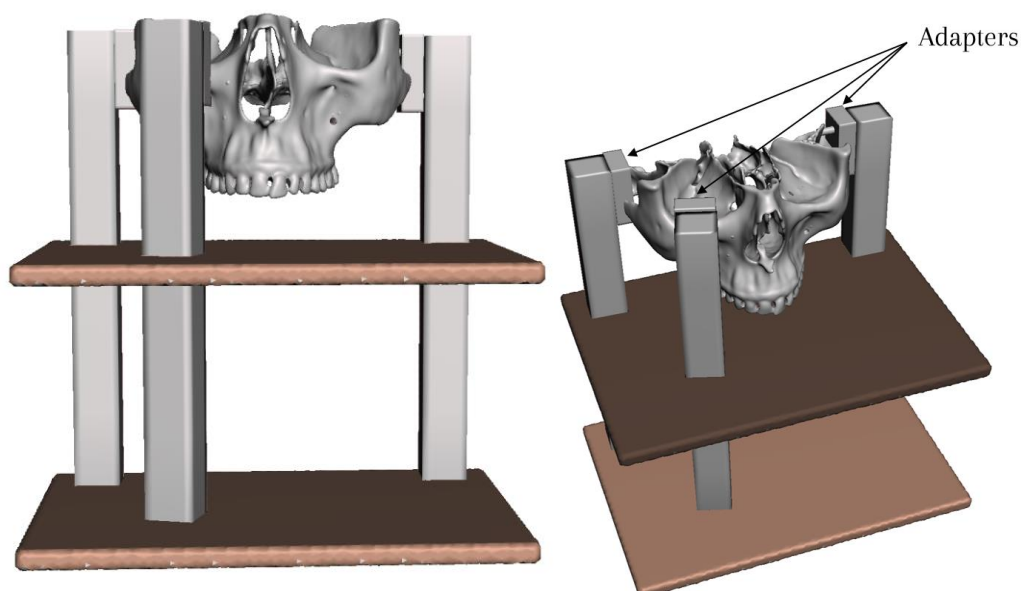


*Figure 6.6. Digital design of the mounting frame with a skull phantom. The adapters are now positioned to the skull phantom, to ensure the right fit.*

## Obturators

For each skull phantom, four 3D-printed hollow obturators are designed according to the state-of-the-art workflow to test the retention methods, each with different combinations of retention methods (see Figure 6.7):

1. Zygomatic wire and boulder + circumferential wires
2. Zygomatic wire and boulder + 3D-printed retention clasps
3. Palatal screw + 3D-printed retention clasps
4. Palatal screw

These designs also include two extra holes so a string can be inserted through them to apply a pulling force to the obturators. These obturators are 3D-printed using the Formlabs SLA printer with Clear V4 Resin.

*Figure **6.7**. Four different combinations of retention methods. 1) Zygomatic wire and boulder, and circumferential wires around M1 and C; 2) zygomatic wire and boulder, and 3D printed retention clasps; 3) palatal screw, and 3D printed retention clasps; and 4) palatal screw. Note the extra holes for a string to be inserted through so a pulling force can be applied to the obturators.*

### Tongue phantom
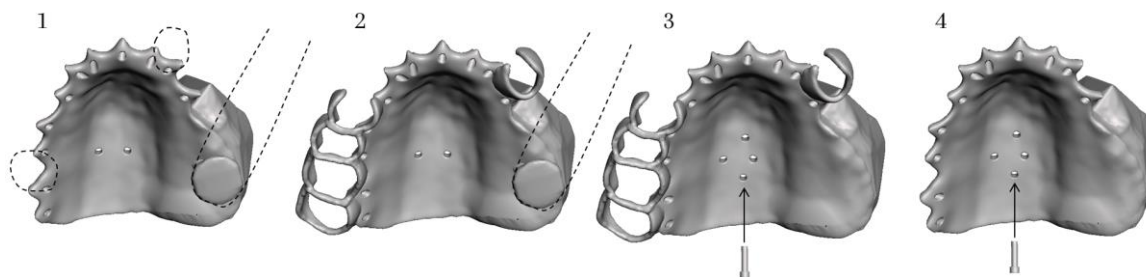
To mimic deglutition, a silicone tongue is developed with three air-filled pockets (anterior, medial, posterior) that can be inflated separately. To create this tongue phantom, a mould is designed in Autodesk Meshmixer (RRID:SCR_015736, ©2020 Autodesk, Inc.), being a block with a cavity in the dimensions of a relaxed tongue that fits within the width of the skull phantom palate (see Figure **6.8**). To ensure enough space for the fixation of tubes to the air pockets, the tongue phantom is longer than the palate.

To get air-filled pockets inside this silicone tongue, a lid is designed that fits onto the mould. This lid has three stems with balls. When the mould is filled with silicone, these stems and balls will ensure a pocket inside the silicone. The stems create connecting tubes, enabling air to get to the pockets separately. Figure **6.9** shows the design of the mould and lid.
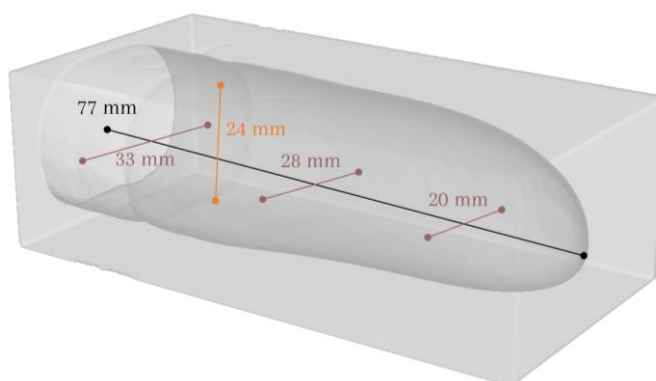


*Figure **6.8**. The design of a mould for a silicone tongue. The measurements are that of a relaxed tongue that will fit into the palate of the skull phantom, with a somewhat extended length.*
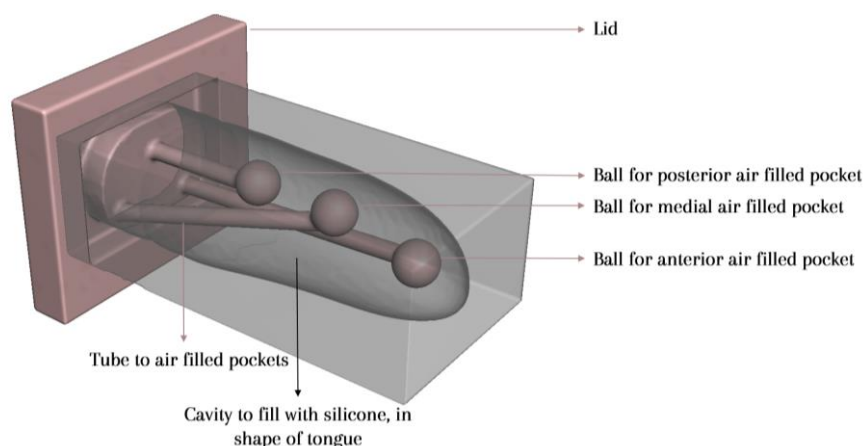


*Figure **6.9**. The digital design of the mould and lid for a silicone tongue phantom with three air pockets. The lid is shown in pink, fitting onto the mould in one way. The lid has three balls with connecting tubes, creating air pockets into the silicone when the mould is filled.*

The mould and lid are also 3D printed with the Formlabs SLA printer. A flexible silicone (EcoFlex 00-30, Smooth-On, Inc. Macungie, Pennsylvania, U.S.A.) is mixed as intended and put in a vacuum chamber to release air bubbles inside the mixture. The mixture is poured into the mould and once again put into the vacuum chamber. The lid is placed onto the mould and all together it is set away to cure for at least 4 hours. After curing, tubes are inserted into the channels. These tubes are connected to a pneumatic valve, which allows air to flow with a certain pressure for a standardized time, expanding the air pockets alternately from anterior to posterior. The time and pressure are set so that on each location, a TPP pressure of 17 kPa is applied. This is tested with the Iowa Oral Performance Instrument (IOPI Medical LCC, Redmond, Washington). A schematic image of the final set-up of the tongue phantom is shown in Figure **6.10**.



*Figure **6.10**. Set-up to determine the displacement of an obturator relative to a skull phantom. A skull phantom is mounted into a frame with adapters, in which an obturator is placed. The silicone tongue phantom with three air-filled pockets is placed on the tongue plate under the skull. The tongue phantom is attached to a pneumatic valve, which allows air to flow to the air pockets alternately from anterior to posterior, creating a 17-kPa pressure between the tongue and the palate. Both the skull and the obturator have an EM sensor to determine the displacement.*

### Contacting scar tissue

To mimic the force of the contracting wound tissue and exudate pushing the bulb out, a pulling force is applied to the obturator. All obturators have two holes around the centre where a string can be put through (see Figure **6.7**). A non-elastic, strong rope is used. The rope is pulled down through a hole in the tongue plate, and at the end hooked to a spring balance, on which the force in Newton can be seen during pulling. Figure **6.11** shows a schematic image of the set-up.
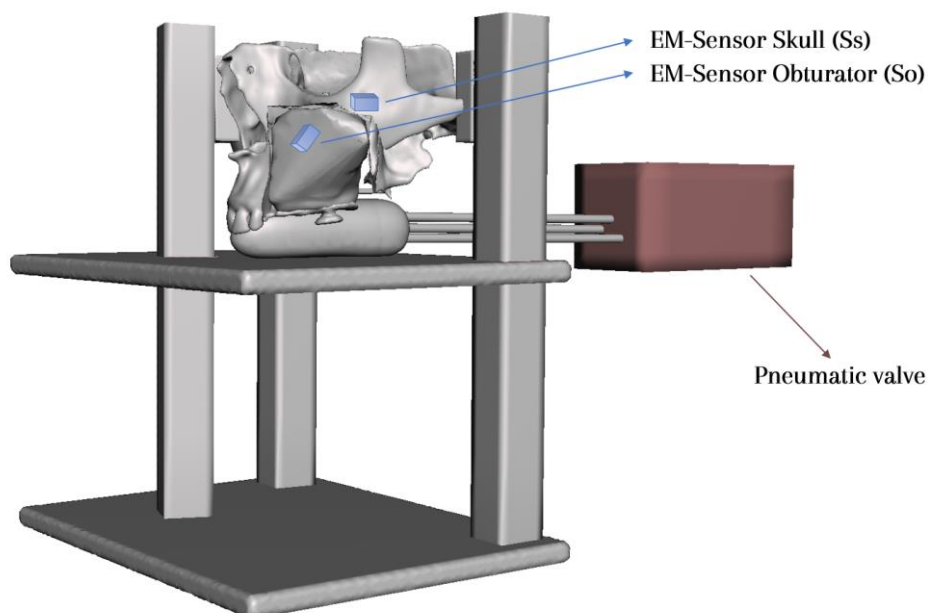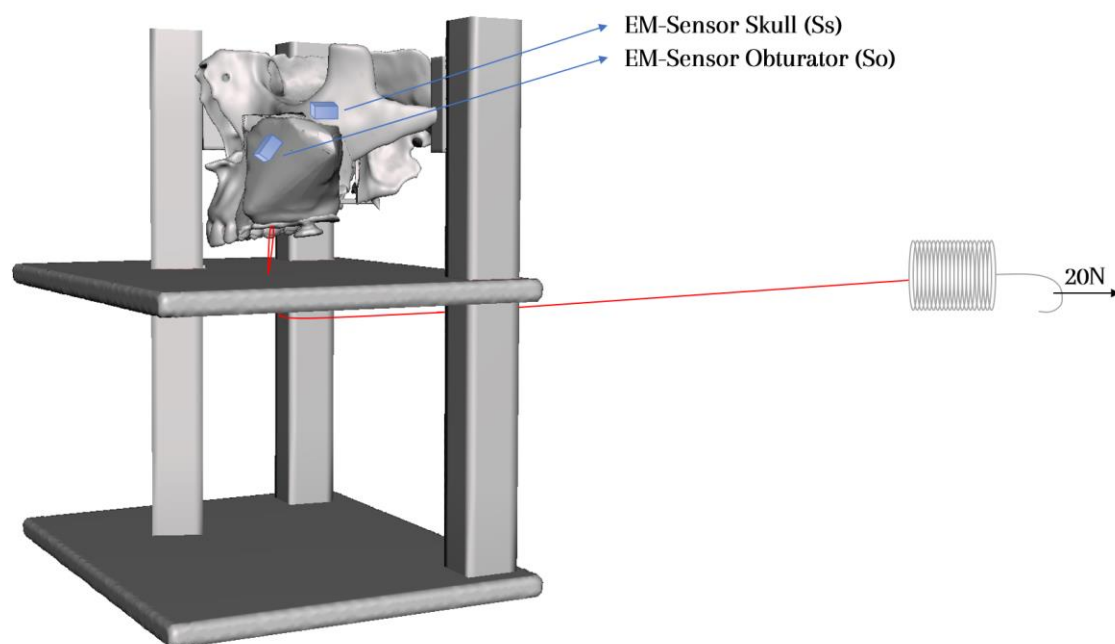
*Figure **6.11**. Set up for the pull test to determine the displacement of an obturator relative to a skull phantom. The skull phantom is mounted into a steady frame with adapters. A fitting obturator is placed into the skull phantom, with a string attached. This string is put through a hole straight down and attached to a spring balance, which is pulled with 20 N. Both the skull and the obturator have an EM sensor to determine the displacement.*

## Measurement protocol

The set-up is placed in the EM field of the NDI Aurora planar field generator. Two cable tools are used with both a 6DOF sensor at the tip. For each skull phantom, the measurement protocol is as follows:

1. Place obturator 1 as intended and add the string through both holes. Pull the string through the tongue plate.
2. Place EM sensor $S_O$ on the bulb of the obturator.
3. Place EM sensor $S_S$ on the skull, close to the field generator.
4. Perform a baseline measurement of 6 seconds.
5. Start a measurement of six seconds when no force is applied to the obturator, pull with 20 Newton and release the force before the measurement is over.
6. Repeat step 5 nine times.

When the pulling measurements are completed, the tongue phantom is placed on the tongue plate. The measurement protocol is as follows:

1. Perform a baseline measurement for three seconds.
2. Start a measurement of three seconds, while each air pocket is inflated from anterior to posterior once.
3. Repeat step 2 nine times.

Now all measurements for the first skull phantom and obturator 1 are performed. Repeat for all obturators. When all four obturators are measured, change the skull phantom and repeat.

## Evaluation

The raw data from both EM sensors for all measurements are processed in MATLAB (The MathWorks, Inc., Natick, Mass). The Aurora has a 40 Hz measurement frequency. For each measurement sample, the distance between $S_S$ and $S_O$ is calculated by a double Pythagoras, after correcting the locations to the position of the sensors at the first sample. To be robust to possible outliers, the 95th percentile maximum displacement is taken for each measurement. This value is determined for all ten measurement rounds.

The first measurement is a baseline measurement, used to evaluate the error of the set-up. The 95th percentile displacement of the other nine measurements is taken together and shown in a boxplot with notches. With the use

of these boxplots and notches, the median of the 95<sup>th</sup> percentile maximal displacements can be compared between obturators per NKI class. The lower the maximal displacement, the stronger the retention method. When notches of two boxplots do not overlap, i.e. the blue or red shaded areas do not overlap, the median of the displacements of the respective obturators is different at a 5% significance level.

One goal is to compare the 3D-printed retention clasps to the conventional circumferential wires. Therefore, obturator 1 and 2 are compared to each other. Obturators 3 and 4 are compared to each other, to evaluate the added value of the 3D-printed retention claps in combination with a palatum screw.

Appendix C elaborates on the MATLAB script that is used for data processing and visualization.

## *Results*

Figure **6.12** shows the boxplots of the maximal displacement of each obturator during the deglutition test per skull phantom. Each boxplot exists of the maximal displacement of nine measurements performed per obturator. The line in the notches show the median of each set of these nine measurements. The x-axis shows numbers 1-4 representing which retention method combination is tested (see Figure **6.7**), and the skull phantom on which is tested (A1-Z3). The y-axis shows the displacement of the $S_O$ relative to the $S_S$ in millimetres.

For skull phantom A1, obturator 1 and 2 do not have overlapping notches, and the displacement of obturator 2 is less than for obturator 1. Obturator 3 has more displacement than obturator 4 with no overlapping notches. For skull phantom A2, obturator 2 has less displacement than obturator 1, with no overlapping notches. Obturator 3 has more displacement than obturator 4 without overlapping notches. For skull phantom A3, obturator 2 has less displacement than obturator 1. Obturator 3 has more displacement than obturator 4 with no overlapping notches. For skull phantom A4, obturator 2 has less displacement than obturator 1, with no overlapping notches. Obturators 3 and 4 have overlapping notches.

For skull phantom Z1, obturator 2 shows more displacement than obturator 1, with no overlapping notches. Obturators 3 and 4 have overlapping notches. For skull phantom Z2, obturator 1 and 2 have overlapping notches, and obturator 3 has less displacement than obturator 4 with no overlapping notches. For skull phantom Z3, obturators 2 and 3 failed, so no comparison is made.



*Figure **6.12**. Boxplots of the maximal displacement of each obturator during the deglutition test per skull phantom. Each boxplot exists of the maximal displacement of 9 measurements done per obturator. The notches show the median of each set of these nine measurements. The x-axis shows the retention method combination and skull phantom. The y-axis shows the displacement of the $S_O$ relative to the $S_S$ in millimetres.*

*\* No measurements are available because of clasp failure*

Figure **6.13** shows the boxplots of the maximal displacement of each obturator during the pull test per skull phantom. The axes are the same as for Figure **6.12**, but note the bigger displacement on the y-axis (2 mm instead of 0.6 mm). Obturator 2 of skull phantom A4 failed, so are obturator 2 and 3 for skull phantom Z3. These are not taken into account.

For skull phantom A1, obturators 1 and 2 have overlapping notches. Obturator 3 has a bigger displacement than obturator 4, with no overlapping notches. For skull phantom A2, obturator 2 has less displacement than obturator 1, with no overlapping notches. Obturator 3 has more displacement than obturator 4 with no overlapping notches. For skull phantom A3, obturator 2 has less displacement than obturator 1, with no overlapping notches. Obturator

3 had less displacement than obturator 4 with no overlapping notches. For skull phantom A4, obturators 3 and 4 have overlapping notches.

For skull phantom Z1, obturator 2 shows less displacement than obturator 1 with no overlapping notches. Obturator 3 shows more displacement than obturator 4 with no overlapping notches. For skull phantom Z2, obturator 2 has more displacement than obturator 1 with no overlapping notches. Obturators 3 and 4 have overlapping notches. No comparison is done for skull phantom Z3.
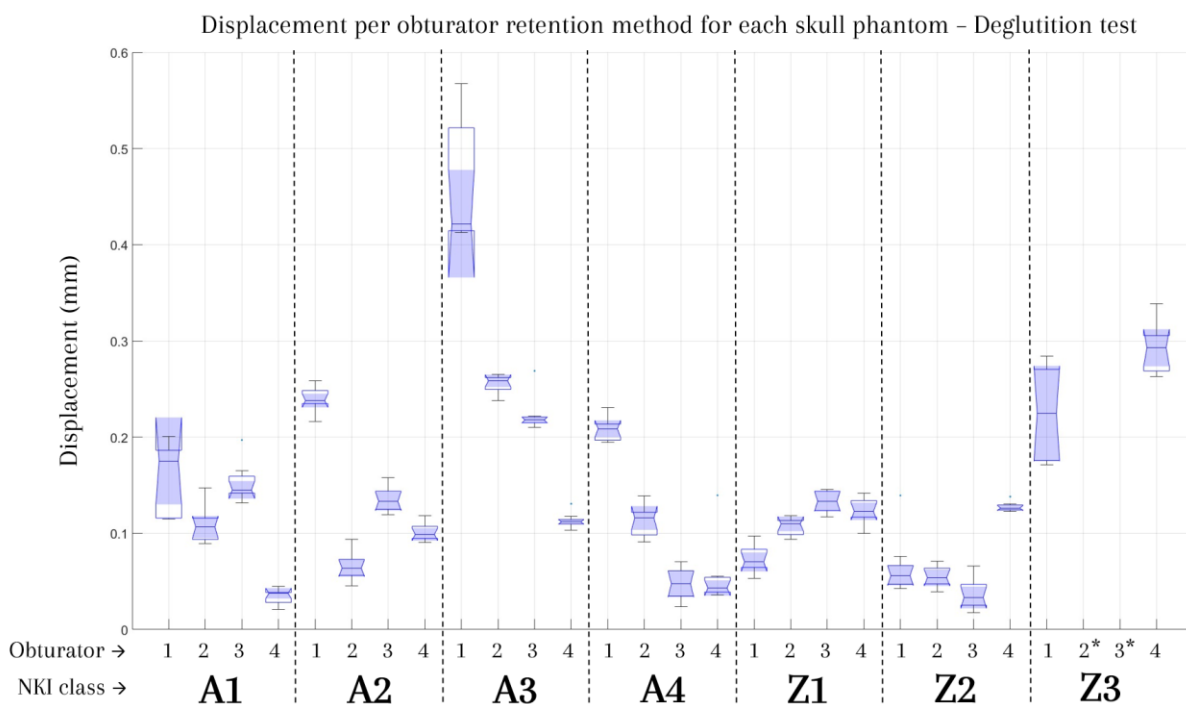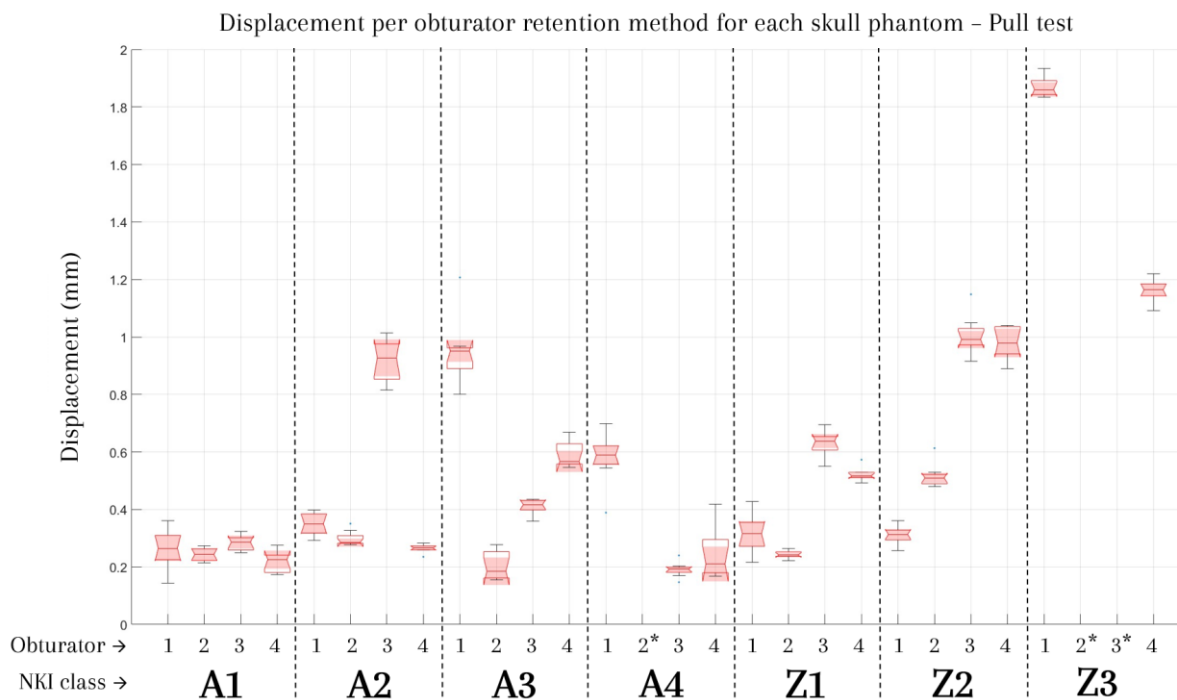


*Figure **6.13**. Boxplots of the maximal displacement of each obturator during the pull test per skull phantom. Each boxplot exists of the maximal displacement of 9 measurements done per obturator. The notches show the median of each set of these nine measurements. The x-axis shows the retention method combination and skull phantom. The y-axis shows the displacement of the $S_O$ relative to the $S_S$ in millimetres.*
*\* No measurements are available because of clasp failure*

Table **6.1** shows if obturator 2 provides equal or better retention compared to obturator 1, for the deglutition and pull test. It also shows if obturator 2 has an equal or better retention when results from both tests are combined.

Table **6.2** shows if obturator 3 has additional retentive value compared to obturator 4 for the deglutition and pull test, and for both tests combined.

**Table 6.1. Does obturator 2 show less displacement than obturator 1, or do both obturators have overlapping boxplot notches?**

|     | Deglutition test | Pull test | Combined |
|-----|:---:|:---:|:---:|
| A1  | ✔ | ✔ | ✔ |
| A2  | ✔ | ✔ | ✔ |
| A3  | ✔ | ✔ | ✔ |
| A4  | ✔ | ● | ✔ |
| Z1  | ✗ | ✔ | o |
| Z2  | ✔ | ✗ | o |
| Z3  | ● | ● | ● |

*Note - legend*

✔ obturator 2 shows less displacement than obturator 1, or the notches overlap.

✗ obturator 2 shows more displacement than obturator 1.

o contradictory results

● failed test.

**Table 6.2. Does obturator 3 show less displacement than obturator 4?**

|     | Deglutition test | Pull test | Combined |
|-----|:---:|:---:|:---:|
| A1  | ✗ | ✗ | ✗ |
| A2  | ✗ | ✗ | ✗ |
| A3  | ✗ | ✔ | o |
| A4  | ✗ | ✗ | ✗ |
| Z1  | ✗ | ✗ | ✗ |
| Z2  | ✔ | ✗ | o |
| Z3  | ● | ● | ● |

*Note - legend*

✔ obturator 3 shows less displacement than obturator 4.

✗ obturator 3 shows more displacement than obturator 4, or the notches overlap

o contradictory results

● failed test.

## Discussion

### Interpretation of results

This study aimed to assess the effectiveness of 3D-printed retention clasps in various combinations for different types of defects through a phantom study. This study involved a tongue phantom to simulate swallowing and a pull test to replicate the outward force caused by exudate and scar tissue contraction. The 3D-printed retention clasps were assessed in combination with a zygomatic wire and boulder. This combination showed comparable or superior retention when compared to circumferential wires around the teeth and a zygomatic wire for the alveolar classes of the NKI classification. For the zygomatic classes of the NKI classification, the clasps showed higher displacement during the tests or the clasps failed. In combination with a palatum screw, the 3D-printed clasps did not provide additional retentive value. The subsequent sections will provide further details on these comparisons.

### Retentive clasps in combination with a boulder and zygomatic wire (obturator 2 compared to obturator 1)

Table 1 shows that obturator 2 has better overall performance than obturator 1 for all alveolar classes (A1-A4). However, for the zygomatic classes, the results of the deglutition test of skull phantom Z1 and the pull test of skull phantom Z2 show more displacement with the retention clasps.

The 3D-printed retention clasps failed for skull phantom Z3, thus no comparison can be made. It is unclear whether the clasps would have failed during the deglutition test because they failed during the pull test that was performed first. The displacements for obturator 1 and 4 for skull phantom Z3 tend to be higher than for the rest of the skull phantoms. Therefore, it is not recommended to use the 3D-printed retention clasps for obturators in class Z3.

For skull phantom Z1, the difference in the median of obturator 1 and 2 is 0.04 (0.11 mm for obturator 2, 0.07 mm for obturator 1) during the deglutition test. It is debatable if this difference in displacement is clinically relevant. The median displacement of 0.11 mm is considered low, which implies that the clasps provide sufficient retention. With the pull test, obturator 2 showed lower displacement than obturator 1. Based on these results, the 3D-printed retention clasps seem useable for hISOs of class Z1.

For the pull test of skull phantom Z2, obturator 2 shows higher displacement than obturator 2. As the notches of obturator 1 and 2 overlap for the deglutition test, the medians are likely to be equal at a 5% significance level. However, it is challenging to draw conclusions based on these two contrasting results as no literature quantifies the extent of displacement and links it to prosthesis failure or dissatisfaction.

Based on these results, the 3D-printed retention clasps can be used for alveolar classes A1-A4 and the zygomatic class Z1. For the obturator of class Z3, the 3D-printed retention clasps are not recommended for use. More research is needed to determine the clinical cut-off value for the displacement linked to prosthesis dissatisfaction for obturators of class Z2. These results are in line with the expectation that retention for bigger and heavier obturators is more challenging[4–6,17,18].

### Retentive clasps in combination with a palatum screw (obturator 3 compared to obturator 4)

This comparison aims to evaluate the additional value of 3D-printed retention clasps when used in combination with a palatal screw, by comparing the retention provided by a palatal screw alone versus a combination of the palatal screw and 3D-printed retention clasps. The results showed that for skull phantoms A1 and A2, the addition of 3D-printed retention clasps did not result in additional retention. However, for skull phantom A3, the deglutition test showed a higher median displacement for obturator 3 than for obturator 4, while the pull test resulted in a lower median displacement for obturator 3 than for obturator 4. These contradictory results suggest that the additive retentive value of the 3D-printed retention clasps cannot be proven.

For skull phantom A4, obturators 3 and 4 have overlapping notches in both the deglutition and pull test, thus the addition of 3D-printed retention clasps did not provide additional retentive value. Similarly, for skull phantom Z1, overlapping notches are seen in the deglutition test. The pull test resulted in more displacement for obturator 3. Thus, the addition of 3D-printed retention clasps to hISOs of class Z1 did not provide additional retentive value in both tests.

However, for skull phantom Z2, the deglutition test showed additional retentive value for the 3D-printed retention clasps, while the pull test resulted in overlapping notches. These results are contradictory and thus the additive retentive value of the 3D-printed retention clasps cannot be proven. As for skull phantom Z3, the retention clasps

failed for obturator 3, so no comparison is made. The results imply not using the 3D-printed retention clasps for obturators in class Z3.

The results showing obturator 3 has more displacement than obturator 4 are unexpected since an extra retention method is added. For example, the pull test for A2 is a strange result, because the displacement is much more for obturator 3 than for obturator 4 (0.92 mm and 0.26 mm resp.). This difference suggests that the retention clasps might have affected the screw's performance or the obturator's fit. However, this is not noticed during measurements.

### Overall retention deglutition test

Overall, the values seen as displacement during the deglutition test are small between 0.03 mm and 0.29 mm. Therefore, it seems that all retention methods could suffice for these forces during swallowing for maxillectomy patients with obturators of all seven NKI classes. The measurement of obturator 1 on skull phantom A3 shows a divergent result, with a median displacement of 0.42 mm.

### Overall retention pull test

The displacement values resulting from the pull test are higher than those resulting from the deglutition test. This can be explained by the bigger force that is exerted on the hISOs. In addition, this force is one-directional, pulling the hISOs down. Overall, the hISO with a boulder and zygomatic wire and the 3D-printed retention clasps seem to provide the most retention. For skull phantom A4, the retention clasps failed, due to the bilateral position of the clasps as described in Chapter 4. Displacement of both the hISOs for skull phantom Z3 show higher displacement, and the retention clasps failed after the first pull. This is in line with larger and heavier bulbs being more challenging in terms of retention.[17,18] This test shows that the retention for bigger obturators such as class Z3 is indeed challenging, even with the weight reduction of 36-39%[10].

Although the displacement values are higher than for the deglutition test, all retention methods for the alveolar classes (except the failed obturator 2 for class A4) and all retention methods for zygomatic classes Z1 and Z2 show a displacement median smaller than 1 mm. It is important to determine which extent of displacement causes prosthesis problems for the patient. A test could be performed, in which air and fluid leakage as measurable results are linked to displacement of their obturator.

## Limitations

### Retentive clasps in combination with a boulder and zygomatic wire

With this phantom study, the 3D-printed retention clasps are compared to the circumferential wires for the CAD/CAM hISO. For the implementation of the hISO with these retention clasps, a comparison with the conventional ISO is desirable. There is no quantitative data on the failure or the displacement of the conventional ISO. Therefore, it is a challenge to state that the 3D-printed hISO with 3D-printed retention clasps and a zygomatic wire provide better - or at least the same - retention as a conventional ISO of the same dimensions with Adams clasps and a zygomatic wire. For clinical testing and implementation, it is very important to prove that the 3D-printed hISO and its clasps are comparable to the conventional ISO.

### Palatal screw

In the clinical situation, the palatal screw is fixated into the remnant hard palatal shelf. The bone quality and quantity play important roles in the success of the palatal screws [19,20]. The hard palate is often mentioned in literature as a place for orthodontic implants or mini-screws, due to the relatively thick bone height and good quality. Unfortunately, the literature also mentions a great individual variability between the anatomy of the hard palate, and thus the vertical bone height of the palate and the bone quality [21,22]. There is a lack of literature about the use of palatal screws for obturators specifically, but the literature on mini-screws shows that the success of the palatal screw is very dependent on patient anatomy.

With this phantom study, the skull phantoms are 3D-printed in Formlabs Tough 1500 Resin, and holes are predrilled into the skull phantom where the screws are fixated into. This is not directly comparable to the clinical situation, since the resin palate does not include layers representing cortical and trabecular bone and does not vary in bone quality and quantity. The vertical bone thickness is true to the anatomy since the skull phantom is directly based on a bone segmentation from a CT scan.

**Overall measurement limitations**

During the measurements, the retention clasps failed for three obturators during the pull test. This was for class A3 and Z3, with both little dentition available for retention. The canine was not included in the retention, which resulted in a suboptimal retention configuration. The results are in line with the literature, stating that retention is more challenging for bigger and heavier obturators. Therefore, it was expected to see bigger displacements, but failure of the clasps was not expected.

The comparison measure in this study is the median, which is determined by an in-built function of MATLAB boxchart. The median is robust for outliers. This measure is chosen because the test is prone to outliers, especially the pull test which is not standardized. In the clinical situation, the maximal displacement is important. When a patient swallows for instance 500 times a day, it is even discouraging if the obturator fails 1 of those times. Because the pull test is not standardized, the median is likely to be associated with the displacement caused by a 20 Newton pull. It could be beneficial to standardize the pull test, and also take into account the maximal value of the maximal displacement per test.

It is also important to mention that the chosen 20 Newton for the pull test is not based on literature or calculations and is reasonably an overestimation. Therefore, the maximal displacements cannot be seen as an absolute displacement happening due to the wound tissue shrinkage and exudate. They have to be seen relative to each other. In addition, the rope is attached to the centre of the obturator. For a proper simulation of the pushing force, the rope should be attached to the centre of gravity of the bulb, or in its vertical line.

The average tongue palate pressure derived from Chapter 5 is used for the deglutition test. It is debatable whether the maximal pressure should have been used to test the maximal displacement because the retention must resist that force. In addition, with the deglutition test a force against the palate with the tongue phantom is provided. This way, the measurements are not solely about retention. According to the definition of retention and support, this test is also looking at the support of the clasps. This is not evaluated specifically in the results. Our initial expectation was the clicking of the obturator due to the force change from anterior to posterior. This was not seen during the tests.

The results of this study are based on the displacement measured with the EM trackers. 6DOF sensors were used, so rotations were also measured but not evaluated. This can be used to evaluate the additional value in the stability of the 3D-printed retention clasps. The use of EM trackers can also be debated. The two main navigation technologies are optical tracking and EM tracking. Optical tracking is very robust to environmental conditions, but the limitation is that a direct line-of-sight is needed between the optical markers and the camera

-up.[23] Within this research, the EM navigation set-up was easily accessible, but optical tracking could enable the phantom set-up to be made of metal and be more rigid.

Overall, the skull phantoms have the true anatomy of a patient but are different from the clinical situation. The teeth are printed as smooth as possible, but true dental enamel together with saliva probably gives less resistance to retention clasps than plastic on plastic. Therefore, these results could overestimate the retention that is provided by the 3D-printed retention clasps. On the other hand, the comparison between the four different obturators is not affected because the set-up is the same.

## *Future perspective*

The present study highlights the limitations of the 3D-printed hISO and retention clasps, which have not been compared to the conventional ISO. To ensure the clinical testing and implementation of the 3D-printed hISO and retention clasps, it is essential to establish that they are at least as retentive as the conventional ISO. Future studies should perform a comparison with conventional ISOs to gain quantitative insight into the retention methods for conventional ISOs, which is currently lacking.

To define "sufficient retention", there is a need for a clinical cut-off value for the displacement of an obturator. There is little to no information about obturator satisfaction linked to displacement of the obturator. Some studies examined the quality of life (QOL) of patients wearing an obturator after maxillectomy, but none linked the QOL to retention, stability and support in a quantitative way.[24–27] Therefore, future studies should perform clinical measurements to quantify the retention, stability and support and link it to patients' prosthesis satisfaction. This could be quantified by measuring the water and air leakage for certain displacements.

Another important factor is the retention of heavy and big bulbs. This study substantiates that retention is challenging for big and heavy bulbs. Therefore, for obturators of class A3, Z2 and Z3 it would be beneficial to look

into different retention methods. A successful retention option mentioned in literature is zygoma implants (ZI), placed into the reminiscing zygoma bone.[28–30] ZI improve the masticatory performance of patients directly after maxillectomy.[31] Mousa et al.[18] wrote a review about finite element studies for biomechanical stress in obturators. They compare ZI with dental implants (DI), often used for definitive obturators. DI have to consolidate into the residual alveolar or maxillary bone, which takes up to 6 weeks. Therefore, DI are not useful for the retention of surgical obturators. For ZI, surgical planning is mandatory because little anatomical landmarks are present, and it is important not to intrude the orbital floor with the risk of ocular perforation.[32] Also, the extent of residual bone is dependent on the maxillectomy planning. ZI are also useful for the retention of obturators for edentulous maxillectomy patients. Future studies should evaluate if ZI are a valid retention method for the CAD/CAM hISO.

The use of 3D-printed clasps in the hISO possibly allows it to serve as an interim obturator, meeting the requirement of easy removal. This is especially advantageous compared to fixation with wires. However, retention clasps are not indicated for use with palatal screws according to this study. Future research should aim at evaluating the retention of clasps without additional retention methods.

## Conclusion

In conclusion, this study assessed the retentive value of 3D-printed retention clasps in each class of the NKI classification, in combination with zygomatic wires and palatal screws in a phantom study. The study simulated deglutition, as well as the outward force of contracting scar tissue and post-op wound exudate. The 3D-printed retention clasps showed positive retentive value when used with zygomatic wires. However, the clasps were not recommended for use in combination with palatal screws. The study also revealed more displacement of the obturators in the zygomatic classes. Therefore, future research should look into alternative retention methods such as zygoma implants.

# REFERENCES

1.    The Glossary of Prosthodontic Terms: Ninth Edition. *J Prosthet Dent*. 2017;117(5):e1-e105. doi:10.1016/j.prosdent.2016.12.001

2.    Singh M, Kapoor S, Kumar L, Pal US, Singh A, Anwar Mohd. Prevalence of maxillectomy defects among patients visiting in an institutionalized hospital setting: A prospective, single-institute study. *Natl J Maxillofac Surg*. 2020;11(2):231. doi:10.4103/NJMS.NJMS_61_20

3.    Mehta S, Mascarenhas E. *Closed Hollow Obturator-An Elixir to the Cancer Patients*. Vol 2.; 2014. www.ijss-sn.com

4.    Devlin H, Barker GR. *Prosthetic Rehabilitation of the Edentulous Patient Requiring a Partial Maxillectomy*.

5.    Keyf F. Review Obturator prostheses for hemimaxillectomy patients. doi:10.1111/j.1365-2842.2001.00754.x

6.    Dalkiz M, Dalkiz AS. The Effect of Immediate Obturator Reconstruction after Radical Maxillary Resections on Speech and other Functions. *Dent J (Basel)*. 2018;6(3). doi:10.3390/DJ6030022

7.    Wu Y low, Schaaf NG. Comparison of weight reduction in different designs of solid and hollow obturator prostheses. *J Prosthet Dent*. 1989;62(2):214-217. doi:10.1016/0022-3913(89)90317-X

8.    Tanaka Y, Gold H 0, Pruzansky S. *A Simplified Technique for Fabricating a Lightweight Obturator*.

9.    Steenhuis A. *Fabrication Process of Maxillary Hollow Bulb Immediate Surgical Oburator Using Intraoral Scanning Technology and Computer Aided Design/Manufacturing*:; 2021.

10.   Ooms A. Optimized and user-friendly workflow for the fabrication of 3D printed maxillary hollow closed surface model obturator using CT, intraoral scanning technology, and computer aided/manufacturing | Master Thesis. 2022;(October).

11.   Murat S, Gurbuz A, Isayev A, Dokmez B, Cetin U. Enhanced retention of a maxillofacial prosthetic obturator using precision attachments: Two case reports. *Eur J Dent*. 2012;6(2):212-217. http://www.ncbi.nlm.nih.gov/pubmed/22509126

12.   Maxillary Prostheses | Iowa Head and Neck Protocols. Accessed January 11, 2023. https://medicine.uiowa.edu/iowaprotocols/maxillary-prostheses

13.   Circum-zygomatic wiring model. | Download Scientific Diagram. Accessed November 1, 2023. https://www.researchgate.net/figure/Circum-zygomatic-wiring-model_fig4_352509564

14.   Specialty Appliances Orthodontic Laboratory | Appliance. Accessed November 1, 2023. https://www.specialtyappliances.com/appliance.php?appliance=43

15.   Craniofacial and Maxillofacial Prosthetics | Plastic Surgery Key. Accessed November 1, 2023. https://plasticsurgerykey.com/craniofacial-and-maxillofacial-prosthetics/

16.   Yamaguchi S. A new design of mini-screw anchored maxillary molar distalizing device applying CAD/CAM technology. *Oral Health and Care*. 2019;4(3). doi:10.15761/OHC.1000170

17.   Patil PG, Patil SP. A hollow definitive obturator fabrication technique for management of partial maxillectomy. *J Adv Prosthodont*. 2012;4(4):248. doi:10.4047/JAP.2012.4.4.248

18.   Mousa MA, Abdullah JY, Jamayet NB, Alam MK, Husein A. Biomechanical stress in obturator prostheses: A systematic review of finite element studies. *Biomed Res Int*. 2021;2021. doi:10.1155/2021/6419774

19.   Bourassa C, Hosein YK, Pollmann SI, et al. In-vitro comparison of different palatal sites for orthodontic miniscrew insertion: Effect of bone quality and quantity on primary stability. *American Journal of Orthodontics and Dentofacial Orthopedics*. 2018;154(6):809-819. doi:10.1016/J.AJODO.2018.02.010

20.   Marquezan M, Lima I, Lopes RT, Sant'Anna EF, Gomes De Souzac MM. Is trabecular bone related to primary stability of miniscrews? *Angle Orthod*. 2014;84(3):500-507. doi:10.2319/052513-39.1

21.     Winsauer H, Vlachojannis C, Bumann A, Vlachojannis J, Chrubasik S. Paramedian vertical palatal bone height for mini-implant insertion: A systematic review. *Eur J Orthod.* 2014;36(5):541-549. doi:10.1093/ejo/cjs068

22.     King KS, Lam EW, Faulkner MG, Heo G, Major PW. Vertical bone volume in the paramedian palate of adolescents: A computed tomography study. *American Journal of Orthodontics and Dentofacial Orthopedics.* 2007;132(6):783-788. doi:10.1016/J.AJODO.2005.11.042

23.     Sorriento A, Porfido MB, Mazzoleni S, et al. Optical and Electromagnetic Tracking Systems for Biomedical Applications: A Critical Review on Potentialities and Limitations. *IEEE Rev Biomed Eng.* 2020;13:212-232. doi:10.1109/RBME.2019.2939091

24.     Irish J, Sandhu N, Simpson C, et al. Quality of life in patients with maxillectomy prostheses. *Head Neck.* 2009;31(6):813-821. doi:10.1002/hed.21042

25.     Ali MM, Khalifa N, Alhajj MN. Quality of life and problems associated with obturators of patients with maxillectomies. *Head Face Med.* 2018;14(1). doi:10.1186/s13005-017-0160-2

26.     Kumar P, Alvi HA, Rao J, et al. Assessment of the quality of life in maxillectomy patients: A longitudinal study. *Journal of Advanced Prosthodontics.* 2013;5(1):29-35. doi:10.4047/jap.2013.5.1.29

27.     Depprich R, Naujoks C, Lind D, et al. Evaluation of the quality of life of patients with maxillofacial defects after prosthodontic therapy with obturator prostheses. *Int J Oral Maxillofac Surg.* 2011;40(1):71-79. doi:10.1016/J.IJOM.2010.09.019

28.     Schmidt BL, Pogrel MA, Young CW, Sharma A. Reconstruction of extensive maxillary defects using zygomaticus implants. *Journal of Oral and Maxillofacial Surgery.* 2004;62(SUPPL. 2):82-89. doi:10.1016/J.JOMS.2004.06.027

29.     Noh K, Pae A, Lee JW, Kwon YD. *Fabricating a Tooth-and Implant-Supported Maxillary Obturator for a Patient after Maxillectomy with Computer-Guided Surgery and CAD/CAM Technology: A Clinical Report.*

30.     Wang M, Qu X, Cao M, Wang D, Zhang C. Biomechanical three-dimensional finite element analysis of prostheses retained with/without zygoma implants in maxillectomy patients. *J Biomech.* 2013;46(6):1155-1161. doi:10.1016/j.jbiomech.2013.01.004

31.     Corsalini M, Barile G, Catapano S, et al. Obturator prosthesis rehabilitation after maxillectomy: Functional and aesthetical analysis in 25 patients. *Int J Environ Res Public Health.* 2021;18(23). doi:10.3390/ijerph182312524

32.     Sender B, Lacroix T, Jaby P, Chaux-Bodard AG. Are zygomatic implants a simple and reliable technique for the stabilization of obturator prostheses? Case report and review of the literature. *Journal of Oral Medicine and Oral Surgery.* 2020;26(2):12. doi:10.1051/mbcb/2020002

# CHAPTER 7. GENERAL DISCUSSION

# Chapter 7.
# General Discussion

## *Overall discussion*

This research aimed to provide the 3D-printed hollow immediate surgical obturator (hISO) with retention. The Chapters of this research all contributed towards an evaluated design of 3D-printable retention for the hISO. The results of the phantom study demonstrate that it is best to use the 3D-printed clasps in combination with a 3D-printed boulder and zygomatic wires. This research provides a workflow for the design of these retention clasps, based on the intraoral scan (IOS) of a patient. It also provides insight into the retention methods and their sufficiency for each class in the proposed NKI classification. With the addition of retention, the 3D-printed hISO is one step further towards clinical testing and implementation within the NKI-AvL.

Retention for obturators is complex because it is dependent on many patient-specific and therapy-dependent factors. To create retention methods for the 3D-printed hISO, we mimicked the methods that are used for the conventional ISO. Specifically for an ISO, the obturator must stay in place to reduce the flow of exudates post-operative, to maintain a clean wound and to hold the skin graft in place when this is needed, and to keep the lip and cheek in position to compensate for scar tissue shrinkage.[1]

To mimic the retention methods of the conventional ISO to the hISO, a 3D-model of a bolder is developed, which can be scaled and added to the digitally designed baseplate on the same location as on the conventional ISO (first molar). A zygomatic wire can be attached to this bolder. For the palatum screws, holes are added to the design. This could also be done after printing, as is done with the conventional ISO. Holes for circumferential wires are also included in the hISO design. To mimic the retention clasps of the conventional ISO, Chapter 4 proposes a CAD/CAM workflow that is developed together with the expertise of a dental technician and a maxillofacial prosthodontist. This resulted in an addition to the existing CAD/CAM workflow for the fabrication of the one-piece hISO including retention clasps.

To evaluate these retention clasps, a phantom study was set up. The retentive value of the 3D-printed retention clasps is evaluated, by determining the displacement of obturators with different combinations of retention methods, for two clinically relevant forces: the force of the wound exudate pushing the bulb outwards, and the force of the tongue during deglutition. To determine the latter, a tongue-palate-pressure (TPP) test is performed on three healthy female subjects. Three locations of the tongue are evaluated: anterior, medial and posterior on the hard palate. The test showed an average pressure of 17 kPa, with no significant difference between the three locations. This is not in line with the results from Yano et al.[2] and Miller et al.[3], who found significant differences in TPP. An explanation could be the size of the balloon of the IOPI, causing the locations to overlap. Another explanation could be the bolus size and viscosity, which both influence the TPP.[3–5] These results are measured for healthy young female subjects. Age can affect tongue pressure, but the literature is inconclusive as to whether gender affects tongue pressure. Ogino et al.[6] performed a retrospective analysis of tongue function and swallowing in maxillectomy patients, and found impaired EAT-10 scores. They also mentioned the importance of obturator retention, because bad retention can lead to impaired tongue functions that can cause dysphagia.

The force of the shrinking scar tissue and the wound exudate is mimicked with a pull test: a non-elastic, strong rope is attached to the obturators, through a hole directly under the obturator. At the end of this rope, a spring balance is attached. This spring balance pulls with a force of 20 Newton on the obturator, mimicking the outward push. There is no literature about this outward pushing force. To extensively test the retention, 20 Newton is chosen as a pulling force. This could well be an overestimation.

The phantom study compared different combinations of retention. Results showed that the 3D-printed retention clasps had better retention than the circumferential wires around the teeth when both in combination with the zygomatic wire for the alveolar classes (A1-A4) and class Z1. For class Z2, greater displacements were seen, and for class Z3 the retention failed. This is in line with the expectation that retention for heavier obturators is more challenging[7–11].

The phantom study showed that the retention clasps did not add retentive value in combination with the palatum screw. The displacement was often higher for the combination of the palatum screw and the retention clasps than

for the obturator with only the palatum screw. This is not expected, because with both obturators, the screw is fixated the same way into the skull phantom. An explanation could be that the retention clasps altered the fit of the baseplate in such a way that the screw is not as tightly screwed. This is not noticed during the tests. Another explanation could be the fact that the palatum screws are normally screwed into the bone. With this phantom study, the screw is placed onto hard resin (Tough 1500, Formlabs). It could cause the screw to be less (or more) fixated, but this does not explain the difference between the displacement with and without retention clasps.

Overall, with this research, a CAD/CAM workflow is created for retention clasps, that are proven 3D-printable together with the hISO. The phantom study substantiates the use of 3D-printed retention clasps and zygomatic wires for the 3D-printed hISO for most of the NKI-obturator classes, but for the big obturators of class Z2 and Z3, retention remains a challenge, even in the phantom study. The addition of retention is a big step towards the implementation of this 3D-printed hollow ISO.

The literature describes the use of CAD/CAM and 3D-printing for the fabrication of hollow obturators. Nyiresy et al.[12] wrote a review about the role of CAD/CAM and 3D-printing in head and neck oncologic surgery. The conclusion states that CAD/CAM and 3D-printing are consistently shown to decrease intraoperative time. In addition, the high costs and delayed manufacturing can be mitigated when in-house workflows are developed. This substantiates the goal of this research line to create the workflow for the fabrication of the hISO in-house. A barrier to this goal is the MDR law, which makes it more difficult to get workflows approved.

Bartellas et al.[13] looked into the creation of a low-cost 3D-printed obturator for rural areas. Meshmixer is free software, and with the use of 3D-scanning with a phone, the patient-specific CT scan may become redundant. Their conclusion is positive towards the applicability of the CAM/CAM and 3D-printing workflow for rural areas.

Tousopoulos et al.[14] describe a method where the 3-month postoperative CT scan is 3D-printed and used as a cast for the design of an interim obturator. Koyoma et al.[15] describe a workflow for the design of a hollow definitive obturator, using a 3D-scan of the definitive cast and hemi-maxillectomy area. The bulb is digitally designed and 3D-printed, and attached to a conventionally fabricated baseplate. They state that materials with adequate mechanical strength, wear resistance, and aesthetics for denture components (teeth and gingiva) are unavailable. Alfaraj et al. describe the same method of 3D-scanning the definitive cast, but they create a 3D-printed one-piece hollow obturator. Jamayet et al.[16] successfully used a merge of an intraoral scan and a 3D-scan of the definitive cast to create a hollow one-piece hollow definitive obturator.

Soltanzadeh et al.[17] also describe the workflow for a 3D-printed definitive obturator, using CAD. This case study also uses the 3D-scan of the definitive cast for the baseplate design. A cobalt-chromium alloy is 3D-printed, and a bulb is conventionally added to this framework, resulting in a solid bulb. These studies all use impressions, unlike our workflow. Callahan et al.[18] describe a case study about a CAD/CAM workflow for an immediate surgical obturator, using the preoperative CT scan of the patient for surgery planning and obturator design. The 3D-printed obturator was successfully situated for 3 weeks until the conventionally fabricated obturator was placed. The report did not design a hollow bulb.

Despite the mentioned reports on the use of CAD/CAM and 3D-printing for definitive and interim obturators, no workflow has yet been described that combines 3D-scanning, virtual planning and 3D-printing to create a hollow immediate surgical obturator. To the best of our knowledge, we are the first to combine all methods to develop an in-house workflow for the hISO.

## Future perspectives

Ultimately, we want to develop an in-house workflow for 3D-printed hollow ISO, which can be clinically used for maxillectomy patients who have surgery in the NKI-AvL. The addition of retention methods is a big step towards this implementation, but to get the CAD/CAM workflow clinically implemented, future steps need to be taken.

One of the biggest limitations of the current workflow is that it is only applicable to dentate patients. The registration of the intraoral scan (IOS) to the CT scan is done by handpicked fiducials on the teeth. For edentulous patients, this is not possible. During this year, another researcher studied the use of markers to (semi)automate the registration of the IOS to the CT scan, and to include edentulous patients in the workflow. First, Mulder[19] evaluated the usability of DentalMark (DentalMark 1.0mm Visionline ball, The Suremark Company) markers, by placing six markers in two volunteers. An IOS is made for both volunteers, directly after the placement of the markers and after 30 minutes. The markers are visible on all IOSs. The results showed submillimeter displacement of all markers, with low inter-observer variability (0.00-0.10 mm). Therefore, the markers are found to be usable, because they are visible on the IOS and have low displacement over time. Mulder also compared the registration

from IOS to CT scan with the markers to the same registration without markers, based on the TRE and FRE. A skull phantom similar to the ones in Chapter 6 is used (see Figure **5.1**). A CT scan and IOS are made of this phantom with eight markers placed on the locations shown in Figure **5.1**.

As the conventional test, five fiducial points on the IOS and CT scan are hand-picked and the IOS is registered to the CT with a linear rigid transformation, as stated in the current workflow. For the tested new method, the markers are used as guidance for the placement of the same hand-picked fiducials and registered with the same method. Different combinations of markers are used to evaluate the optimal marker placement. The marker on location 7 (see Figure **5.1**) is used as a target in both tests. The current workflow resulted in an FRE of 1.012 mm and a TRE of 0.95 mm. The workflow including the markers configuration of location 1, 3, 5 and 8 showed the lowest FRE and TRE, which is 0.2583 mm and 0.0789 mm respectively. These results show that the use of markers results in a lower registration error. The use of markers also results in a quick and easy workflow, that is less dependent on the operator skill and patient anatomy.

The markers can also be used for edentulous patients with dentures. The workflow for edentulous patients will include two CT scans – one CT scan of the patient's head with dentures in place, and one CT scan of the dentures itself. This protocol is already in use for CT-based implant planning. Mulder started with the automation of the registration of the two CT scans, but further research is needed to finish this objective. To ensure useful data for this research and for the automation of the registration of IOS to CT for (partially) dentate patients, an IRB is approved to include 25 patients in the next 4 years. These patients are coming for a CT scan of their head. When included in the study, a dentate patient will get the markers on their gingiva and palate (locations 1,3,5 and 8) and get their CT scan as standard care. Also, an IOS will be made with the markers in place. When patients are edentulous and have a denture or obturator, markers will be placed and two CT scans will be made as stated at the beginning of this section.
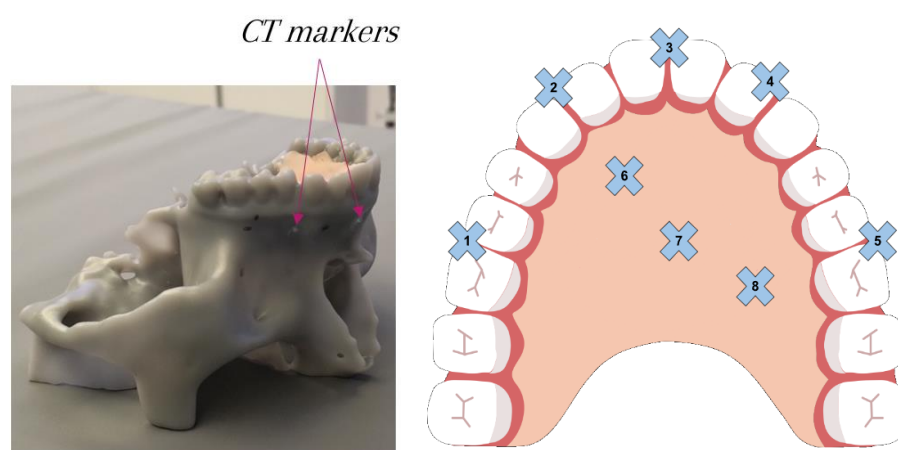


*Figure **5.1**. A 3D-printed skull phantom with CT markers is shown on the left. The illustration on the right shows the eight locations of the CT markers on the skull phantom.*

Before clinical implementation, an approved material and workflow are necessary. Therefore, when the workflow is comprehensive and includes edentulous patients, tests should be performed with biocompatible material. For the Formlabs 3D-printers, the Dental LT Clear Resin can bear more load (449 J/m vs 25 J/m for the now-used Clear V4 Resin, measured with the Notched Izod test). The Dental LT Clear Resin is a Class IIa resin and is certified biocompatible by ISO 10993-1:2018 and ISO 7405:2018.[20] In-house tests should be performed to evaluate this resin for the retention clasps. Next to the use of biocompatible material, the workflow and design must be approved according to the infection prevention within the NKI-AVL. In addition, the workflow and design should be evaluated according to the General Safety and Performance Requirements (GSPR) to comply with the MDR.

According to the research and the phantom study of Chapter 6, the 3D-printed retention clasp is indicated for use together with the zygoma wire for classes A1, A2, A4, and Z1. For the heavier and bigger classes (A3, Z2 and Z3), the 3D-printed retention clasps were not sufficient. Circumferential wires around the teeth are a retention option, but stability and support are not provided with this method. Future research should look into different retention options. One viable option is to use zygoma implants (ZI), placed in the reminiscing zygoma bone. This method is already described in the literature, with positive outcomes and the additional improvement of masticatory performance directly after surgery.[10,21–24] Surgical planning is very important for the placement of ZI because no anatomical landmarks exist, and it is important to prevent orbital floor intrusion and ocular perforation.[25]

Therefore, further studies should be performed to develop an in-house workflow for the planning and placement of ZI, and how to connect the 3D-printed hISO to the implant. In addition, the additional value of ZI and specific indications should be examined.

When these steps are taken, all patients are included in the workflow and the hISO can be used for clinical tests. These tests should focus on the patient satisfaction with the hISO. Also, the advantages of this in-house 3D-printed workflow must be examined, compared to the conventional method. It is important to test the retention methods in a clinical setting because all forces that play a role are complex and could differ for each patient. In addition, the use of the hISO as an interim obturator should be evaluated: is this easy to do and what alterations are needed? The main question should be answered: Does this 3D-printed hollow lightweight obturator result in better treatment and patient satisfaction?

Next to these appointed future studies, some future studies can be performed to improve the current hISO design. The current design does not include dentition. Dentition is not necessary for the hISO to fulfil its primary goals, but especially when anterior teeth are included in the resection, social impact can be huge when no teeth are included in the design. In the NKI-AvL, a study has been performed aimed at extending the current CAD/CAM workflow with prosthetic teeth to improve the aesthetics of the 3D-printed surgical obturator prosthesis.[26] Unfortunately, this research resulted in poor outcomes in terms of poor clinical scores from the prosthodontist, and due to high Hausdorff Distances (HD) between the IOS and the 3D-scan of the final obturator with dentition in place. Follow-up studies should focus on different methods to include dentition, for example by adding pockets into the design, to place conventionally made teeth separately.

Next to design additions and alterations, the surgery navigation method can also be evaluated. In the current workflow, EM navigation is used. The planned bone resection is turned black in the preoperative CT scan, which gives guidance during the surgery. With this approach, the cutting edges are not completely straightforward. Therefore, future studies could look into the use of saw and drill guides. Within the NKI-AvL, a lot of research is done for saw and drill guides for the mandibula (commando resection). Because the maxillectomy includes bone and has a unique and complex structure the use of saw and drill guides would be a good fit for maxillectomies.

# REFERENCES

1.      Haribhakti V V. *Restoration, Reconstruction and Rehabilitation in Head and Neck Cancer*. Springer Singapore; 2019. doi:10.1007/978-981-13-2736-0

2.      Yano J, Kumakura I, Hori K, Tamine KI, Ono T. Differences in biomechanical features of tongue pressure production between articulation and swallow. *J Oral Rehabil*. 2012;39(2):118-125. doi:10.1111/j.1365-2842.2011.02258.x

3.      Miller JL, Watkin KL. *The Influence of Bolus Volume and Viscosity on Anterior Lingual Force During the Oral Stage of Swallowing*: Vol 11.; 1996.

4.      Shaker R, Dodds WI, Hogan WJ. *Pressure-Flow Dynamics of the Oral Phase of Swallowing*.

5.      Sugita K, Inoue M, Taniguchi H, Ootaki S, Igarashi A, Yamada Y. Effects of Food Consistency on Tongue Pressure during Swallowing. *J Oral Biosci*. 2006;48(4):278-285. doi:10.1016/S1349-0079(06)80010-1

6.      Ogino Y, Fujikawa N, Koga S, Moroi R, Koyano K. A retrospective cross-sectional analysis of swallowing and tongue functions in maxillectomy patients. doi:10.1007/s00520-021-06186-w/Published

7.      Devlin H, Barker GR. *Prosthetic Rehabilitation of the Edentulous Patient Requiring a Partial Maxillectomy*.

8.      Keyf F. Review Obturator prostheses for hemimaxillectomy patients. doi:10.1111/j.1365-2842.2001.00754.x

9.      Dalkiz M, Dalkiz AS. The Effect of Immediate Obturator Reconstruction after Radical Maxillary Resections on Speech and other Functions. *Dent J (Basel)*. 2018;6(3). doi:10.3390/DJ6030022

10.     Mousa MA, Abdullah JY, Jamayet NB, Alam MK, Husein A. Biomechanical stress in obturator prostheses: A systematic review of finite element studies. *Biomed Res Int*. 2021;2021. doi:10.1155/2021/6419774

11.     Patil PG, Patil SP. A hollow definitive obturator fabrication technique for management of partial maxillectomy. *J Adv Prosthodont*. 2012;4(4):248. doi:10.4047/JAP.2012.4.4.248

12.     Nyirjesy SC, Heller M, von Windheim N, et al. The role of computer aided design/computer assisted manufacturing (CAD/CAM) and 3-dimensional printing in head and neck oncologic surgery: A review and future directions. *Oral Oncol*. 2022;132. doi:10.1016/j.oraloncology.2022.105976

13.     Bartellas M, Tibbo J, Angel D, Rideout A, Gillis J. Three-Dimensional Printing: A Novel Approach to the Creation of Obturator Prostheses Following Palatal Resection for Malignant Palate Tumors. *Journal of Craniofacial Surgery*. 2018;29(1):e12-e15. doi:10.1097/SCS.0000000000003987

14.     Tasopoulos T, Kouveliotis G, Polyzois G, Karathanasi V. Fabrication of a 3D Printing Definitive Obturator Prosthesis: a Clinical Report. *Acta Stomatol Croat*. 2017;51(1):53. doi:10.15644/ASC51/1/7

15.     Koyama S, Kato H, Harata T, Sasaki K. *A Workflow for Fabricating a Hollow Obturator by Using 3D Digital Technologies*.

16.     Jamayet N Bin, Farook TH, Al-Oulabi A, Johari Y, Patil PG. *Digital Workflow and Virtual Validation of a 3D-Printed Definitive Hollow Obturator for a Large Palatal Defect*.

17.     Soltanzadeh P, Su JM, Habibabadi SR, Kattadiyil MT. *Obturator Fabrication Incorporating Computer-Aided Design and 3-Dimensional Printing Technology: A Clinical Report*.

18.     Callahan N, Moles SL, Markiewicz MR. The Use of a CAD/CAM Surgical Obturator Without Impressions to Restore a Maxillectomy Defect. *Craniomaxillofacial Trauma & Reconstruction Open*. 2021;6:247275122199297. doi:10.1177/2472751221992972

19.     Mulder I. *Automatic Registration of Intra-Oral 3D Scan to CT for the Design of a 3D-Printed Maxilla Obturator*.; 2023.

20.     Technical Datasheet - Formlabs. *Dental LT Clear (V2) Biocompatible Photopolymer Resin for Form 2 and Form 3B*.

21.     Schmidt BL, Pogrel MA, Young CW, Sharma A. Reconstruction of extensive maxillary defects using zygomaticus implants. *Journal of Oral and Maxillofacial Surgery*. 2004;62(SUPPL. 2):82-89. doi:10.1016/J.JOMS.2004.06.027

22.     Noh K, Pae A, Lee JW, Kwon YD. *Fabricating a Tooth-and Implant-Supported Maxillary Obturator for a Patient after Maxillectomy with Computer-Guided Surgery and CAD/CAM Technology: A Clinical Report.*

23.     Wang M, Qu X, Cao M, Wang D, Zhang C. Biomechanical three-dimensional finite element analysis of prostheses retained with/without zygoma implants in maxillectomy patients. *J Biomech*. 2013;46(6):1155-1161. doi:10.1016/j.jbiomech.2013.01.004

24.     Corsalini M, Barile G, Catapano S, et al. Obturator prosthesis rehabilitation after maxillectomy: Functional and aesthetical analysis in 25 patients. *Int J Environ Res Public Health*. 2021;18(23). doi:10.3390/ijerph182312524

25.     Sender B, Lacroix T, Jaby P, Chaux-Bodard AG. Are zygomatic implants a simple and reliable technique for the stabilization of obturator prostheses? Case report and review of the literature. *Journal of Oral Medicine and Oral Surgery*. 2020;26(2):12. doi:10.1051/mbcb/2020002

26.     Michels V. Adding prosthetic teeth to the workflow for the fabrication of a 3D printed maxillary obturator prosthesis. Published online 2022.

# APPENDICES

# APPENDIX A.
# Proposed method for a Digital Surveyor

As described in chapter 4, a first set-up of a digital surveyor is proposed. A digital surveyor should identify the undercuts in a digital dental cast model.

The digital cast models used during this research build from a triangular polygon mesh, which in turn exists of faces and vertices (see Figure **A.1**). Each vertex has a normal, which is described with its direction in the x- y and z-axis.
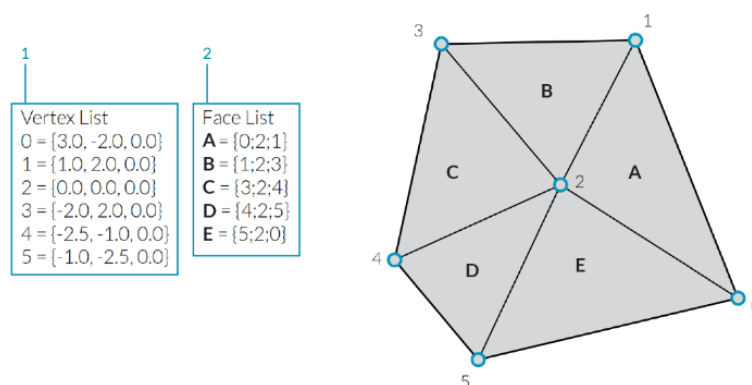


*Figure **A.1**. Example of a triangular polygon mesh, existing of faces (the grey surface indicated with a letter) and vertices (the blue dots, having an x- y- and z- axis location).*[1]

In this approach, the undercuts are identified by evaluating the z-direction of the normals of each vertex. First, a 3D model of the intraoral scan is plotted for visibility. The function pcread is used to create a point cloud ptCloud. The normals of each point can be found in ptCloud.Normal. The point is plotted as red when the z-direction of the normal is upwards (z>0). Otherwise, the point is plotted as white. This is done in MATLAB (The MathWorks, Inc., Natick, Mass) with the following code:

```
ptCloud = pcread('IntraOralScan.ply');
c1 = [255 0 0];
c2 = [255 255 255];
for i=1:ptCloud.Count
    if ptCloud.Normal(i,3)>= 0
     ptCloud.Color(i,:) = c1;
    else
     ptCloud.Color(i,:) = c2;
    end
end
pcshow(ptCloud)
```

1.      What is a Mesh? | The Grasshopper Primer (EN). Accessed October 30, 2023.
        http://grasshopperprimer.com/en/1-foundations/1-6/1_What%20is%20a%20Mesh.html

The points are plotted over the mesh of the intraoral scan for visibility. Figure **A.2** shows the result of a digital surveyed intraoral scan. The red shows the undercuts of the teeth. At first impression, this method seems to work as a digital surveyor.
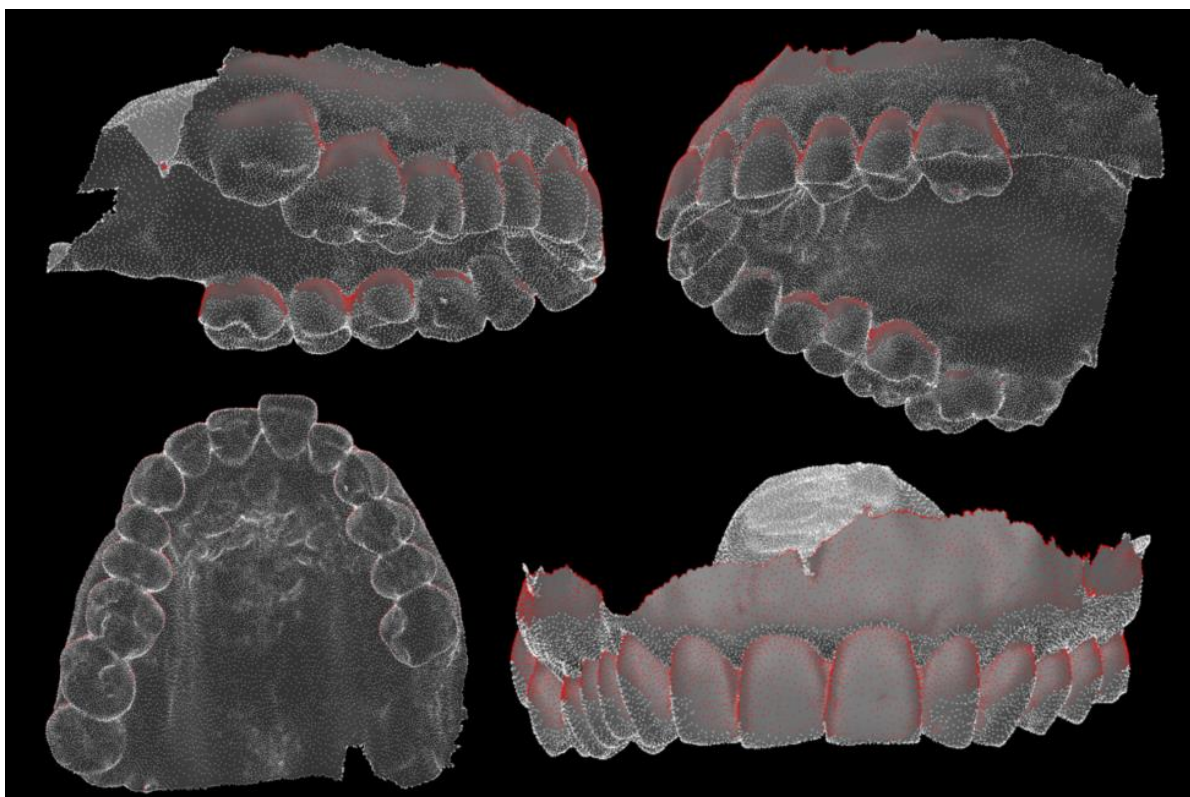


*Figure **A.2**. Results from the digital surveyor in MATLAB. In red, the undercuts are shown.*

# APPENDIX B.
# Tongue-Palate Pressure test: raw data

In chapter 5, tongue-palate pressure (TPP) tests are performed on three female, healthy subjects. The raw data of these tests is shown in table **B.1**. Three subjects each performed three rounds of measurements. One round of measurements exist of three sips of water for each measurement location. The TPP is measured anterior ($TPP_a$) on the tongue, and medial ($TPP_m$) and posterior ($TPP_p$).

Table **B.1**. Tongue-Palate pressure measured on three locations for three subjects when swallowing sips of water.

| Unit: kPa | Subject | 1 | | | 2 | | | 3 | | |
|---|---|---|---|---|---|---|---|---|---|---|
| Round | swallow→ location↓ | 1 | 2 | 3 | 1 | 2 | 3 | 1 | 2 | 3 |
| 1 | $TPP_a$ | 21 | 24 | 12 | 10 | 14 | 18 | 12 | 11 | 11 |
| | $TPP_m$ | 20 | 13 | 17 | 13 | 32 | 14 | 15 | 23 | 16 |
| | $TPP_p$ | 16 | 16 | 16 | 17 | 20 | 13 | 24 | 18 | 18 |
| 2 | $TPP_a$ | 19 | 26 | 19 | 23 | 16 | 15 | 13 | 16 | 17 |
| | $TPP_m$ | 14 | 15 | 15 | 23 | 21 | 21 | 15 | 13 | 19 |
| | $TPP_p$ | 16 | 18 | 20 | 15 | 27 | 19 | 21 | 14 | 15 |
| 3 | $TPP_a$ | 34 | 16 | 22 | 9 | 19 | 12 | 16 | 12 | 15 |
| | $TPP_m$ | 22 | 16 | 17 | 18 | 14 | 9 | 21 | 20 | 18 |
| | $TPP_p$ | 13 | 16 | 17 | 12 | 18 | 17 | 17 | 17 | 21 |

# APPENDIX C.
# Data processing and visualization of the phantom study for evaluation of 3D-printed retention clasps for surgical obturators.

In Chapter 6, a phantom study is performed. Measurements include two EM sensor locations during different tests. The maximal distance between those sensors at some point in time, is the result of one measurement. For every test, ten measurements are performed. The sensors are located on the obturator and the skull phantom. The distance is calculated with Pythagoras. A cut-off value is set to be robust for outliers.

```
co_value = 0.99  # or 0.95 for the pull test

# Create a new figure
# Set the figure position and size
hold on

for i = 1 to 10        # Because there are 10 measurements
    xo = x location of EM sensor on the obturator
    xo = xo - xo(1)  # Normalize to the initial position
    yo = y location of EM sensor on the obturator
    yo = yo - yo(1)  # Normalize to the initial position
    zo = z location of EM sensor on the obturator
    zo = zo - zo(1)  # Normalize to the initial position
    xs = x location of EM sensor on the skull phantom
    xs = xs - xs(1)  # Normalize to the initial position
    ys = y location of EM sensor on the skull phantom
    ys = ys - ys(1)  # Normalize to the initial position
    zs = z location of EM sensor on the skull phantom
    zs = zs - zs(1)  # Normalize to the initial position


    for k = 1 to number of measurement samples
        distances(k) = sqrt((xo(k) - xs(k))^2 + (yo(k) - ys(k))^2 + (zo(k) - zs(k))^2)
                # Normalize for the movement of the EM sensor on the skull, double
        pythagoras
    end

    plot(distances)
    A = sort(distances)
    max = A[round(co_value * length(A))]
    maxDisplacement(i) = max
end

hold off
```